

The Messenger



No. 162 – December 2015

Scientific return of VLT programmes
New fibre link for HARPS
Re-opening of VLTI
Dynamics of RSG atmospheres



The Scientific Return of VLT Programmes

Michael Sterzik¹
 Christophe Dumas²
 Uta Grothkopf¹
 Andreas Kaufer¹
 Bruno Leibundgut¹
 Stephane Marteau¹
 Silvia Meakins¹
 Ferdinando Patat¹
 Francesca Primas¹
 Marina Rejkuba¹
 Martino Romaniello¹
 Felix Stoehr¹
 Lowell Tacconi-Garman¹
 Ignacio Vera¹

¹ ESO

² TMT Observatory Corporation,
 Pasadena, USA

An in-depth analysis of the publications from 8414 distinct scheduled VLT observing programmes between April 1999 and March 2015 (Periods 63 to 94) is presented. The productivity by mode (Visitor or Service Mode) and type (Normal and Large, Guaranteed Time, Target of Opportunity, Director's Discretionary Time) are examined through their publication records. We investigate how Service Mode rank classes impact the scientific return. Several results derive from this study: Large Programmes result in the highest productivity, whereas only about half of all scheduled observing programmes produce a refereed publication. Programmes that result in a publication yield on average two refereed papers. B rank class Service Mode Programmes appear to be slightly less productive. Follow-up studies will investigate in more detail the parameters that influence the productivity of the Observatory.

Introduction

Very Large Telescope (VLT) observing programmes have been offered in Visitor Mode (VM) and Service Mode (SM) since the beginning of regular operations in 1999. Observing programmes* are imple-

mented through a variety of different programme types such as Normal Programmes, Large Programmes (LP), Guaranteed Time Observations (GTO), Director's Discretionary Time (DDT), Target of Opportunity (ToO; including Rapid Response Mode), Calibration, and Monitoring Programmes, each attuned to the needs of proposers or operations. All programme types are described in detail in the ESO Call for Proposals¹. GTO Programmes are almost exclusively executed in VM, while Monitoring, Calibration, DDT, and ToO Programmes are usually done in SM. Normal Programmes and LPs are pursued in both SM and VM.

Both Visitor Mode and Service Mode offer specific advantages. VM allows visiting astronomers to adapt their observing strategy in real time and ensures close relations between the visiting astronomers and the observatory staff. It also provides an opportunity for young researchers to gain hands-on observing experience at the Observatory. SM is designed to optimally use the range of observing conditions according to the observing constraints of the different science cases and enables execution of science programmes requiring particularly stringent conditions (Silva, 2001). For SM Programmes, different rank classes (A, B, C) are assigned by ESO, following the evaluations by the Observing Programmes Committee (OPC) according to the VLT/VLTI Science Operations Policy². The top-ranked SM proposals are assigned an A rank, followed by B rank and the filler programmes, with more relaxed observing constraints, receive rank class C. Hence the rank classes set priorities for the execution of SM observations. It should be noted that VM Programmes are only scheduled if they are rated at the same level as SM A rank class Programmes.

The scientific productivity of the VLT (and other ESO facilities) compares very well with other observatories in terms of global bibliometrics³. Here we investigate the impact of science operations, in particular on how programme modes, types and rank classes compare to each other in terms of their scientific return.

Through the identification of specific strengths and weaknesses of the current

operational model, as revealed through this analysis, we hope to enable improvements in the mid-term and to prepare for the future integrated VLT and European Extremely Large Telescope (E-ELT) operations scheme in the next decade.

Methodology

We utilise ESO-internal databases that collect information from Phase 1 (proposal submission) and Phase 2 (observation preparation and execution). Some of these databases were set up before the start of VLT operations, and over time, several modifications have been introduced to improve consistency and completeness. Among other studies, these databases enable the analysis of operational metrics and efficiency, which have been presented in Primas et al. (2014). We extracted the following information from the databases: scheduled observing proposal with its associated unique programme identification (ID, e.g., 089.A-0118), telescope, instrument, observing mode (VM or SM) and allocated time (nights for VM and hours for SM).

Observing programmes may consist of several runs, and these are identified through their run IDs (alphabetical letter added to the programme ID, e.g., 089.A-0118(B)). Each of these runs has its own time allocation, instrument, mode, etc. Observing runs are evaluated and ranked individually by the OPC.

A large fraction of programmes ask for only a few runs (68 % have one run and another 20 % two runs per programme). The number of "mixed mode" programmes (with SM and VM runs) is low (4 % by number and 9 % in time). Programmes with allocations on the VLT together with other ESO telescopes are more frequent (5 % by number and 12 % in time). Many multi-run programmes are LPs, while some Normal Programmes have multiple runs requesting, for example, different instruments to cover the same objects in one programme, different constraint sets or specification of several epochs to follow a variable object. The OPC rarely recommends different rank classes for individual runs within a programme. Other reasons for runs with different rank classes within an observing

* For the purposes of this study, we disregard VLTI programmes and spectroscopic surveys. Surveys on the VLT were introduced only in 2011. There are currently three such surveys: Gaia-ESO with FLAMES; Lega-C and VANDELS with VIMOS.

programme can be different pressures on telescopes or operational reasons, e.g., when a pre-imaging run receives a rank A while the corresponding spectroscopy run has B rank. The number of programmes with mixed rank classes amounts to 6 % by number and 9 % in time. Since the analysis is carried out at the programme level, we had to decide which rank class to assign to a programme. We added the time allocated to all runs and picked the rank class with the largest time allocation.

The ESO Telescope Bibliography (telbib⁴) provides the bibliometric information on the refereed publications for this study. The association of a publication with an observing programme is accomplished through the ESO programme ID. Cross-references between papers and programmes within the database are considered to be complete to over 95 %. We selected all papers associated with a programme including archival papers. Citations are drawn from the Astrophysics Data System (ADS) and the caveats on completeness of the ADS apply⁵.

Table 1 summarises the 8414 distinct observing programmes scheduled between the start of Unit Telescope 1 (UT1) operations in April 1999 (ESO Period 63) and March 2015 (end of Period 94). The analysis was restricted to the programme types Normal, Large, DDT, GTO and ToO. Short Programmes, which were offered between Periods 80 and 86 have been grouped with Normal Programmes. Calibration Programmes and Monitoring Programmes were first implemented in Periods 82 and 92, respectively. Since both Calibration and Monitoring Programmes are very few in number, we refrained from a separate analysis.

The fractional time distribution between VM/SM Programmes is 32 %/68 % (and 26 %/74 % in terms of number of programmes). VM Programmes typically received a median (mean) time allocation per programme 64 % (30 %) higher than SM Programmes. This is due to a combination of VM Programmes applying for full or half nights and many SM Programmes requesting short observations of less than one night. Among the SM Programmes, C rank class Programmes contribute approximately 10 % to the total

Programme (Mode, Rank, Type)	No. of programmes	Median TTA per programme (hrs)	Mean TTA per programme (hrs)	TTA (nights)
Total	8414	12.2	17.1	16028
VM	2228	18	20.7	5130
SM	6186	11	15.9	10898
A rank	2672	9.6	16.2	4807
B rank	2841	11.5	14.3	4515
C rank	673	16	21.1	1576
Normal	6705	14.0	16.4	12216
Large	80	170	209.4	1862
GTO	498	9	15.8	872
DDT	689	3.5	4.8	371
ToO	416	12	14.6	672
Calibration	17	8	8.1	15
Monitoring	9	16.5	19.7	20

Table 1. The Total Time Allocation (TTA) statistics for the different observing programme modes, SM rank classes and types for Periods 63 to 94. A night is taken to be nine hours.

number and intentionally over-schedule the observing queues. This procedure ensures that the available observing parameter space is filled, statistically, with suitable programmes (Silva, 2001).

Although there are relatively few Large Programmes (less than 1 % by number), they account for a fair fraction of the observing time (12 %). The selection process for LPs occasionally resulted in the reduction of the allocation to only one period and hence to LPs with scheduled time below 100 hours. We kept all LPs, independent of their total allocation, in our sample. One VLT Imager and Spectrometer for the mid-InfraRed (VISIR) Large Programme, which was not started due to the delayed VISIR upgrade, was excluded. Twenty LPs had runs scheduled at the VLT and other ESO telescopes. We tried to assess the relative importance of the respective telescope allocations by examining the scheduled time per telescope. Fourteen LPs have a majority allocation on the VLT and are counted as VLT LPs. The remaining six LPs were excluded from the analysis. The number of LPs considered in our VLT analysis is 80 as given in Table 1.

It should be noted that LPs in Service Mode are normally allocated an A rank, but a few LPs requiring very loose observing constraints were scheduled as filler programmes with a C rank class.

Productivity

The number of refereed publications can be used as an indicator of the scientific productivity of a programme. This implicitly assumes that all programmes received the full requested observations and the corresponding data, which is not true in all cases. Weather or technical time losses during VM and non-completion of SM Programmes will affect the ability of the community to produce scientific results.

Effects of programme completeness

The productivity of programmes depends on the completeness level of observing programmes, in particular for B and C rank-class SM Programmes. As examples we mention here the fact that some ToO Programmes did not trigger observations as no suitable transient object appeared during the allocated time. About 50 % of the allocated ToO time is typically not used. This explains some of the low numbers of publications per allocated night. Conversely, the fraction of DDT publications is fairly high as the programmes often have a very direct scientific goal and the small allocation leads to fast publication.

An analysis of the completeness for SM runs has recently been presented (Primas et al., 2014). Since ESO Observing Period 78 (October 2006), the overall completeness distribution fractions in terms of number of runs and number of hours for the different SM rank classes have been systematically recorded. The completeness fraction is defined as the

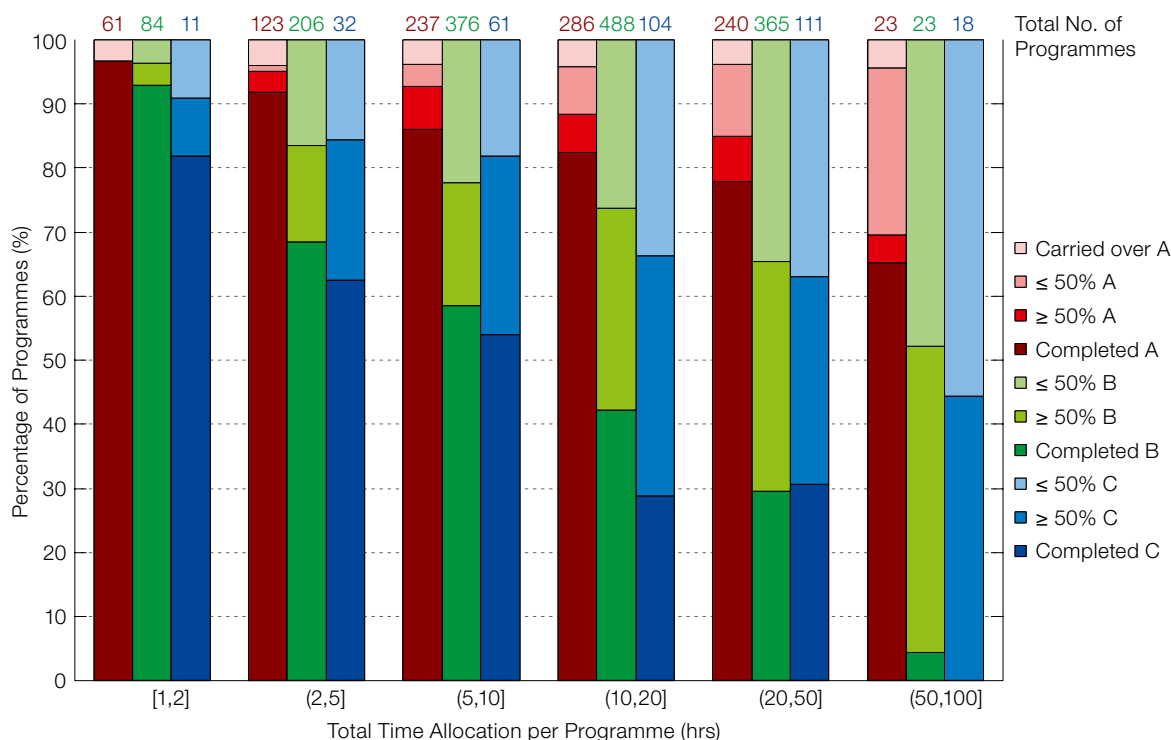


Figure 1. The fraction of observing programmes with different completeness levels separated by rank classes A, B, C, binned by total time allocation in hours. Each bar in a given allocation bin gives the completed, “ $\geq 50\%$ ” and “ $\leq 50\%$ ” fractions. For A rank class Programmes, the fraction of programmes with a carry-over status at April 2015 are included. The numbers at the top of the plot refer to the total number of programmes in each bin (= 100%).

actual time successfully executed for a given run divided by the total time allocated to this run. At the end of every period, incomplete A rank class observing runs are judged on their science status and are either declared completed (in most cases the runs are nearly fully complete) or are carried over into the next period. Some runs may be terminated for external reasons (e.g., users request that the programme be stopped or technical feasibility issues require its curtailment). About 15% of the B rank class runs were not started at all (Primas et al., 2014, Figure 6). The percentage of programmes that have not been started is even smaller. As long as there is only one run in a programme, the individual run completeness fraction applies. For multi-run programmes, we determined the completeness fraction as the average over all its runs weighted by the allocated time.

In the following we compare SM Programmes of the same type only. Therefore, we have selected a number of 968 A rank, 1550 B rank and 338 C rank class Programmes of type Normal and Short between Periods 78 and 94, for which we have reliable completeness information. We introduce three completeness groups: fully completed; more

than half, but not fully, completed (designated “ $\geq 50\%$ ” in the following); less than half ($\leq 50\%$) completed. Also a few (38) programmes that currently hold carry-over status are included. We do not include 282 programmes in the same period range that were never started, and consequently have a completeness fraction of 0%. Most of these programmes were in B rank class.

Figure 1 displays how the completeness level of Normal and Short Programmes with different rank classes depends on the programme length. The fraction of completed A rank class Programmes is generally high as the Observatory commits to these programmes, e.g., through carry-over into future observing periods. More than 80% of all A rank class Programmes with less than 50 hours allocated time were completed. We also explicitly show the fraction of A rank class Programmes being carried over in April 2015. Less than half of the B and C rank class Programmes with more than ten hours allocated time were fully completed; for the C rank class Programmes this is almost by design as they are filler programmes.

Table 2 compiles the productivities for subsamples with different completeness

levels for these A, B and C rank class Programmes. It presents the fraction of programmes leading to a publication (4th column), the average fraction of publications over all programmes (6th column) and the average number of publications per programme that produced a publication (7th column). Analysis of publications is presented in the following section.

As expected, higher levels of completeness usually lead to higher productivity for the programmes. Completed programmes, and those with more than 50% completeness, result in a significantly larger number of publications than those with a low observational return. This emphasises the importance of programme completion as an essential parameter to ensure the science return.

Amongst the fully completed programmes, the B rank class Programmes produce on average fewer publications per programme than A or C ranked Programmes. This effect is much smaller for the programmes that are at least half completed. Interestingly, the programmes that lead to publications typically produce more than one paper in all rank classes. This appears to be true even for programmes that obtained only very limited data.

Programme (Rank)	No. of programmes	No. of programmes with publications	Fraction of programmes producing a publication	No. of publications	Fraction of publications per programme (all programmes)	No. of publications per programme
Completed	1709	605	0.35	1023	0.60	1.69
<i>A rank</i>	820	303	0.37	553	0.67	1.83
<i>B rank</i>	762	248	0.33	368	0.48	1.48
<i>C rank</i>	127	54	0.43	102	0.80	1.89
≥ 50% completed	582	211	0.36	382	0.66	1.81
<i>A rank</i>	72	24	0.33	40	0.56	1.67
<i>B rank</i>	402	147	0.37	263	0.65	1.79
<i>C rank</i>	108	40	0.37	79	0.73	1.98
≤ 50% completed	565	108	0.19	162	0.29	1.50
<i>A rank</i>	76	11	0.14	19	0.25	1.73
<i>B rank</i>	386	76	0.20	111	0.29	1.46
<i>C rank</i>	103	21	0.20	32	0.31	1.52

Table 2. Average productivities of Normal Programmes in Service Mode (starting with Period 78) by completeness level for different rank classes. Three completeness categories are presented: fully completed (Completed); more than half, but not fully completed (≥ 50% completed); less than half completed (≤ 50%).

Further investigations considering the impact by actual observed time and including additional parameters — like programme length, instrument, observing conditions and observing requirements — need to be considered to interpret the findings.

Publication analysis

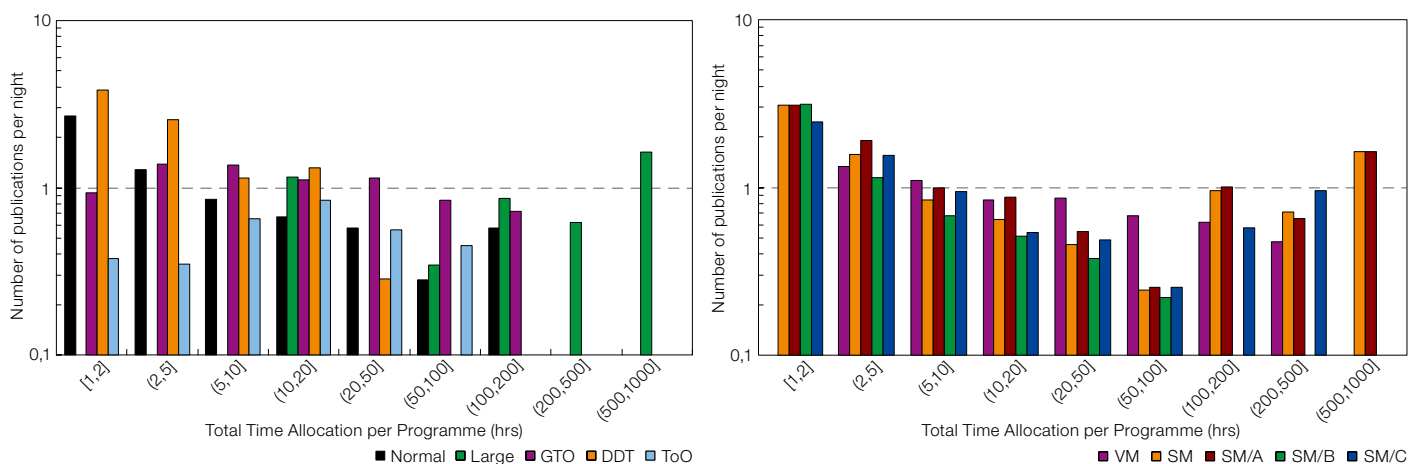
We have used the telbib database to correlate the ESO observing programmes with their refereed publications for all programme types and for the full length of VLT operations (Period 63 to 94). The results can be found in Table 3. There were 5907 publications based on VLT data to April 2015. Of the 8414 programmes allocated time, 3675 have contributed to publications. Many programmes contribute to more than one publication (compare columns 3 and 4 in Table 3) and conversely many papers are based

on several programmes: the 3675 programmes are mentioned 11 291 times in refereed papers. During the last 16 years a VLT programme contributed on average to 1.34 publications (= 11291/8414). The publications are based on only 44% (= 3675/8414) of all observing programmes. These are lower limits as there are a number of programmes that were not started (e.g., ToO, some SM Programmes) and hence the total number of programmes that received data is smaller. On average, one VLT Unit Telescope (UT) night resulted in 0.7 publications (= 11291/16028). Primas et al. (2014, Figure 9) have shown that typically only 75% of the scheduled time results in useful science observations and hence the previous number can be corrected to 0.9 publications per useful UT night. A further increase is expected as we have also included recent programmes, and many

of these may not yet have produced a publication.

There appears to be a significant fraction of observing programmes that do not result in publications and it is in the Observatory's interest to understand the reasons. It should be noted that the above statistics are based on allocated programmes and not on completed observations and hence the numbers are strict lower limits. The exact impact of completeness of the individual programmes is difficult to assess, as it may depend on many parameters (see discussion above) and we did not try to correct for it.

Figure 2. The dependence of productivity, by programme type (left panel) and observing mode and SM rank classes (right panel), in terms of publications per night is shown for the total time allocation per programme.

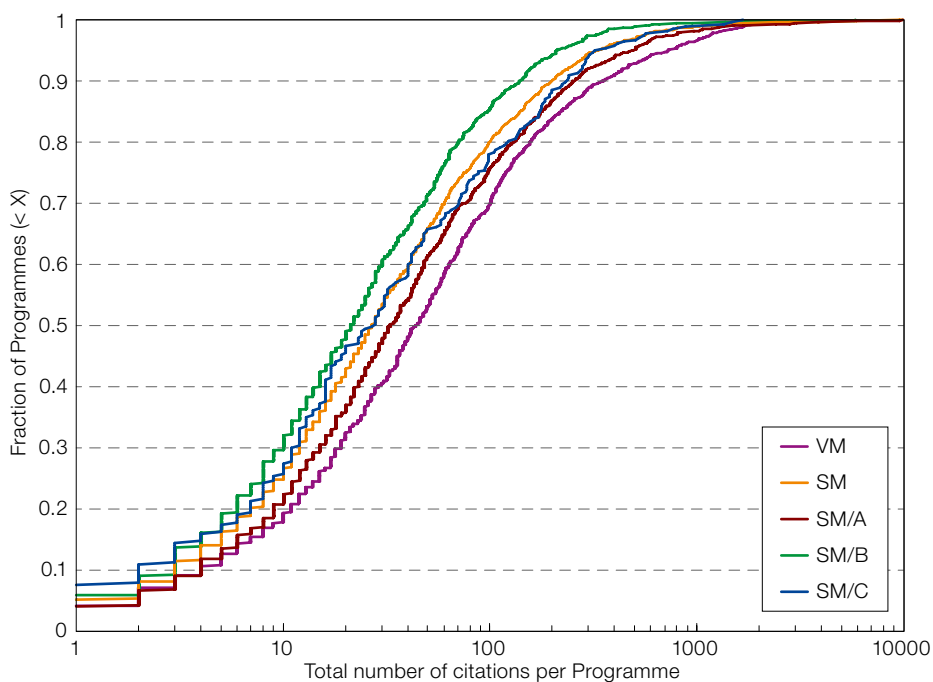
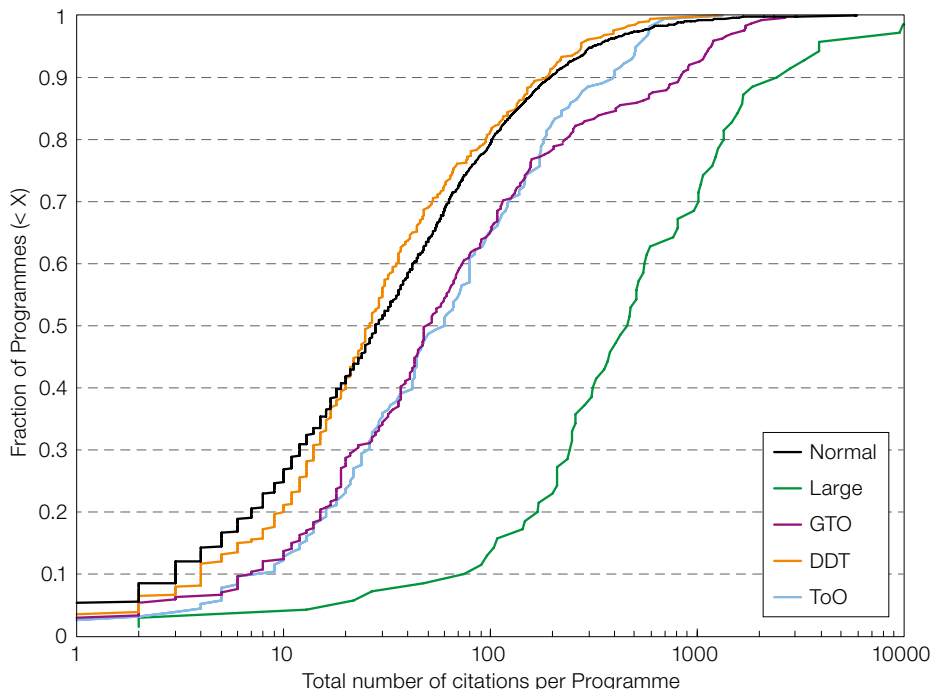


The productivity of the different observing modes and programme types shows some interesting features. It is noteworthy that Large Programmes produce many publications and are as productive per night as the other programme types. The GTO publication rate is high, which points towards a good match of the GTO science cases with the instrument and a high level of preparation of the GTO teams for the data analysis, e.g., through exquisite knowledge of the instrument and preparation of the instrument pipeline. Also the productivity of DDT Programmes is quite remarkable, profiting from their short duration and fast return. The least productive observing modes are SM Programmes in rank classes B and C.

Figure 2 shows the distribution of productivity per night for the different programme types (left panel), and modes and SM rank classes (right panel) as a function of allocated time. Programmes with a small allocation producing a publication are clearly favoured in such a comparison. Examination of Figure 2 demonstrates that:

- Large Programmes exhibit relatively constant normalised productivities. In general, LPs are allocated over 100 hours, but in rare cases the OPC recommended smaller allocations. These programmes are still listed as LPs in the database. This explains the small number of LPs with less than 100 hours in Figure 2. The number of publications per night is still rather high (mostly above 0.6) despite the large time allocations.
- DDT and Normal Programmes show decreasing normalised productivities with increasing allocated time, while GTO and ToO Programmes have a relatively flat distribution.
- VM Programmes also exhibit a rather flat normalised productivity distribution. They have the highest normalised productivities for programme lengths between 20 and 100 hours (approximately 2 to 11 nights).
- SM Programmes exhibit a high publication rate for short programmes and again for the LPs with > 100 hours allocations.

The trend for A, B and C rank class Programmes is very similar below 100 hours. A strong drop can be observed for pro-



grammes with more than 30 hours allocated. The fraction of completed programmes in this range is 30% or less for B and C rank classes, while it drops below the 80% mark for A rank class. However, given that non-completed programmes do publish, and that the fraction of programmes producing a publication is not dramatically lower for the programmes

Figure 3. The cumulative distribution of the total number of citations for those programmes that produced at least one publication. The sum of all citation counts is used in case more than one publication contributes. The top panel shows the distribution by programme type and the lower panel by observing mode and SM rank class.

Programme (Mode, Rank, Type)	No. of programmes	No. of programmes with publications	Contributions to publications	No. of publications per programme	No. of publications per allocated night
Total	8414	3675	11291	1.34	0.70
<i>VM</i>	2228	1205	4211	1.89	0.82
<i>SM</i>	6186	2470	7080	1.14	0.65
<i>A rank</i>	2672	1186	3956	1.48	0.82
<i>B rank</i>	2841	1014	2292	0.81	0.51
<i>C rank</i>	673	270	832	1.24	0.53
<i>Normal</i>	6705	2863	7776	1.16	0.64
<i>Large</i>	80	70	1483	18.5	0.80
<i>GTO</i>	498	241	960	1.93	1.10
<i>DDT</i>	689	342	633	0.92	1.70
<i>ToO</i>	416	156	436	1.05	0.65
<i>Calibration</i>	17	3	3	0.18	0.20
<i>Monitoring</i>	9	0	0	0	0

Table 3. Publication statistics of VLT observing programmes by mode and SM rank class and type.

that are $\geq 50\%$ completed, the impact of completeness is not so straightforward to analyse. The cause for this distribution requires further investigation.

Impact

Citations can provide a measure of the scientific impact of observing programmes. We have obtained the number of citations for a given publication from the ADS.

The cumulative distributions of the total number of citations for the different programme types and the modes are shown in Figure 3. All citations of all publications for a given programme are summed. We chose to present the cumulative distributions to remove the effects of the sometimes very different sample sizes (cf., Table 1).

The median for Normal Programmes is approximately 20 citations, i.e., about 50% of all Normal Programmes have produced more than 20 citations from their publications. The highest number of citations is reached by the Large Programmes: half of them resulted in more than 300 citations. The median citation count for GTO and ToO Programmes is around 50, while it is about 20 citations for DDT Programmes.

The median for all SM Programmes is around 25 citations and is the same for C rank class Programmes bracketed by A and B rank classes with 30 and 20 citations, respectively. VM Programmes have a median citation of about 40.

Nevertheless, all programme types produce a high science impact of more than 100 citations. Ninety percent of the LPs achieve more than 100 citations and some 20% over 1000 citations. About 20% of ToO and GTO Programmes also generated more than 100 citations.

Caveats

Some of the approximations and assumptions that have been made for this analysis have already been described in the relevant sections. In particular, we have not accounted for the fact that typically a delay of several years is seen between receipt of data and publication. Considering that it takes roughly five years on average for a publication to appear and hence we have not accounted for almost a third of the lifetime of the VLT, we expect the number of publications to increase by about 30% in the future.

The programme implementation and classification policies have changed relatively little, but new instruments have been offered and the underlying model has evolved. Therefore subtle biases in the programme distribution and their performance over time cannot be excluded.

The records contained in the telbib database do not consider or evaluate the contributions of individual datasets of programmes to the scientific goal of a publication. On the one hand, some data (and programmes) contribute critically and others just provide complementary or ancillary data. Effectively, this may

overestimate the scientific return for some programmes in publications contributing multiple datasets. On the other hand, the total time required to contribute specific data to a publication may not use the entire time allocation of the full programme. The assumption of accounting for the total time of an entire programme therefore overestimates the actual observing time attributed to a publication. There is no simple methodology to weight the different contributions objectively and we have not attempted to do so.

The incompleteness of SM Programmes of different rank classes introduces various biases. We have investigated its effect on programme productivity, but not on its associated citation statistics. Incomplete programmes lack specific observations and likely reasons are the (expected or actual) violation of observing constraints or some statistical over-scheduling of constraint parameter space. The dependency of observing constraints and conditions for a given programme on its subsequent science return is another important performance indicator of SM Programmes and their implementation, and deserves further analysis.

Results and conclusions

The main findings of this study of the scientific return of VLT observing programmes are as follows:

1. Large Programmes (LPs) have by far the highest scientific productivity and impact. As expected, they fulfil their role of providing major scientific

- advances, breakthroughs and often have a high legacy value. Normalised by the allocation time, their productivity per night is at least as high as for Normal Programmes. Thus LPs have proven to be a highly valuable asset in the strategic distribution and implementation of VLT programmes.
2. Most of the telescope time available at the VLT is allocated for the execution of Normal Programmes. They produce most of the VLT publications. However, their impact is relatively small when compared to the other programme types (cf., Figure 3). Still, the community prefers Normal Programmes as shown by the results of the ESO2020+ Users' Poll (Primas et al., 2015).
 3. GTO Programmes have on average a higher impact than Normal Programmes, supporting their role as pathfinders using novel instrumentation for cutting-edge science cases. Some GTO Programmes are coordinated observations over several periods and resemble LPs in this respect.
 4. ToO Programmes have on average a higher impact than Normal Programmes. Considering that many ToO Programmes are not triggered, the impact has to be regarded as even higher. This reflects the growing interest in the astrophysics of the variable sky.
 5. DDT Programmes typically constitute small investments of telescope time and are targeted at specific, "hot" scientific questions that can lead to quick publication. Often they complement existing data to confirm or strengthen a result and represent less than 2% of the scheduled observing time. They are productive in terms of number of publications per telescope night, but their absolute impact (in terms of citations) remains limited, as shown by Figure 3.
 6. VM Programmes exhibit high productivity and impact, in particular for Normal Programmes with telescope time allocation of a few nights. In this parameter range, the specific strengths of VM allocations pay off: the visiting astronomer can optimise the observing strategy and implement back-up programmes to adjust in quasi real-time to changing observing conditions, thus possibly securing a higher data return.
 7. A and C rank class SM Programmes yield, on average, nearly two refereed publications for programmes that produced a publication. B rank class Programmes do not produce as many publications. If one compares the number of publications per night, B and C rank class Programmes show lower publications than A rank class and Visitor Mode Programmes.
 8. SM A rank class and VM Programmes have similar completion fractions, if we assume that statistically Visitor Mode Programmes receive about 85% of the allocated time (allowing for ~ 15% weather and technical downtime; Primas et al. [2014], Figure 9) while the B and C rank class Programmes are more incomplete. The number of publications per programme, and per allocated time, increases with completeness fraction for all ranks. It is quite possible that statistically most B rank class Programmes lose their programme execution competition to A rank class Programmes in the same, demanding, observing constraint conditions. We plan to investigate this aspect in the future in more detail.
 9. The publication ratio for all VLT programmes (i.e., the number of programmes that published at least one refereed paper, divided by the number of all VLT scheduled programmes) is 44%. This is a strict lower limit as the time between observations and publication is typically five years and we can expect an increase of about 30% in this number over the next few years.
- It is clear that attention must be given to the implementation of B rank class Programmes, and in particular to facilitate, if possible, an increase of their completion rates. C rank class Programmes exhibit a relatively strong performance.
- Together with the community we should also try to better understand the reasons why a significant fraction of VLT programmes do not lead to results published in refereed journals. ESO plans to poll the principal investigators for the reasons for not publishing.
- An important scientific return comes from archival research. We have included archival papers in our analysis, but did

not separate them out for study, as we were primarily interested in the operational aspects. The impact of archive research will be investigated in a separate article (Romaniello et al., in preparation).

Several aspects of this study require follow-up analysis. The statistical investigation presented here is only one step towards a better global understanding of the complexity of the various processes that lead to advancement of scientific knowledge. The individual science cases, but also sociological factors within the science teams, may influence the scientific return, an aspect which is well beyond the scope of the present analysis.

Acknowledgements

We thank Piero Rosati for sharing his unpublished study with a similar scope made in 2011. Discussions with Ralf Siebenmorgen about the methodology and with Jeremy Walsh and Olivier Hainaut about the presentation of this article are highly appreciated. This research made use of the NASA Astrophysics Data System.

References

- Grothkopf, U. et al. 2007, *The Messenger*, 128, 62
 Grothkopf, U. & Meakins, S. 2012, *The Messenger*, 147, 41
 Primas, F. et al. 2014, *The Messenger*, 158, 8
 Primas, F. et al. 2015, *The Messenger*, 161, 6
 Silva, D. 2001, *The Messenger*, 105, 18

Links

- ¹ ESO Call for Proposals, e.g., the most recent: <http://www.eso.org/sci/observing/phase1/p97/CfP97.pdf>
- ² ESO Council resolution on VLT/VLTI Science Operations Policy: <http://www.eso.org/sci/observing/policies/Cou996-rev.pdf>
- ³ telbib statistical summary: <http://www.eso.org/sci/libraries/edocs/ESO/ESOstats.pdf>
- ⁴ ESO telescope bibliography, telbib: <http://telbib.eso.org>
- ⁵ ADS citations: http://doc.adsabs.harvard.edu/abs_doc/faq.html#citations

HARPS Gets New Fibres After 12 Years of Operations

Gaspare Lo Curto¹
 Francesco Pepe²
 Gerardo Avila¹
 Henri Boffin¹
 Sebastian Bovay²
 Bruno Chazelas²
 Adrien Coffinet²
 Michel Fleury²
 Ian Hughes²
 Christophe Lovis²
 Charles Maire²
 Antonio Manescau¹
 Luca Pasquini¹
 Samuel Rihs²
 Peter Sinclair¹
 Stéphane Udry²

¹ ESO

² Université de Genève, Département d'Astronomie, Versoix, Switzerland

In June 2015, as part of the HARPS Upgrade 2 Agreement signed in 2013 between ESO and Geneva University, a new set of non-circular (octagonal) optical fibres, with improved mode-scrambling capabilities, has been installed. The motivation for the exchange of the fibre link and the results from the commissioning tests are presented. The throughput of the instrument (+40% at 550 nm), its illumination uniformity and stability, and thus its radial velocity (RV) stability, are significantly improved. An RV offset correlated with the width of the stellar lines is found with the new fibres from observations of RV standards. As a result of this major upgrade, and once the laser frequency comb that is already assembled in the HARPS room is fully functional, we expect to reach an RV precision better than 0.5 m s^{-1} on bright stars.

Rationale for a fibre upgrade

The High Accuracy Radial velocity Planet Searcher (HARPS) was developed between 2000 and 2003 to measure stellar radial velocities with a precision of 1 m s^{-1} or better (Mayor et al., 2003) and has proved to be a spectacularly successful workhorse spectrograph for the discovery and monitoring of extrasolar planets. The spectrograph is based on the simultaneous-reference technique

(Baranne et al., 1996), which has the great advantage with respect to the self-calibration technique (iodine absorption cell) of using the whole visible spectrum without any light loss and spectral contamination.

Since the simultaneous-reference technique relies on the stability of the instrumental profile (IP), at least on timescales of an observing night, the technique requires the use of optical fibres. They ensure that the stellar image injected into the fibre at the telescope focus is well scrambled, i.e., the light distribution at the fibre exit is homogeneous and does not change with time¹. However, an optical fibre only scrambles the near field (i.e., the light distribution on the fibre tip) in a satisfactory way, but not its far field (the angular distribution within the light cone leaving the fibre). It was therefore necessary to introduce the concept of a double scrambler — a set of two fibres connected by a simple optical system that exchanges the near field of the first fibre with the far field of the second fibre, and vice versa (Baranne et al., 1996). This fibre link ensures a good scrambling of both near and far field.

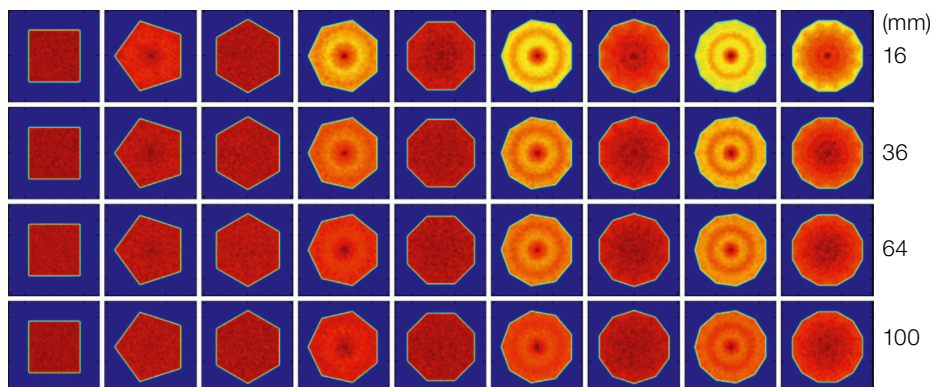
During the design phase of HARPS, and following tests on CORALIE, we could estimate the level of scrambling to be expected with HARPS (Pepe et al., 2002). It became clear that the scrambling alone would not be sufficient to achieve the 1 m s^{-1} requirement, and that a requirement on the centring precision of the star on the fibre during the scientific exposure had to be set. It was estimated, and confirmed, that a systematic de-centring of the stellar image to the fibre edge would induce an RV effect of the

order of 3 m s^{-1} (Mayor et al., 2003). While de-centring was addressed first by an improvement to the 3.6-metre guiding system, followed by the introduction of a tip-tilt system (Lo Curto et al., 2010), in the absence of other solutions this issue of imperfect scrambling has been accepted for many years.

It was already known that circular fibres carry some memory effect of the angular and spatial distribution of the injected light. However, only later it was understood that far-field changes dramatically impact the IP of the spectrograph in presence of optical aberrations (Perruchot et al., 2010). In the meantime, non-circular fibres had become available and it was demonstrated, by simulation and laboratory tests, that their scrambling efficiency is far superior to that of circular fibres (see Figure 1 and Chazelas et al. [2010], Figures 5 and 10).

On account of their advantages, octagonal fibres were quickly employed in SOPHIE (Bouchy et al., 2013) at the Observatoire de Haute-Provence and in the northern copy of HARPS at the Telescopio Nazionale Galileo (Cosentino et al., 2012) with excellent results. The improvement was so convincing that it was proposed that a copy of the HARPS-N fibre link on HARPS at the 3.6-metre telescope should be implemented within a new HARPS Upgrade 2

Figure 1. Near-field fibre scrambling (Zemax simulation) is shown as a function of fibre shape (horizontal axis) and fibre length (vertical axis). The output face of the fibre is shown in each case. The simulation assumes an input spot of $10 \mu\text{m}$ in diameter at the centre of the fibre with a core thickness of $100 \mu\text{m}$. Hexagonal, octagonal and square fibres show very good uniformity for lengths above 16 mm.



project (see Figure 2). The agreement between the Geneva Observatory and ESO also foresaw an upgrade of the HARPS data reduction pipeline, which was necessary to cope with the new laser frequency comb (LFC; Lo Curto et al., 2012) and the fibre upgrade, as well as an improvement of the thermal stability of the instrument and its maintenance for an additional three years.

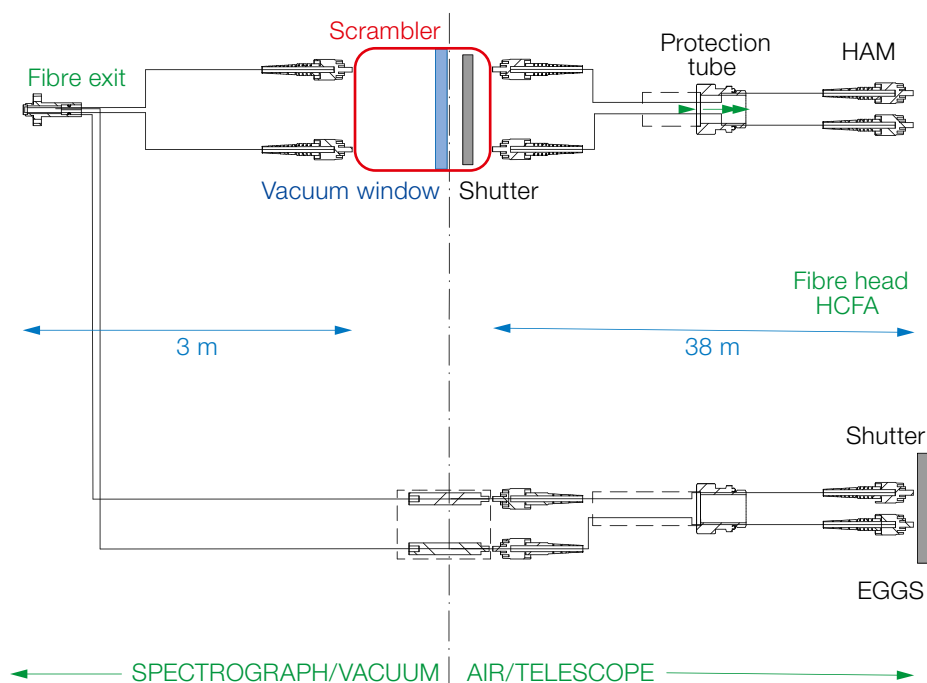
An optical fibre link is often considered as a necessary evil for the sake of precision. The original HARPS fibre link (40 metres of fibre and a double scrambler) achieves an efficiency of only about 55 % at peak, without taking into account additional slit losses occurring in poor seeing or with non-optimum telescope image quality. By harnessing the improved fibre technology, we had demonstrated on HARPS-N that the fibre-link efficiency could be improved to about 70 %, and that only about 10 % of the 30% loss was due to the double scrambler. For this reason, ESO and the Geneva Observatory agreed on a goal of 20 % relative efficiency improvement with respect to the old HAM (high accuracy mode) fibre link on HARPS at the 3.6-metre.

Together with the new fibre link (Figure 2), we also replaced the homemade HAM shutter with a commercial bi-stable Uniblitz shutter and developed a new miniaturised shutter for the high efficiency mode (EGGS) fibre head. Finally, to improve the functionality of the EGGS mode, the upgrade provided the opportunity to repair its broken sky (or simultaneous reference) fibre.

The HARPS Upgrade 2 Agreement also foresaw the update of the data-reduction pipeline, the installation of thermally controlled vacuum-vessel feet for better thermal stabilisation of the instrument, a new (spare) vacuum pump and other minor maintenance tasks on the instrument. All these aspects were successfully executed during the fibre upgrade mission.

A new fibre link

The new HAM fibre link is conceptually identical to the old fibre link (Mayor et al., 2003) with the only difference being the



use of octagonal fibres, instead of circular fibres (Figure 3), of the same effective diameter. The detailed mechanical and optical design of the fibre head, the scrambler and the fibre exit were copied from HARPS-N because of the slightly improved optical performance. On the fibre exit side, the EGGS fibres are integrated in the same ferrule and use the same relay optics as the HAM fibres. However, the EGGS fibres do not use a double scrambler. It would have been very difficult to safely handle a 40-metre long EGGS fibres and a vacuum feedthrough attached to the fibre exit and the HAM scrambler, while pulling the whole system through the telescope Coudé path and into the vacuum vessel. For this reason, we decided to split the EGGS fibres at the vacuum feedthrough and install fibre connectors on the external side of the vacuum flange. Furthermore, we changed the fibre head of EGGS in order to adopt the same solution and optics as for the HAM fibres. In addition to being easy to align, the new fibre-head optics of EGGS fibres now injects the stellar image instead of the telescope pupil into the fibre's near field. Since the pupil is stable by definition, and the near-field (stellar image) is perfectly scrambled by the octagonal fibre, we can also expect better radial velocity performance for the EGGS fibres.

Figure 2. Configuration of the fibre link for the HAM and EGGS fibre links from the telescope (fibre head) to the spectrograph (fibre exit).

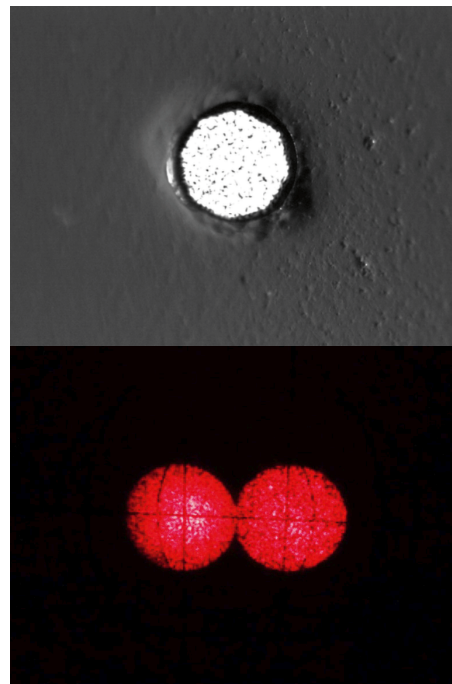


Figure 3. Top: Near-field image of the back-illuminated octagonal object fibre observed with a microscope through the 140 μm pinhole in the HARPS guiding mirror during alignment and focusing. Bottom: Far-field image of the back-illuminated fibres (object and sky fibre) during alignment of the optical axis.

A complete fibre link for HARPS, plus one set of spare fibres, was assembled, aligned and successfully tested in the laboratory with respect to total transmittance and focal ratio degradation (FRD). At La Silla, the optical alignment of the fibre-link optics was re-verified before installation (Figure 3). On 19 May 2015 HARPS stopped operations and the instrument was opened. Installation and alignment of the fibre link lasted roughly one week. On 29 May, the vacuum vessel was closed and evacuated for the last time. Finally, a formal commissioning of the new fibre took place, finishing on 3 June, when the instrument was handed back to Science Operations.

Table 1 shows laboratory measurements of the total efficiency and FRD of the two HAM fibres of the new fibre link, at three different wavelengths. The total throughput has been measured in nominal conditions, i.e., injecting a 3.6-metre telescope-like $F/8$ beam and measuring the total transmitted flux within the $F/7.5$ acceptance beam of the spectrograph. Values higher than 75 % were obtained in the green–red part of the spectrum, where the internal transmittance of the fibres is excellent. These values have to be compared to the 55 % total throughput measured for the original HARPS fibres in 2002.

The FRD indicates the fraction of the light falling within the $F/7.5$ cone compared to the total flux exiting the fibre. The values show that only about 6 % of the light falls outside the nominal acceptance cone. Such very low FRD losses are achieved when the fibres are prepared in a suitable way. Experience has shown that stress-free mounting is essential and can be obtained by using soft glue when connecting the fibres. Also, the thick cladding and buffer makes the fibre less sensitive to stress. Nevertheless, another aspect must be considered: the HARPS solution foresees gluing the relay lenses directly on to the fibre tip. By this means reflection losses are avoided and, even more important, the remaining surface defects on the fibre tip, which would produce stray light and FRD, are levelled out. Finally, after subtracting FRD losses and internal transmittance losses, less than 10 % loss can be assigned to the scrambler optics. In fact, most of the losses

Wavelength [nm]	Fibre A (object)		Fibre B (sky or simultaneous)	
	FRD	Throughput	FRD	Throughput
600	94.2%	79.8%	94.7%	79.3%
550	94.8%	77.3%	95.5%	76.8%
450	94.0%	68.4%	93.8%	66.2%

Table 1. Laboratory measurements of FRD and throughput of the new HAM fibres.

reported in the past occurred in the scrambler, and were due to the poor FRD of the first and long fibre section from a coupling-efficiency loss.

The scrambling power of the new fibres has been demonstrated to be a factor of at least ten times the value measured using circular fibres (Cosentino et al., 2012). Also, it has been shown that the far field was stabilised to much better than 10 % relative variation, even when moving the injected test light source from the centre to the edge of the fibre. Altogether, we expected (and demonstrated on HARPS-N) that any de-centring of the star on the fibre would result in an RV effect of less than 0.5 m s^{-1} .

Commissioning results

Spectral format, point spread function and resolution

The fibre upgrade project foresaw the opening of the vacuum vessel in order to access the vacuum side of the fibre link. The fibre link had been prepared to allow a plug-and-play installation, but nevertheless, the new fibre exit that defined the spectrograph slit had to be re-aligned and re-focused. The alignment was performed in such a way as to match the spectral format recorded by the science

detector (charge coupled device [CCD]) prior to the upgrade. This objective was indeed achieved within a couple of pixels in both spectral (dispersion) and spatial (cross-dispersion) directions. For the focus however, two iterations of evacuating and re-opening the vacuum vessel had to be performed in order to obtain a form of through-focus test and define the best focus position. The focus was physically adjusted by mechanically moving the fibre exit.

Figure 4 shows the result of the last through-focus procedure performed when the vacuum vessel had been evacuated for the last time before the restart of operations. The measurements show the full width at half maximum (FWHM) of the thorium–argon spectral lines recorded by the CCD at various locations both in Y (dispersion) and X (cross-dispersion). The values are minimum, and the curve becomes flat, towards 0 mbar, the pressure at which the spectrograph is operated, demonstrating that we had achieved optimum focus.

Another measure of the focus quality is shown in Figure 5, where the width of the spectral orders is plotted as a function of time. It can easily be seen that the orders became wider with time indicating a clear defocus of the instrument.

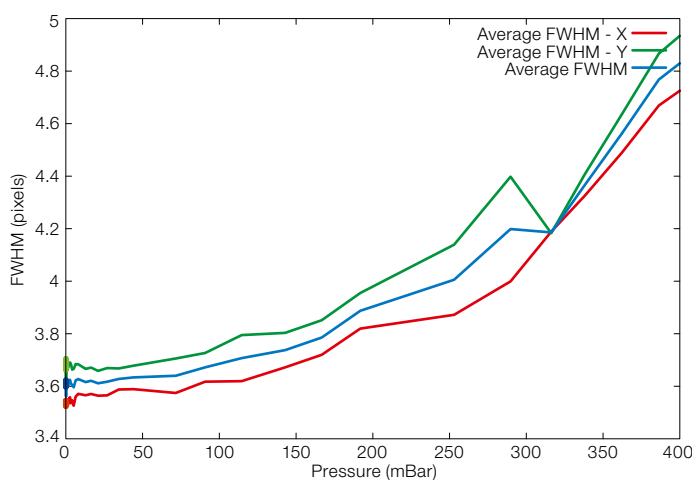


Figure 4. Through-focus of the new fibres as a function of vacuum pressure during the last evacuation of the vacuum vessel. At 0 mbar (operating condition), both the FWHM in dispersion and cross-dispersion direction are minimum and flat.

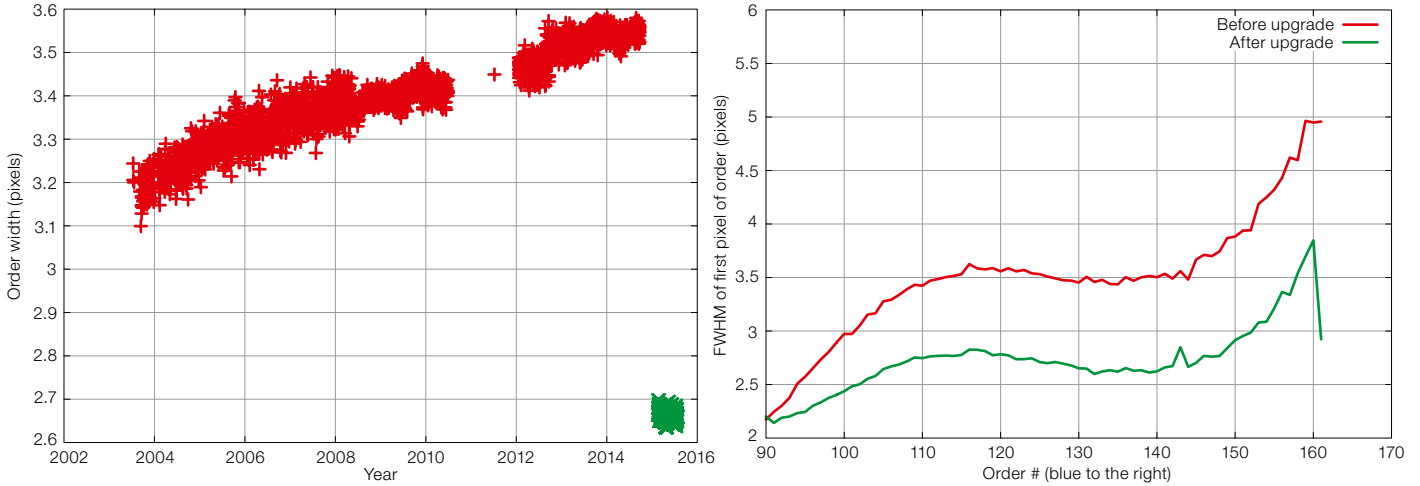


Figure 5. Width of the spectral orders measured at the CCD serial register are shown. Left panel: Time evolution for order #120. The width is measured by the online pipeline via a three Gaussian fit and recorded in the FITS header. Right panel: Order width as a function of order number before (19 May 2015) in red and after (29 May 2015) in green the intervention.

FWHM in dispersion direction showed that the focus was better on most locations across the CCD, but slightly worse on the centre-high part (red part) of the spectrum. The resulting (flux-averaged) resolving power remained almost unchanged (before: $R = 115\,000$; after: $R = 114\,000$). However, the homogeneity of the focus and the symmetry of the focus spots were greatly improved. This can be appreciated, for instance, by the right panel of Figure 5, which shows that the change of the spot size across the order is much smaller after the intervention and much closer to the expected anamorphic effect of the echelle spectrograph. Overall the focus and the homogeneity of the focal plane was improved by the intervention and the re-alignment. It is important to note that minor changes of the focal plane did not require develop-

ing a new version of the data-reduction pipeline. Nevertheless, significant work had to be invested to adapt the data-reduction system (DRS) to the slightly different spectral format and to cope with other changes, e.g., the altered flux calibration and the modified IP. An optimisation of the DRS to take best advantage of the new configuration is still in progress.

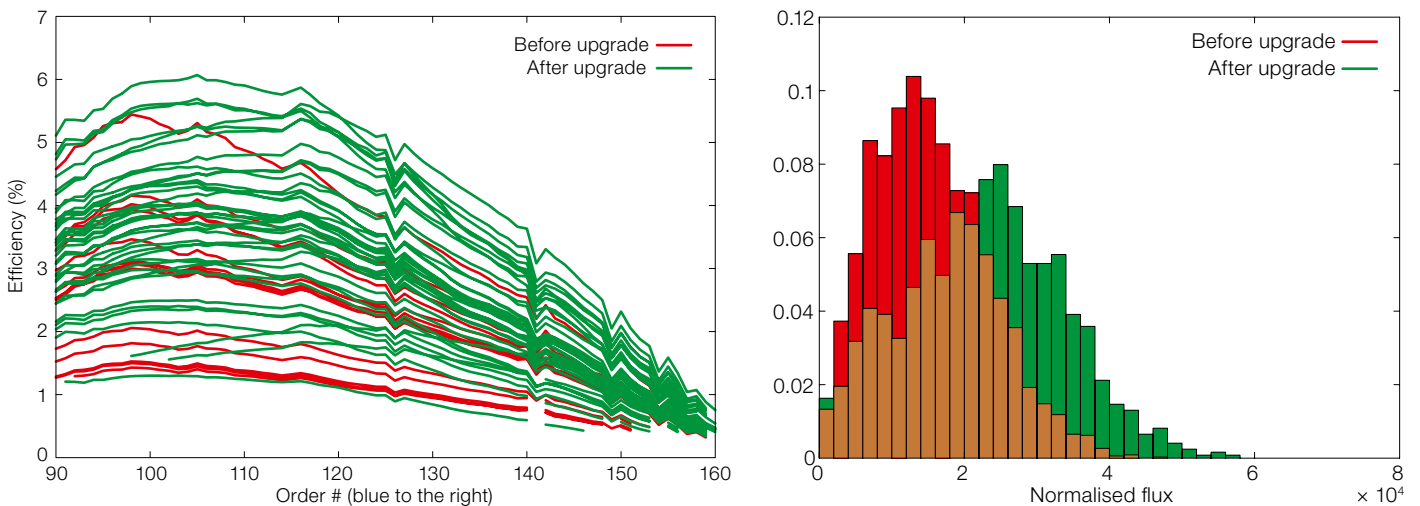
Throughput and efficiency

The increase in throughput was not one of the main motivations of this upgrade, however we expected a noticeable improvement given the experience gained with optical fibres, stress-free mounting

After the intervention (green points and line in Figure 5) the FWHM of the orders decreased considerably, demonstrating again the effectiveness of the focus procedure. The order width along a selected order is shown in the right panel of Figure 5, providing further evidence for the difference between pre- and post-intervention of the focus.

The improvement of the focus is not as dramatic in the dispersion direction as in the cross-dispersion direction. Nevertheless, a preliminary analysis of the

Figure 6. Left: Improvement of the overall instrumental throughput as measured from spectrophotometric standards. Right: Histogram of the direct comparison of the integrated flux (normalised by object magnitude and exposure time) of science targets.



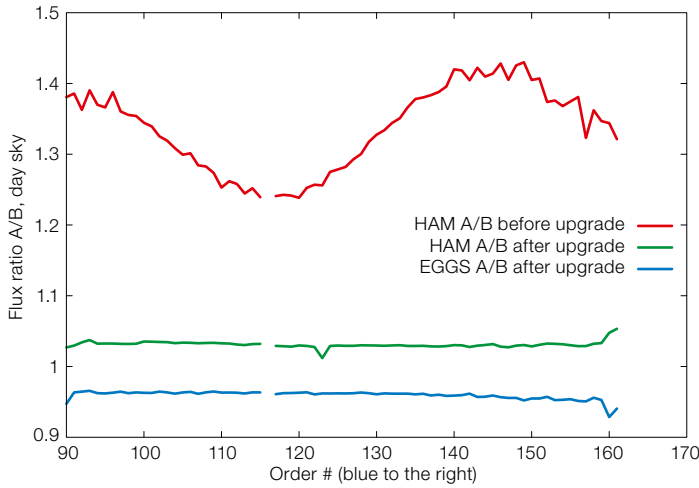


Figure 7. Fibre throughput ratio: science (A)/reference (B) integrated flux as measured from the diffuse light of the daytime sky. The curves obtained after the upgrade are very uniform and close to unity both for the HAM and the EGGS modes.

Before the upgrade, the throughput ratio between the two fibres of the HAM mode was about 1.35 and strongly colour dependent (Figure 7). After the upgrade, not only did the value get much closer to unity, but also the colour dependence had almost disappeared. In addition, by replacing the EGGS fibres, the broken fibre B of this mode was replaced. The flux ratio A/B for this mode was also measured and we obtained a value very close to unity and very uniform as a function of wavelength.

The same spectrophotometric standard stars as for the HAM efficiency measurement (Figure 6) were used to compare the efficiency of the HAM versus the EGGS mode. Figure 8 displays the efficiency of both modes at different air-masses. The seeing was about 1 arcsecond, and each EGGS spectrum was taken just after the HAM one, on the same target and without moving the telescope. The EGGS/HAM throughput ratio is shown in blue and is close to a factor of two. This is as expected given the larger fibre diameter (factor 1.4) and the absence of the image scrambler in the EGGS fibre link. It is interesting to note that the gain of EGGS versus HAM increases towards the blue, probably due to the fact that the effective seeing degrades towards the blue and the larger EGGS fibre is less affected than the smaller HAM fibre.

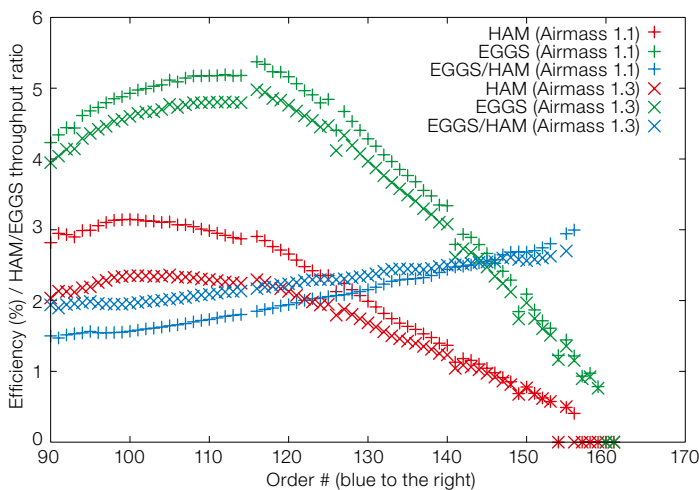


Figure 8. HAM & EGGS efficiency in % and relative EGGS/HAM throughput (on the same scale) are compared.

of fibre connectors, optical alignment and better injection optics. However, the gain had also to be demonstrated at the telescope. The efficiency was measured via observations of spectrophotometric standard stars. We collected about 20 spectra of standard stars within 2015 before, and 20 after, the intervention. The efficiency curves are shown in Figure 6 (left). The red curves are the efficiencies before the fibre link exchange, and the green curves after. The scatter is due to various atmospheric conditions, but the new curves are on average well above the old ones. From this dataset, we notice an approximately 40% average increase in efficiency at 550 nm for the new fibre link with respect to the old.

A more statistical way to demonstrate the efficiency gain, despite the short time basis, is to compare the flux of all

the stars of the HARPS Large Programme (PI: S. Udry) and the high-precision programme (PI: F. Pepe) observed before and after the upgrade. Figure 6, (right), shows the histogram of the integrated flux normalised by the stellar magnitude and the exposure time, before (red) and after (green) the upgrade. To avoid strong biases due to astroclimatic conditions, the period after the upgrade (1 June to 31 August 2015) was compared with the same period for the preceding year. The average efficiency appears to be as much as a factor of two higher. A more conservative estimate of the improvement is obtained by computing the ratio of the highest values, which should reflect the best-possible astroclimatic conditions in the two distributions. The resulting increase of 33% is consistent with that measured for the spectrophotometric standard stars, i.e., about 40%.

Effects of telescope decentring & defocus on the radial velocity

The main purpose of this upgrade was to install the new octagonal fibres to improve the scrambling of the spatial modes inside the fibres and in this way obtain a very uniform and stable light distribution at the exit of the fibre. The key performance indicator in this regard is the instrument sensitivity to de-centring. This indicator was evaluated before the upgrade by an RV drift of 3 m s^{-1} when de-centring the star by 0.5 arcseconds from the fibre centre. We repeated the same test after the upgrade and cannot detect any variation, down to the measurement uncertainty (Table 2). For each position of the star with respect to the fibre centre, we acquired three spectra and used the standard deviation (SD) of

Offset	ΔRV (m s ⁻¹)	SD(RV) (m s ⁻¹)	δRV (m s ⁻¹)
0.5" E	-0.22	1.19	0.52
0.5" W	0.05	0.90	0.42
0.5" N	0.13	1.54	0.87
0.5" S	-0.42	1.91	0.99

Table 2. Effect of de-centring on RV, measured on the star HD190248 with the HAM mode. The ΔRV s are measured with respect to the spectra acquired with the star centred on the fibre. The standard deviation (SD) over three acquired spectra is a better estimation of the RV uncertainty than the photon noise (δ), due to the intrinsic stellar RV jitter.

the measurements to express an uncertainty including the stellar jitter. The average RV offset is: $-12 \text{ cm s}^{-1} \pm 37 \text{ cm s}^{-1}$ (photon noise only, 12 data points); or $-12 \text{ cm s}^{-1} \pm 72 \text{ cm s}^{-1}$ (photon noise and stellar jitter included, 12 data points).

We have also measured RV variations with respect to changes of the telescope focus within a 0.6 mm range around its optimum position. In this case as well, RV variations are within the measurement uncertainty (the seeing was about 1 arc-second).

These are the main results achieved with this upgrade. Before, our RV precision was limited, by, among other factors, the centring of the star on the fibre. Even a small decentring of 0.05 arcseconds would give approximately a 30 cm s^{-1} effect on the RV measurement. This variation should be at least a factor ten lower, and small decentring or defocusing events, likely to happen during normal operations, will have now a negligible impact on the RV precision.

Radial velocity offset

By changing the fibres and re-adjusting the spectrograph focus, the IP of the spectrograph has changed significantly. Most of these changes are taken into account by the nightly wavelength calibration, which allows detection and correction of zero and first order effects on the radial velocity measurement introduced by a displacement or stretch of the focal plane. IP changes, however, especially if the IP is not perfectly symmetric, affect absorption and emission lines differently. An asymmetric IP may introduce a shift of the spectral line that depends on the

Star name	Spectral type	RV offset [m s ⁻¹]	Dispersion [m s ⁻¹]	CCF-FWHM [km s ⁻¹]	Mask used
HD109200	K1V	11.202	1.713	5.903	K5V
HD10700	G8.5V	15.935	1.509	6.287	G2V
HD1581	F9.5V	20.020	1.838	7.291	G2V
HD3823	G0V	17.488	2.449	7.252	G2V
HD20794	G8V	17.028	1.702	6.401	G2V
HD210918	G2V	16.145	1.622	6.858	G2V
HD26965A	K0.5V	16.732	2.017	5.927	K5V
HD177565	G6V	17.491	2.489	6.833	G2V
HD65907A	F9.5V	17.632	1.965	7.162	G2V
HD199288	G2V	14.124	1.739	6.509	G2V
HD207869	G6V	9.934	2.459	6.477	G2V
HD199604	G2V	15.916	1.946	6.643	G2V
HD210752	G0	14.371	1.745	6.665	G2V
HD55	K4.5V	15.297	2.178	6.049	K5V
Gl87	M2.5V	0.736	2.043	3.687	M2V
HD154577	K2.5V	12.061	1.782	5.773	K5V
HD131653	G5	11.088	2.123	6.181	G2V
HD134088	G0V	11.637	1.802	6.388	G2V
HD147518	G4V	12.494	2.041	6.387	G2V
HD144628	K1V	11.599	1.768	5.873	K5V
Gl588	M2.5V	-2.281	1.966	3.866	M2V

line width. For these reasons, we were expecting small RV offsets to be introduced by the new fibre link with respect to measurements prior to the upgrade.

We therefore observed a set of RV standard stars and compared their radial velocities before and after the upgrade. The results are summarised in Table 3 and show that such RV offsets indeed exist and are statistically significant. Furthermore, the offset is not a constant value for all stars. Indeed an effect due to IP changes and their interaction with the line width might be expected. This is confirmed by the data presented in Table 3, where the FWHM of the cross-correlation function (CCF) is shown together with the RV offset: the trend is for the RV offset to be smaller for narrower stellar lines. This trend implies that narrow stellar lines are affected by the IP change in a way similar to the (narrow) thorium–argon lines, such that the differential effect, and thus the RV offset, is small. For wider lines however, the differential effect is larger and thus the RV offset larger. Unfortunately the relation is not so well established, mainly because of stellar jitter and the fact that the CCF is a convolution of the stellar line width with the cross-correlation mask. The precise results depend also on the wavelength

Table 3. RV offsets measured for selected RV stable stars from various HARPS programmes. Column 4 lists the dispersion of the offset and column 5 the cross-correlation function FWHM for the particular mask used (column 6).

calibration algorithms and the data reduction in general. An in-depth study and optimisation of the wavelength calibration are underway. They are expected to lead to more quantitative results and a reduction of the observed offsets.

Prospects

A series of improvements to HARPS have been achieved with this latest upgrade: new fibre links, including new shutter systems; improved thermal stability; start of continuous operation of the vacuum pump; and vacuum-pump maintenance. The polarimetric optics have also been re-aligned to the new fibre link, and, consequent on the fibre change, we have improved the throughput and the RV precision of HARPS for both the HAM and the EGGs modes. On stellar targets a small RV offset is now observed after the change, and this offset is slightly different from star to star. We recommend users to consider the measurements before and after the upgrade as two dif-

ferent datasets, leaving an additional free parameter for the differential velocity of the two sets.

Once the laser frequency comb, which is already installed in the HARPS laboratory, becomes fully operational, we will be able to improve the wavelength calibration process significantly. As a result of these interventions, two of the most serious limitations, the illumination stability and the wavelength calibration, will have been solved. With HARPS we may then expect a long-term radial velocity precision of better than 50 cm s^{-1} and to achieve detection of a large number of super-earths in the habitable zone of Solar-type stars. Together with the upcoming Echelle SPectrograph for Rocky Exoplanet and Stable Spectroscopic Observations (ESPRESSO) instrument at the Very Large Telescope, HARPS promises to continue to be a pivotal player in

the exoplanet field, highly complementary to the upcoming space missions dedicated to extrasolar planets, such as the European Space Agency (ESA) CHaracterising ExOPlanet Satellite (CHEOPS), the US National Aeronautics and Space Administration (NASA) Transiting Exoplanet Survey Satellite (TESS) and the ESA PLANetary Transits and Oscillations of stars (PLATO).

Acknowledgements

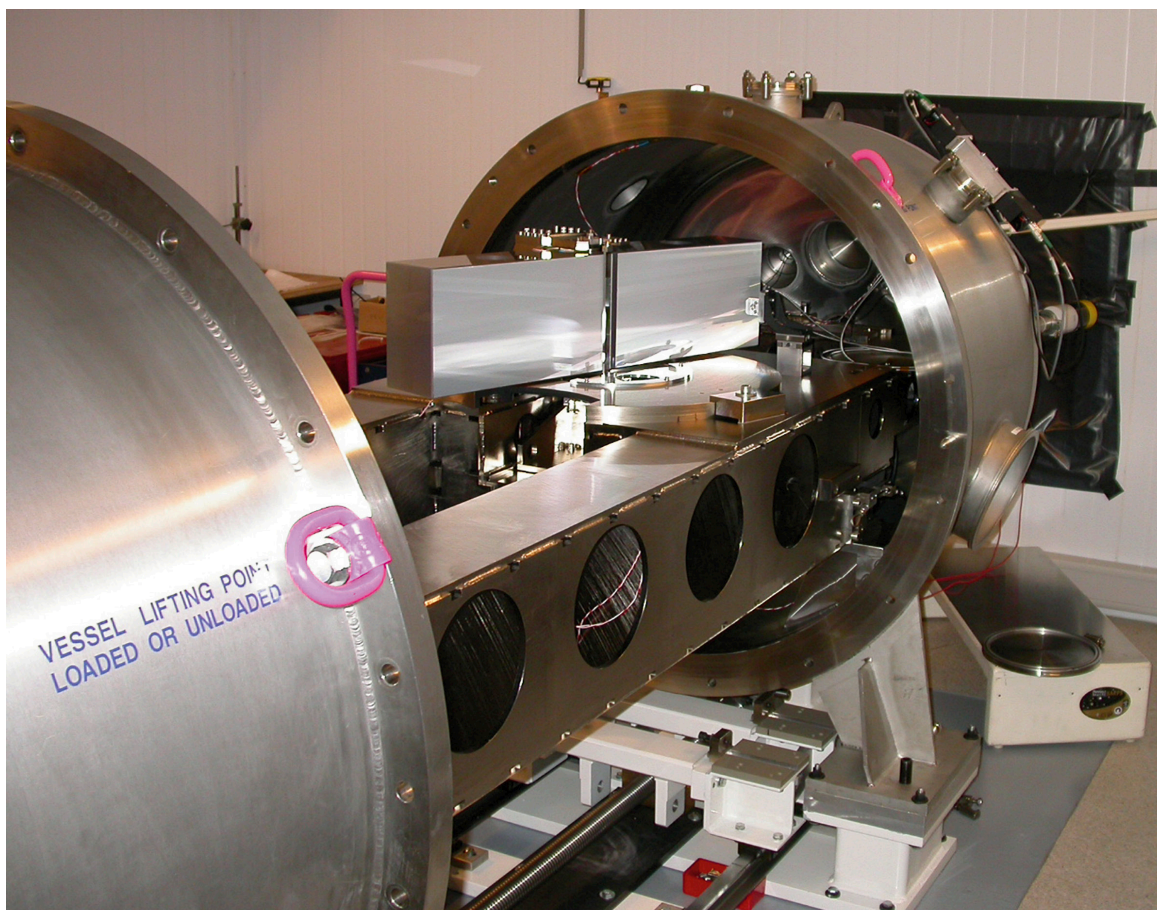
We acknowledge the enthusiastic support of the La Silla Observatory personnel and warmly thank the technical and the administrative personnel of the Geneva Observatory and everyone who contributed with enthusiasm and dedication to the success of the HARPS upgrade. Francesco Pepe acknowledges the Swiss National Science Foundation for the continuous support of this project through research grant Nr. 200020_152721. The presented work was executed under the HARPS Upgrade 2 Agreement between ESO and Geneva University.

References

- Baranne, A. et al. 1996, A&AS, 119, 373
- Bouchy, F. et al. 2013, A&A, 549, A49
- Chazelas, B. et al. 2010, Proc. SPIE, 7739E, 134
- Chazelas, B. et al. 2012, Proc. SPIE, 8450E, 13
- Cosentino, R. et al. 2012, Proc. SPIE, 8446E, 1V
- Lo Curto, G. et al. 2012, The Messenger, 149, 2
- Lo Curto, G. et al. 2010, Proc. SPIE, 7735E, 33
- Mayor, M. et al. 2003, The Messenger, 114, 20
- Pepe, F. et al. 2002, A&A, 388, 682
- Pepe, F. et al. 2002, The Messenger, 110, 9
- Perruchot, S. et al. 2011, Proc. SPIE, 8151E, 37

Notes

- ¹ A spectrograph forms a monochromatic image of the fibre tip on the detector. The fibre image defines the "slit" and thus the spectral resolution. A change of the fibre illumination would be seen as a change in the IP. If we consider that a spectral line has a width of 3 km s^{-1} at $R = 100\,000$, one understands that a small IP change can induce a line shift well above the 1 m s^{-1} precision goal.



The vacuum vessel of the High Accuracy Radial velocity Planet Searcher (HARPS) instrument open in the 3.6-metre telescope Coudé room, showing the optical bench and the diffraction grating.

VLTI: First Light for the Second Generation

Julien Woillez¹
 Frederic Gonté¹
 José Antonio Abad¹
 Sergio Abadie¹
 Roberto Abuter¹
 Matteo Accardo¹
 Margarita Acuña¹
 Jaime Alonso¹
 Luigi Andolfato¹
 Gerardo Avila¹
 Pablo José Barriga¹
 Juan Beltran¹
 Jean-Philippe Berger¹
 Carlos Bollados¹
 Pierre Bourget¹
 Roland Brast¹
 Paul Bristow¹
 Luis Caniguante¹
 Roberto Castillo¹
 Ralf Conzelmann¹
 Angela Cortes¹
 Françoise Delplancke¹
 Diego Del Valle¹
 Frederic Derie¹
 Alvaro Diaz¹
 Reinaldo Donoso¹
 Philippe Duhoux¹
 Christophe Dupuy¹
 Christian Elao¹
 Sebastian Egner¹
 Eloy Fuenteseca¹
 Ruben Fernandez²
 Daniel Gaytan¹
 Andreas Glindemann¹
 Jaime Gonzales¹
 Stephane Guisard¹
 Pierre Hagenauer¹
 Andreas Haimerl¹
 Volker Heinz¹
 Juan Pablo Henriquez¹
 Pierre van der Heyden¹
 Norbert Hubin¹
 Rodrigo Huerta¹
 Lieselotte Jochum¹
 Jean-Paul Kirchbauer¹
 Alfredo Leiva¹
 Samule Lévêque¹
 Jean-Louis Lizon¹
 Fernando Luco¹
 Pedro Mardones¹
 Angel Mellado¹
 Antoine Mérand¹
 Juan Osorio¹
 Jürgen Ott²
 Laurent Pallanca¹
 Marcus Pavez¹
 Luca Pasquini¹
 Isabelle Percheron¹
 Jean-François Pirard¹

Duc Than Phan¹
 Juan Carlos Pineda¹
 Andres Pino¹
 Sebastien Poupard¹
 Andres Ramirez¹
 Claudio Reinero¹
 Miguel Riquelme¹
 Juan Romero³
 Thomas Rivinius¹
 Chester Rojas¹
 Felix Rozas¹
 Fernando Salgado¹
 Markus Schöller¹
 Nicolas Schuhler¹
 Waldo Siclari¹
 Christian Stephan¹
 Richard Tamblay¹
 Mario Tapia¹
 Konrad Tristram¹
 Guillermo Valdes¹
 Willem-Jan de Wit¹
 Andy Wright¹
 Gerard Zins¹

¹ ESO

² redlogix, Gilching, Germany

³ MT Mecatronica SpA, Chile

The Very Large Telescope Interferometer (VLTI) stopped operation on 4 March 2015 with the objective of upgrading its infrastructure in preparation for the second generation VLTI instruments GRAVITY and MATISSE. A brief account of the eight bustling months it took our interferometer to metamorphose into its second generation, under the supervision of the VLTI Facility Project, is presented.

Decommissioning of MIDI and PRIMA and move of PIONIER

The first operation was to decommission the Mid-infrared Interferometric Instrument (MIDI), in order to make room for its replacement, the Multi AperTure mid-Infrared SpectroScopic Experiment (MATISSE; Lopez et al., 2014). One after the other, warm optics, cryostat, cooling, cabling, and control electronics were removed from the VLTI Laboratory (Figure 1). Then, following the termination of the astrometric mode of the Phase Referenced Imaging and Microarcsecond Astrometry instrument (PRIMA; van Belle

et al., 2008), its fringe sensor unit was partly dismantled, preserving just the metrology equipment for possible use in vibration metrology for the Unit Telescopes (UTs). Finally, the *H*-band instrument PIONIER (Zins et al., 2011) was moved to a new optical bench located on top of the FINITO fringe tracker (see Figure 2), this time to make room for GRAVITY (Eisenhauer et al., 2011) and its feeding optics (Figure 3). New dichroic mirrors mounted on movable periscopes were installed to pick up the *H*-band, while keeping transmission of the *K*-band to the IRIS tip-tilt sensor. With this move complete, the VLTI was verified to be operational one last time, before a more extensive and transformational shutdown.

Upgrade of the VLTI infrastructure

Over the past few years, as the next generation VLTI instruments GRAVITY and MATISSE were being developed, it became obvious that many aspects of the infrastructure of the VLTI needed to be upgraded.

Therefore in April 2015, the instruments in the VLTI Laboratory were covered with protective tarpaulins, just before beginning the major transformation. Very quickly, Paranal turned into a beehive, but not just in the VLTI Laboratory. Upgrade activities took place in many different locations: the four Coudé rooms of the UTs; the VLTI and the Combined Coudé Laboratories; and the VLTI computer room. In order to accommodate the new instruments, the

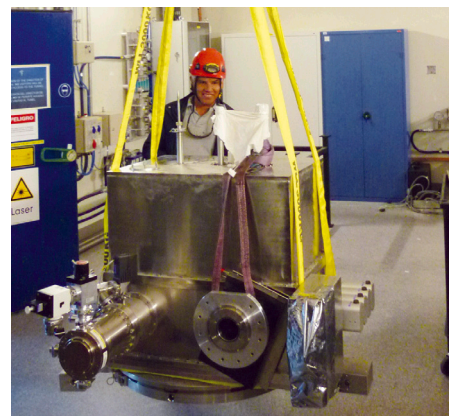


Figure 1. The MIDI cryostat is craned away from its base in the VLTI Laboratory after 12 years of productive work.

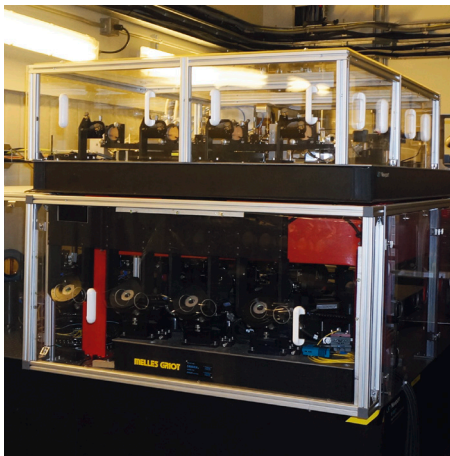


Figure 2. PIONIER, now located above FINITO in the VLTI Laboratory, is fed by four periscopes.

entire electrical, cooling, cryogenic, and network layout had to be modified. Drilling through the walls to open new cable ways, installing pipes for the new cooling system, changing the cooling pumps, feeding thick and heavy electrical cables, relocating and installing new service connection points and power distribution, all kept the teams extremely busy. See some examples in Figure 4.

The infrastructure of the inner and outer UT Coudé rooms had to be upgraded as well, to prepare the arrival of CIAO, the infrared wavefront sensors of GRAVITY. This was also the occasion to relocate

the control equipment for the newly refurbished visible wavefront sensor of the Multiple Application Adaptive Optics instrument (MACAO; Arsenault et al., 2003), and the star separators, into new cabinets.

The challenging star separator upgrade of the Auxiliary Telescopes

The GRAVITY instrument needs the star separators on the Auxiliary Telescopes (ATs) to provide the field of view required by its dual field mode (Eisenhauer et al., 2011). As such, they are the only relay optics equipped with tip-tilt metrology feeding the GRAVITY beam combiner. As a consequence of the PRIMA astrometry demonstrator, AT3 and AT4 were already equipped with star separators. They however needed to be upgraded with variable curvature mirrors, in order to relay the pupil to the entrance of the delay lines, at a distance depending on the telescope station on the platform (Figure 5).

Providing better access to the relay optics under the Auxiliary Telescopes than the old maintenance station (G2), a new maintenance station (I2) became available (Figure 5). It was envisioned to support the AT upgrade as well as their long-term maintenance, without having to send the telescopes down to base camp.

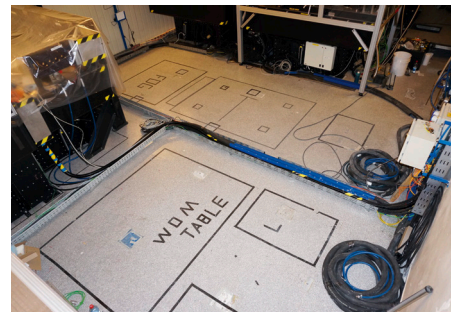


Figure 3. With MIDI removed and PIONIER relocated, the VLTI Laboratory was one step closer to receiving GRAVITY (location upper right) and MATISSE (location lower left).

Along with its control software, the variable curvature mirror upgrade on AT3 and AT4 was performed in April 2015. Then in May 2015, the upgrade of AT2 started, but very quickly appeared significantly more challenging than anticipated. Even though the opto-mechanical installation was progressing, work on the electrical front was not keeping pace, thus significantly delaying the testing of the control software and the system integration.

The need to schedule an unplanned emergency trip to Paranal to recover the electrical situation of the telescopes, combined with accumulating delays on the VLTI and the Combined Coudé Laboratories and UT Coudé rooms, forced the VLTI Facility Project to raise a red flag in June 2015. The recovery plan called for a significant increase in the number of staff involved, including the external contractors on site. Only then was it possible to complete the upgrades on AT2, and carry out the one on AT1 by the end of August 2015.

The upgrade of the Interferometer Supervisor and second light

The Interferometer Supervisory Software, the single gateway between the instru-



Figure 4. An album of work in progress for the VLTI upgrade: installation of the new false floor covering the cable trays running from the instruments (upper left); installation of a new cooling distribution system in the Combined Coudé Laboratory (upper right); integration of a more powerful pump to provide cooling for the second generation instruments (lower left); drilling of a new feedthrough between the Combined Coudé and the VLTI Laboratories (lower right).



Figure 5. Integration of a new star separator inside the relay optics structure of one of the Auxiliary Telescopes, as seen from the inside of the new maintenance station.

ments and the VLTI infrastructure, had to be adapted as well. Specifically, the objective was to make the VLTI behave like the single field interferometer it was before the upgrade, despite the installation of the star separators and its latent dual-field capability. This upgrade was successfully implemented in June and August 2015, leading to a straightforward and successful second light for the first generation instruments PIONIER and AMBER/FINITO on 23 August 2015. For observers, nothing has apparently changed. Yet, under the hood, the telescopes now point to a small offset position of the requested target, in order to avoid the edge of the star separator located at the Coudé focus. The same behaviour is planned for the UTs.

The readiness review and the re-commissioning of VLTI

On 26–28 August 2015, the upgrades of the ATs, the VLTI Laboratory, the Combined Coudé Laboratory and the UT Coudé room infrastructures were reviewed by an ESO internal board including observers from the GRAVITY, MATISSE, and ESPRESSO¹ instrument consortia. The objective was to assess the readiness for a re-opening of opera-

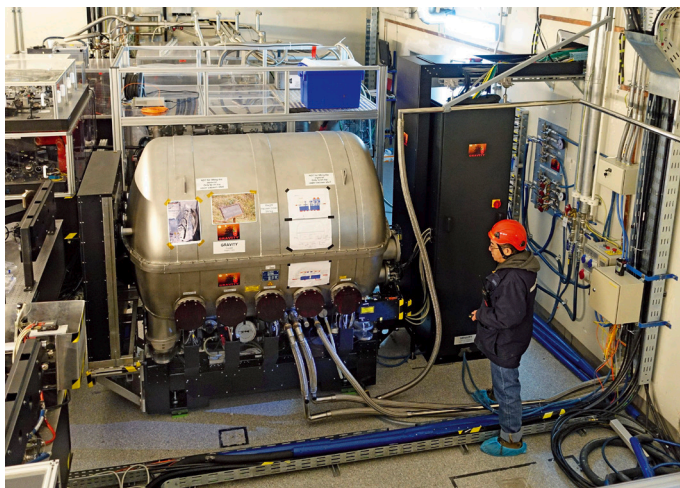


Figure 6. The GRAVITY beam combiner freshly installed in the VLTI Laboratory.

tions, and the integration of the GRAVITY beam combiner into the VLTI Laboratory. No show-stoppers were identified, although finalisation of the as-built documentation demands further attention. The month of September 2015 was used to re-commission the VLTI, verify the performance of the instruments, and open the three AT configurations (small: A0–B2–D0–C1; medium: D0–G2–J3–K0; large: A0–G1–J2–J3) planned for the operations in Period 96 (October 2015–March 2016).

The arrival of GRAVITY and the coming years

With only one month's delay on the schedule, the GRAVITY beam combiner was installed in the VLTI during October 2015 (Figure 6). The upgrade of the VLTI, especially at the level of the software interfaces, continued over this period, providing GRAVITY with the control it needs to achieve its mission. As a side effect of this installation and the presence of the consortium on the mountain, we have already received very valuable feedback on the performance of the upgraded VLTI, with a list of points to be addressed in the coming months.

Even though science operations started again in mid-November 2015, the pace of the VLTI Facility upgrades is not slowing down. The installation of star separators in the Coudé rooms of the Unit Telescopes 2 and 4 should be completed by February 2016, before the progressive arrival of the four CIAO infrared wavefront sensors in the March–September 2016

timeframe. In late 2016 – early 2017, the optics of the Coudé trains of the Auxiliary Telescopes will be replaced to improve the transmission of the VLTI imaging array. The adaptive optics instrument NAOMI (Dorn et al., 2014) will significantly improve the sensitivity, robustness, and fringe-tacking performance of the ATs by the end of 2018. All these activities will have to be carried out while GRAVITY expands its commissioning to astrometry and is made ready for observation of the S2 Galactic Centre event in 2017–2018. In the same timeframe, MATISSE will re-open the mid-infrared window of VLTI, and achieve its design sensitivity once the GRAVITY-for-MATISSE developments allow the two instruments to work together.

Without doubt, the VLTI will continue to be challenging and exciting for ESO and its community.

References

- Arsenault, R. et al. 2003, *The Messenger*, 112, 7
- Dorn, R. et al. 2014, *The Messenger*, 156, 12
- Eisenhauer, F. et al. 2011, *The Messenger*, 143, 16
- Lopez, B. et al. 2014, *The Messenger*, 157, 5
- Pepe, F. et al. 2013, *The Messenger*, 153, 6
- Van Belle, G. T. et al. 2008, *The Messenger*, 134, 6
- Zins, G. et al. 2011, *The Messenger*, 146, 12

Notes

- ¹ The Echelle SPectrograph for Rocky Exoplanet and Stable Spectroscopic Observations (ESPRESSO; Pepe et al., 2013) will be located in the Combined Coudé Laboratory and share its infrastructure with the VLTI instruments. As such, some of the infrastructure upgrades executed by the VLTI Facility Project will benefit this instrument.

The First Component of the Adaptive Optics Facility Enters Operations: The Laser Traffic Control System on Paranal

Paola Amico¹
 Paula Santos¹
 Doug Summers²
 Philippe Duhoux¹
 Robin Arsenaault¹
 Thomas Bierwirth¹
 Harald Kuntschner¹
 Pierre-Yves Madec¹
 Michael Prümml^{1,3}
 Marina Rejkuba¹

¹ ESO

² Large Binocular Telescope Observatory, Tucson, Arizona, USA

³ Informaté

The Laser Traffic Control System (LTCS) entered routine operations on 1 October 2015 at the Paranal Observatory as the first component of the Adaptive Optics Facility (AOF). LTCS allows the night operators to plan and execute the observations without having to worry about possible collisions between the AOF's powerful laser beams and other telescopes with laser-sensitive instruments. LTCS provides observers with real-time information about ongoing collisions, predictive information for possible collisions and priority resolution between telescope pairs, where at least one telescope is operating a laser. LTCS is now deployed and embedded in the observatory's operational environment, supporting high configurability of telescopes and instruments, right-of-way priority

rules and interfacing with ESO's observing tools for Service and Visitor Mode observations.

The Laser Traffic Control System of Paranal (LTCS-Paranal or LTCS hereafter) is the first (small) piece of the Adaptive Optics Facility to enter routine operations, on 1 October 2015. Its genesis dates back to the 2009 AOF Final Design Review, when the need for a laser beam avoidance tool was recognised as the best way to support operations of an observatory equipped with four powerful lasers (MLGSF — Multiple Laser Guide Star Facility) and a large number of non-laser telescopes and instruments sensitive to laser light. Every visible-light instrument sensitive to the wavelength of the Na lines (589 nm) can “see” laser light if it enters the optical path.

LTCS encompasses software tools, both developed by third parties and within ESO, which allow the night operators to plan and execute their observations without having to worry about possible collisions between the laser beam and other laser-sensitive equipment. As requested by Paranal Science Operations (SciOps), this is an early release, which

also supports PARLA laser (Lewis et al., 2014) operations, before the AOF comes online; moreover, the tool will be fully tested in routine operations and possibly further tuned to best serve the observatory during the AOF operations era.

What is a laser collision?

The collision geometry is shown in Figure 1. To quote Summers et al. (2003): “a beam collision occurs when any portion of the cone volume determined by the field of view of the (non-laser) telescope intersects with any portion of the laser beam cone defined within the Rayleigh scattering limits or sodium fluorescence limits, provided that the non-laser telescope instrument or other systems are sensitive to the laser wavelength”.

A common misconception is that, if two telescopes point to the same target, there is necessarily a collision — this is not always the case. On Paranal this is only true for the Very Large Telescope (VLT) Unit Telescope 4 (UT4) and the VLT Survey Telescope (VST) operating OmegaCAM. More importantly, collisions are possible when telescopes are pointing to different targets (see Figure 1).

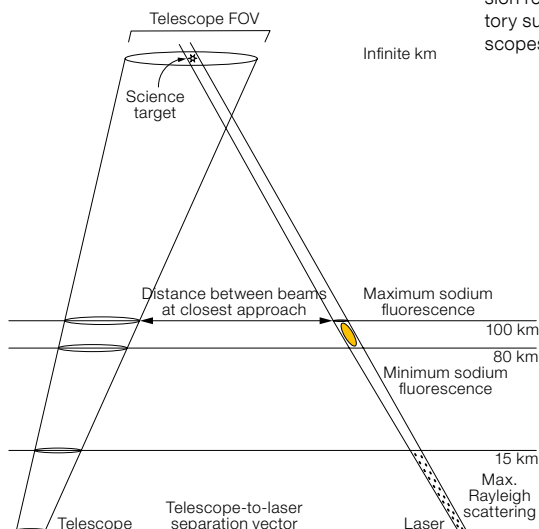
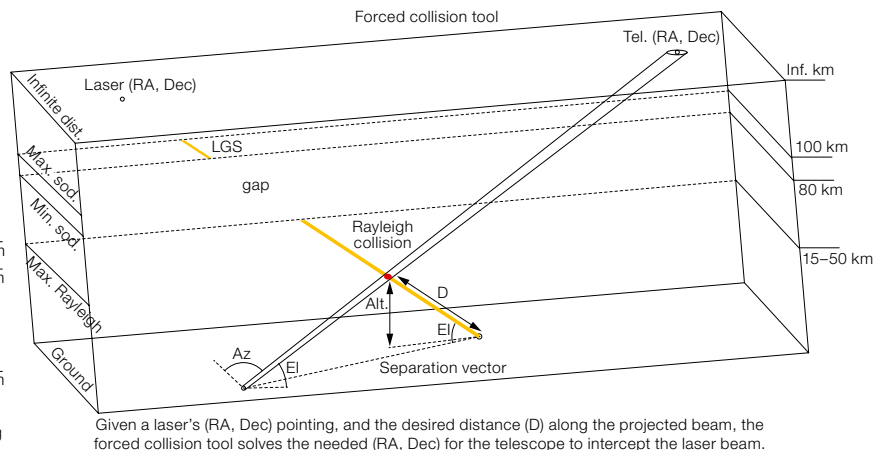


Figure 1. Left: Schematic representation of the geometry involved in the interaction between a laser and a non-laser telescope (Summers et al., 2003; 2006). The heights of the Rayleigh scattering and the sodium fluorescence limits are location-dependent parameters that were measured during the March 2014 commissioning run. The calculation of a collision requires an accurate knowledge of the observatory survey, the relative position in space of all telescopes with respect to the laser-equipped telescope



(e.g., telescope-to-laser separation vector and relative height difference between telescopes, as in the case of the VISTA–UT4 pair). Right: Schematic of the forced collision tool to calculate the Right Ascension (RA) and Declination (Dec) for a telescope to intercept the laser beam. Given the (RA, Dec) of a laser pointing and the desired distance along the projected beam (D), the tool solves the needed (RA, Dec) that intercepts the laser beam and produces a Rayleigh collision at an altitude (Alt).

Laser-light contamination can adversely affect telescope operations (Amico et al., 2010), such as guiding systems and active optics, monitoring systems and science frames. Examples of the latter, images and spectra, were obtained in the 2014 LTCS commissioning run with the PARLA laser. In the case of UT3 and the VST, they are at higher risk of collision due to their proximity to UT4 (57 and 80 metres respectively), but in general for all telescopes at the observatory, light contamination can significantly affect optical imaging and spectroscopy. Figure 2 shows an image of the Rayleigh beam as seen by the FOcal Reducer and Spectrograph (FORS2) and a spectrum taken with the 1200R grism. Figure 3 shows an image of the laser beam and spot as seen by OmegaCAM on the VST.

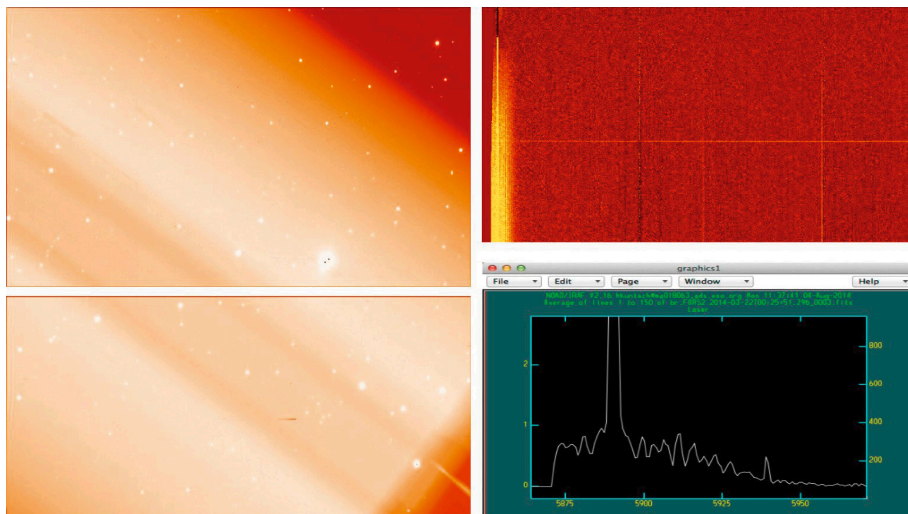


Figure 2. Left: FORS2 1-second acquisition image (chip1 and chip2) of the Rayleigh beam. The beam brightness peaks at ~ 500 counts above the sky background. Upper right: 60 s 1200R spectrum of the Rayleigh beam as seen by FORS2. Lower right: Plot of the line profile of the Rayleigh beam as observed with the FORS2 1200R grating. Assuming that the wings are symmetric, the total width is 12 nm. The average count levels of the wings are between 0 and 0.7 counts. The laser light peaks at 430 counts and the full width at half maximum of the laser line is 0.222 nm.

LTCS: Laser Traffic Control System

LTCS is a system that comprises four main components, as shown in Figure 4:

- 1) LTCS Publisher: An ESO application that provides and updates files containing the Telescope and Instrument Position Information (TIPI) for each telescope, as required by the LTCS Core process for assessing the beam collision geometry when the laser is propagating. The LTCS Publisher collects the dynamic pointing data and the telescope configuration (focus in use) in real time from the telescope databases.

- 2) LTCS Core: A third-party application, originally developed for Mauna Kea (Summers et al., 2003; 2006), composed of three executable UNIX processes and HTML/PHP displays. The source code makes use of some third party software (mySql, Apache, Log4J, PHP and SLALIB). The LTCS-Paranal version is run on ESO-standard scientific LINUX with LAMP extension. The processes are the collector, the geometric analysis engine, the status manager and web displays and have the following functions:

- a. The collector sends position updates only when the change in telescope positions is sufficient to warrant recalculation of prediction data;
- b. The geometric analysis software calculates and predicts collision events for all telescopes that are sensitive

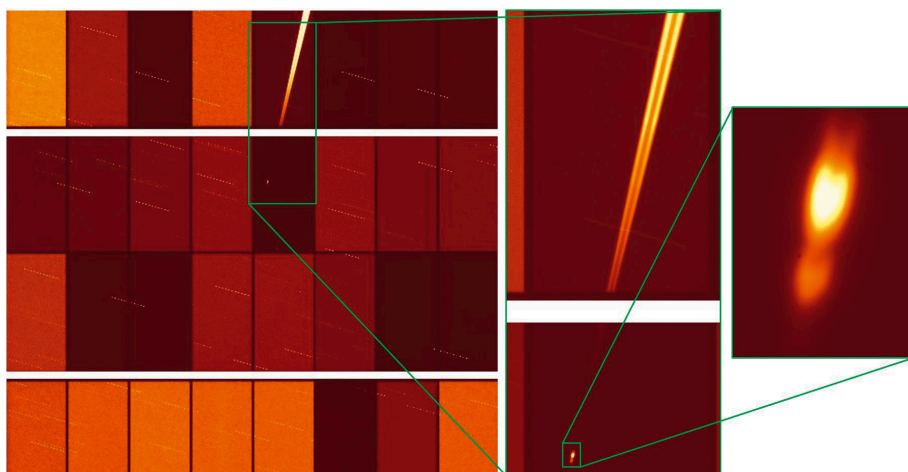
to laser emission and for all lasers that are actively propagating;

- c. The status manager and web displays provide interface to the users. The graphical user interface (GUI) is different for laser telescopes, which are provided with a full overview of the status of all other telescopes, and non-laser telescopes, which only receive information concerning their status with respect to the laser telescope(s) (see Figure 5). The GUI provides additional tools for checking the overall health of the software, for overriding parameters (such as laser sensitivity or laser status) and for manual queries.

All these processes were developed in Java with the exception of the geometric analysis engine, which was written in Java and C. The C portion is a shared library which performs a single

telescope-to-laser collision calculation using calls to the SLALIB astronomy library functions. Modifications to these processes were implemented for use at Paranal, but kept generic so that they

Figure 3. OmegaCAM 20 s image with details of the laser beam, including the Rayleigh cone and the sodium fluorescence spot. There is an increase of ≥ 2000 counts above the sky level. The test was done at zenith with no telescope tracking.



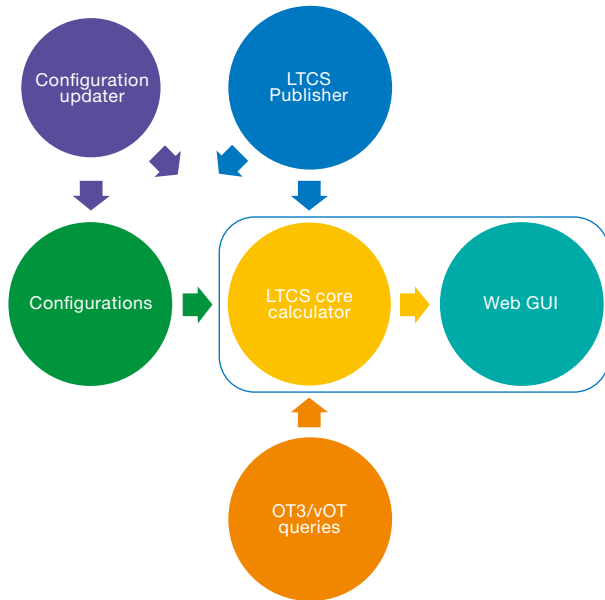


Figure 4. Schematic representation of LTCS-Paranal. Its four main components are included (see text). In addition, the configuration updater allows the user to re-configure the system and restarts the appropriate process of LTCS-Core once a configuration change is committed.

can be inserted as part of the general worldwide distribution of the package, since LTCS has been deployed to various observatories in the world after Mauna Kea (Summers et al., 2012).

3) Configurations: Files with the information regarding static data for the observatory (e.g., Auxiliary Telescope [AT] positions on the platform), environmental parameters (e.g., measured height of the Rayleigh beam at Paranal), instrument sensitivity table, and priority rules for the night (e.g., which, between laser and telescope, has the right of way in case of a collision). The latter take into account the SciOps policies for laser operations. The configuration files are modified on a need-to basis by means of VLT-software compatible scripts developed at ESO: at least once a day, during startup, but also during the night, if, for instance, the right of way changes (e.g., when a telescope switches from Service Mode [SM] to Visitor Mode [VM]). The reconfiguration is done automatically upon change of focus on a telescope, as well as the handling of both the PARLA and MLGSF lasers, which will coexist and be operated alternately on UT4.

4) Query Server + Observing Tools: External clients, such as the Observing Tool (OT) and visitor OT (vOT), can interface directly to the external query server. The query server deals with the calculation of external queries itself, instead of the core calculator; however, it accesses the LTCS database for information on dynamic pointing data.

The LTCS implementation is meant to be operated stand-alone: all processes are running in background, and no manual operation is required to update the configurations, except for setting the night-time priorities between telescope pairs (UT4 vs. non-laser telescope). The only interface to the users is through a web browser and PHP queries from OT/vOT.

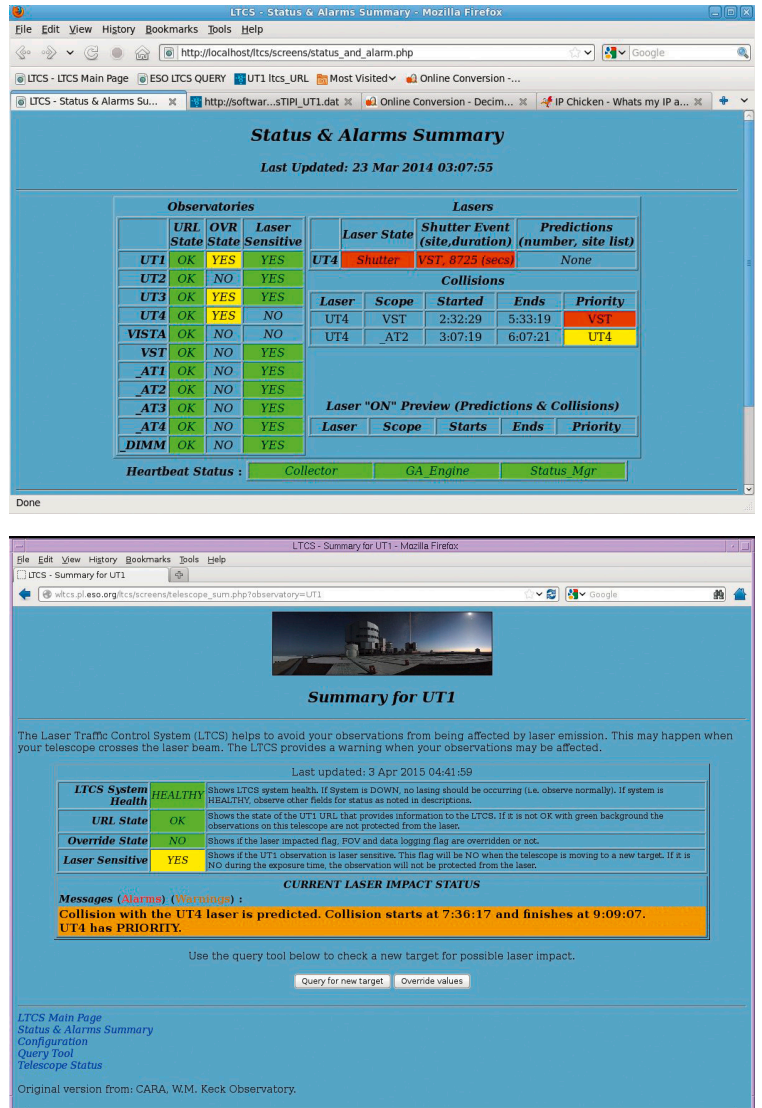


Figure 5. Upper: LTCS Main Summary panel, as seen by the laser telescope. This panel informs the operator of the status of all telescopes at the observatory and of all collisions and predictions, including priority information and all details concerning the collision, such as start time, end time, duration, plus relevant geometric parameters. Lower: Non-laser telescope (UT1) panel, as seen by the operators, provides information via written and audio messages on the real-time status. In the case shown, there is a prediction of a collision where UT1 has to yield to UT4.

OT/vOT interface to LTCS

The Observing Tool and the visitor Observing Tool are Java desktop applications used on Paranal to perform Service and Visitor Mode observations, respectively. With the OT, the operators can browse through the Observing

Blocks (OBs) in the queues and, through OT's ranking engine (ORANG), filter and sort (rank) them according to the current conditions. The OBs to be executed next are then put into an execution sequence from where they can be fetched with BOB (Broker of Observing Blocks) for observation. vOT, with very similar features to P2PP, the service mode Phase 2 Proposal Preparation tool, also interfaces with BOB and is mainly used by the visiting astronomers to create and execute their OBs.

The AOF project brought new requirements to OT and vOT: adding laser collision detection features to facilitate the short-term observation planning; and informing the users of any laser collisions before starting an observation in a what-if scenario (e.g., what if I started this observation now, would there be any laser collisions?).

To fulfil this requirement, these tools now interface with LTCS, asking this question through an HTTP get request that includes the telescope, the target's coordinates and equinox, the instrument field of view and the laser state on sky. As a reply, LTCS sends a list of ongoing/future collisions, including the colliding telescope pair, the start/end of collision and the telescope with priority — or "none" if there are no collisions.

In OT, this check is done on the OBs in the execution sequence, either on demand, by pressing a collision check button, or automatically at a specified frequency. Most importantly, given the dynamic nature of the Observatory, a check is automatically performed whenever the user fetches an OB for execution. If collisions or predictions are detected, the OT requests confirmation to proceed. In the execution sequence, the OBs are highlighted according to their collision status: green (no collision), orange (predicted collision), red (collision now), grey (unknown) and white (unchecked). Collision details are displayed upon selection of the OB (Figure 6).

In the vOT, the user can also check for collisions on demand, by selecting the OBs and pressing the collision check button. Once the check is done, vOT displays a report with basic collision infor-

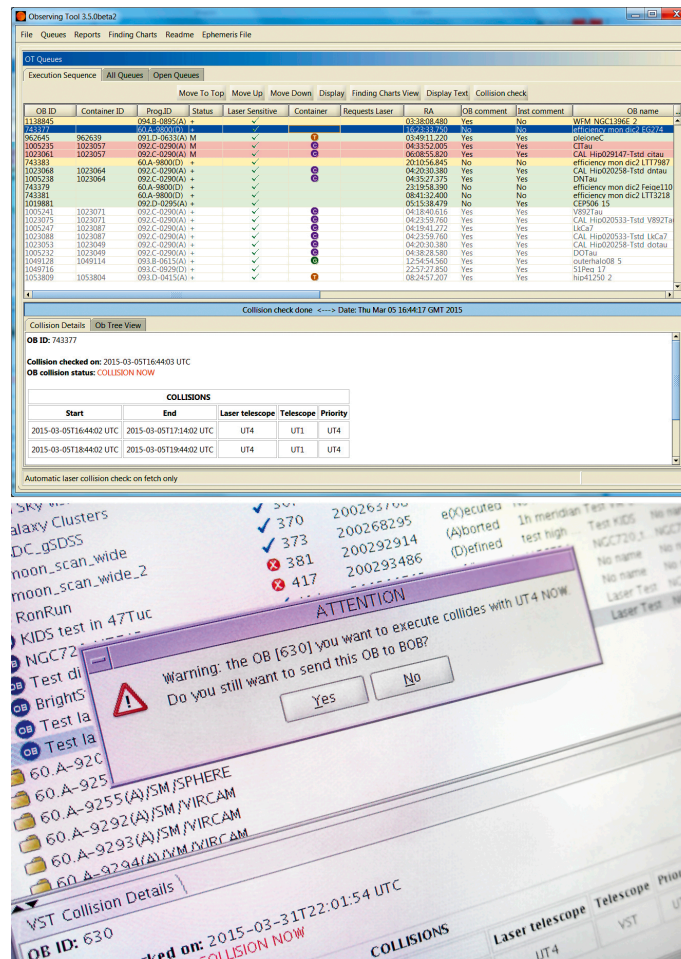


Figure 6. Upper: Snapshot of OT execution sequence as tested in March 2015. The colour-coding informs the operators of the possibility of collision if the OBs were executed right away. The semaphore logic applies in all cases: green means no collision; yellow means prediction of a collision; red means collision; grey means the collision status is unknown; and white means no checks were performed. The tool deals with all possible aspects of operations, including flagging equally OBs in a concatenation, dealing with multiple telescope queries for VLTI, etc. Lower: Photo of a monitor in the Paranal Control Room showing vOT after an OB was fetched for execution. A dialogue is presented to the user, informing that a collision will happen if the selected OB is started and requesting confirmation before proceeding.

mation — further collision details are displayed once the report is closed. Again, an automatic collision check is triggered on fetching an OB.

For the VLTI, both tools include an option to select the baseline: all ATs, all UTs or all UTs + ATs. The collision check is performed for all telescopes included in that baseline, and it is the operator's task to analyse the result and understand if the reported collisions present an impediment, depending on which telescopes are effectively being used for each VLTI observation.

Since the observing tools have access to the full OB setup, they can evaluate whether or not an OB is laser sensitive. Information on which setups are sensitive is read from the instrument configuration files in the Instrument Packages. If an OB is not laser sensitive, no checks need to be done with respect to UT4 (laser tele-

scope) — these OBs are therefore shown as green. Nevertheless, there is an option to force the collision check, which is useful when using a different setup other than that specified in the OB (e.g., visitor filters), or manually edit it in BOB. In the same fashion, when starting an OB from UT4, a check for possible collisions with observations on other telescopes is only done if UT4 uses the laser guide star.

The first versions to include these features were OT3.5.0 and vOT3.4.0, deployed and tested at the Observatory in integration with LTCS during the March 2015 mission to Paranal. These versions have been in use since 1 October 2015.

Operations

LTCS+OT/vOT form together a user-friendly system that supports nighttime operations with the laser. Both the real-

time operations and the what-if scenarios are supported by the LTCS GUIs (Figure 5) and the OT/vOT interfaces (Figure 6). In real time, LTCS calculates whether the geometry of the pointing of each telescope pair formed by UT4 + laser-sensitive telescope + instrument generates a collision or a prediction. Contamination from indirect laser stray light cannot be taken into account. In the what-if scenarios, LTCS is used as a predictive tool.

The tools do not replace human intervention, since the final decision to act (e.g., shutter the laser) on a collision or a prediction event is in the UT4 operator's hands. It is expected that nighttime operators will negotiate in all those cases where the collision cannot be avoided and the application of the rules, as indicated by the tools, is not efficient: for instance, in all those cases when the yielding telescope has little time left to observe and it is expected to move soon from that patch in the sky.

The tools are designed to support both SM and VM operations. The visitors, who typically have higher priority observations than SM, will be able to plan their night following the real-time recommendations of the tool. This is especially useful when more than one visitor, one on UT4 and another on a laser-sensitive instrument elsewhere, are on the mountain together.

Future developments

LTCS has been designed with the future in mind: not only the onset of AOF operations with MLGSF, but also the case of multiple laser-telescopes, e.g., when the E-ELT comes to the observatory. LTCS can be easily configured to add or remove telescopes from the observatory survey and to redefine laser sensitivity.

Additional upgrades have been discussed with SciOps colleagues, the main users of the tools, and include:

- A first upgrade already planned for April next year, when a new version of LTCS will offer automatic nighttime reload of configuration changes, such as an OB priority change or laser constellation changes.
- LTCS configuration scripts will be modified to support all the different AOF constellation setups, to provide better collision calculations in all specific cases, including that of ERIS, the new AOF instrument foreseen for the Cassegrain focus of UT4, which has the option to use one out of the four available lasers.
- Third-party software will be fully integrated within the VLT software release (VLTSW2015) with 64-bit support, so that LTCS becomes a fully VLTSW-compliant subsystem.
- New versions of the OT and vOT also aim to support further laser-equipped telescopes on site. In such a scenario, UT4 would not only act as a laser propagator, but also as a laser-impacted telescope. After the tests carried out at Paranal, we realised that some minor

changes are still required to fully cover this scenario.

- To support the AOF, the OT and vOT will have to be modified to allow queries for all the different laser constellations.
- Lastly, the significantly different laser setup of ERIS may present some restrictions to our current assumptions and will be a topic for future discussion.

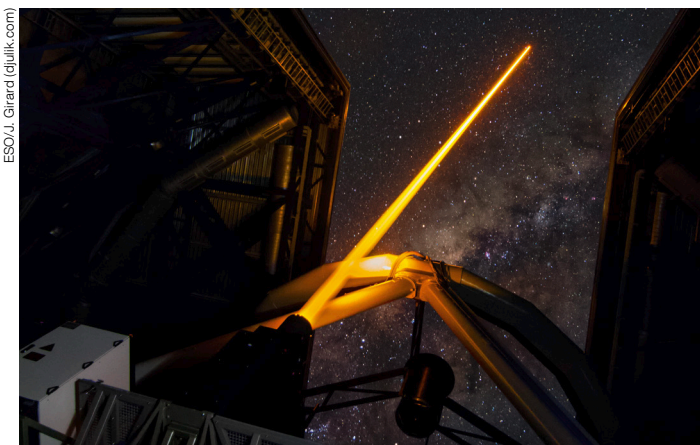
As of today, the observing tools can fully support laser collision detection with PARLA, providing a good trial period for users to become acquainted with the changes in the workflow and an opportunity to provide feedback. New versions of LTCS, to be deployed in the near future before the MLGSF starts operations, will include support for the missing functionalities mentioned above.

Acknowledgements

LTCS-Paranal, including the update of the observing tools, was developed and commissioned thanks to the help of many contributors: the original LTCS-Mauna Kea software was courteously made available to us by the Keck Observatory; the SciOps staff, in particular S. Brilliant, A. Smette, S. Cerda, and all the operators who worked with us during the commissioning runs; M. Pasquato, who led general OT testing and support; and last but not least, the ESO Laser and Photonics group, without whose "annoying" lasers this project would not exist.

References

- Amico, P. et al. 2010, SPIE Proc., 7737-10
 Lewis, S. et al. 2014, The Messenger, 155, 6
 Summers, D. et al. 2003, SPIE Proc., 4839-57
 Summers, D. et al. 2006, SPIE Proc., 6272
 Summers, D. et al. 2012, SPIE Proc., 88474S-1, 2012



First light of the 4 Laser Guide Star Facility (4LGSF) on Unit Telescope 4 occurred in April 2015. See Announcement eso15034 for more details.

ESO/J. Girard (djulik.com)

The European ALMA Regional Centre Network: A Geographically Distributed User Support Model

Evanthia Hatziminaoglou¹
 Martin Zwaan¹
 Paola Andreani¹
 Miroslav Barta²
 Frank Bertoldi³
 Jan Brand⁴
 Frédérique Gueth⁵
 Michiel Hogerheijde⁶
 Matthias Maercker⁷
 Marcella Massardi⁴
 Stefanie Muehle³
 Thomas Muxlow⁸
 Anita Richards⁸
 Peter Schilke⁹
 Remo Tilanus⁶
 Wouter Vlemmings⁷
 José Afonso¹⁰
 Hugo Messias¹⁰

¹ ESO

² Astronomical Institute of the Czech Academy of Sciences, Ondřejov, Czech Republic

³ Argelander-Institut für Astronomie, University of Bonn, Germany

⁴ INAF-Osservatorio di Radioastronomia, Bologna, Italy

⁵ Institut de Radio Astronomie Millimétrique (IRAM), Grenoble, France

⁶ University of Leiden, the Netherlands

⁷ Onsala Space Observatory, Chalmers University of Technology, Sweden

⁸ Jodrell Bank Centre for Astrophysics (JBCA), University of Manchester, United Kingdom

⁹ I. Physikalisches Institut, Universität zu Köln, Germany

¹⁰ Institute for Astrophysics and Space Science, Lisbon, Portugal

In recent years there has been a paradigm shift from centralised to geographically distributed resources. Individual entities are no longer able to host or afford the necessary expertise in-house, and, as a consequence, society increasingly relies on widespread collaborations. Although such collaborations are now the norm for scientific projects, more technical structures providing support to a distributed scientific community without direct financial or other material benefits are scarce. The network of European ALMA Regional Centre (ARC) nodes is an example of such an internationally distributed user support network. It is an

European ARC nodes

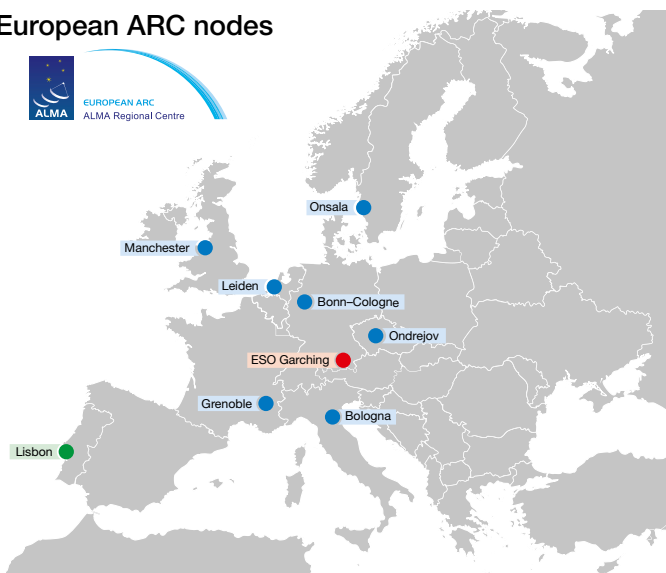


Figure 1. The locations of all the European ARC nodes are shown on a map of Europe and including the Centre of Expertise in Lisbon.

organised effort to provide the European ALMA user community with uniform expert support to enable optimal usage and scientific output of the ALMA facility. The network model for the European ARC nodes is described in terms of its organisation, communication strategies and user support.

The European ARC

A fundamental concept within the Atacama Large Millimeter/submillimeter Array (ALMA) operations model is that direct ALMA user support is not provided by the Joint ALMA Observatory¹, but by the ALMA Regional Centres. These are set up in East Asia (serving Japan and Taiwan), North America (USA, Canada) and Europe. Taiwanese users can choose to receive support from either the East Asian or North American nodes. These ARCs deliver a comprehensive ensemble of user services, ranging from general user support, helping astronomers to develop their scientific goals, all the way to assisting users with optimising data reduction and getting the most out of their ALMA observing project. Each executive (ESO, NAOJ², NRAO³) has some freedom in setting up their ARC, as long as the services agreed by all three parties are delivered.

At an early ALMA Community Day in Garching in 2002 (Shaver & van Dishoeck, 2002), the attendees voted for a European

ARC model with a central, coordinating node at ESO and a number of smaller nodes in the community. The ESO Scientific Technical Committee (STC) and ESO Council approved a Call for Statements of Interest to establish local ARC nodes, which was sent out in 2004, and resulted in responses from six institutes in Europe. The initial model of the European ARC was described in Andreani & Zwaan (2006). A Memorandum of Understanding between ESO and the six ARC nodes was signed in 2008, marking the official start of the European (EU) ARC network.

Today, in 2015, the EU ARC network still operates with the same six founding members: Italian (located in Bologna), German (in Bonn/Cologne), IRAM (in Grenoble), Dutch (Allegro; in Leiden), British (in Manchester) and Nordic countries (based in Onsala). In addition, an ARC node in Ondrejov (Czech Republic) was created in 2009. The most recent extension of the European ARC network is the Portuguese Centre of Expertise (CoE), which has been operating in Lisbon since early summer 2014. A CoE is a temporary status through which potential new nodes may have to transition while they build up the required expertise and user base. Figure 1 shows the geographical distribution of these nodes and the CoE.

For convenience, the nodes are named after the communities that they primarily serve. They also serve users from outside

these communities who do not have a “local” node, or simply wish to take advantage of the expertise and experience available at a particular node. Each node has the mandate to primarily serve their local community. The staff at each ARC node are scientists covering a range of expertise in interferometry, (sub-)millimetre observing and ALMA data reduction and interpretation. The ARC nodes are based at locations in Europe that have a long history in radio and/or millimetre observing and data analysis. The ARC network therefore makes optimal use of the immense knowledge and expertise that exists in Europe, without having to build this up at ESO alone.

The central node, usually referred to as “the ARC”, is located at ESO Headquarters in Garching. The ARC is set up as a department within the European ALMA Support Centre (EASC), a cross-divisional structure within ESO, which, in addition to the ARC, also houses the ALMA Technical Support Group, the ALMA Science Programme and ALMA Outreach.

ARC network management and coordination concepts

An interesting question to consider is why the European ARC network functions, if there are no contractual obligations between ESO or ALMA and the ARC nodes. ESO plays a managing and coordinating role, but the ARC nodes are autonomous in the way they set up their local structures. They have complete freedom over the number of staff they hire, the expertise areas on which they wish to concentrate, and so on. Furthermore, ESO does not provide financial support for the ARC nodes. The ARC nodes seek their own funding through a range of national schemes. Therefore, funding horizons may vary from one to five years between the different nodes.

Rather than having formal or legal agreements, the ARC network partnership is based on the Memorandum of Understanding, but above all on trust and collegiality. This collaboration, that at first sight may seem vulnerable, functions well because of its symbiotic nature: through the ARC nodes ESO is able to



Figure 2. Many of the staff of the nodes of the European ARC pictured during the most recent all-hands meeting in Smögen, Sweden, 28–30 September 2015.

provide the European ALMA users with services that far exceed what would have been possible without the network, while the ARC nodes are able to build up expertise in ALMA operations and technical developments and secure funding for their institutes.

Coordinating and managing the ARC network requires a dedicated effort from ESO and each of the ARC nodes. Three ESO astronomers are tasked with bringing the diverse elements of the complex ARC structure into one efficient working model, referred to as the EU ARC manager, liaison and coordinator. The European ARC manager is responsible for the successful operation of the European ARC. The ARC manager is also member of the ALMA Science Operations Team and the EASC management team, and has a number of different roles, including being responsible for running the ARC at ESO. In addition, the ARC manager provides a crucial link between the ALMA Director’s Office and ESO Management, and is directly accountable to the ALMA Director for Board-approved operational deliverables. The ARC node liaison is responsible for matters related to the nodes, and oversees the provision of support and overall coordination, working closely with the ARC manager. Finally, the ARC node coordinator acts as the contact person for all ARC staff, and is responsible for maintaining communica-

This team of three people is referred to as the ARC network management team and together they are responsible for the

smooth functioning of the ARC network. In addition to this team, at each of the ARC nodes one representative is responsible for the communication with the network and the local coordination of their node. The ARC node representatives, together with the ARC network management team, are collectively referred to as the ARC Coordinating Committee, or ACC. Important decisions within the ARC network are taken by the ACC through consensus decision-making.

Communication scheme at the heart of a uniform user experience

The dispersal of ALMA user support in Europe to a number of geographically separated institutions (Figure 1) often makes it a challenge to ensure the dissemination of information in a steady and effective way. In addition, the geographical separation of the ARC nodes from the ALMA Observatory implies that activities in the European ARC nodes run the risk of not being optimally aligned with ALMA developments carried out elsewhere, or that the nodes might feel detached from the observatory, and not an integral part of the ALMA project. Information flow in all relevant directions is therefore essential and, in turn, results in a high level of homogeneous user support across the network, while satisfying the specific needs of the local communities.

A number of interfaces between the ARC at ESO and the nodes are in place to enable and promote communication. The ARC TWiki, hosted and maintained by ESO, is a document repository and a means to homogeneously disseminate and store information within the network. All European ARC staff have access to it. Monthly telecons/videocons, organised and chaired by ESO and attended by the ACC, facilitate dialogue and coordination among the nodes, keep people up to speed with the latest ALMA developments and network news, and help to identify and rapidly react to any problems.

Face-to-face meetings are still the most effective ways of communicating and diffusing information. Once a year an “all-hands” meeting, open to all European ARC staff, is organised and the venue rotates through each of the nodes and ESO. This year’s meeting was held in Sweden (see Figure 2). This is a superb opportunity to go through the ARC activities over the past year, discuss ALMA operations in general and plan for the future. In a geographically dispersed network these yearly meetings are essential. ARC staff are informed of the latest ALMA news and developments and get a chance to discuss issues and concerns openly or in smaller groups. But most importantly, staff get to know each other and strengthen working relationships that could otherwise remain formal and impersonal due to the distance.

A second type of yearly face-to-face meeting takes place among ACC members, including the ARC network

management team, with the participation of one additional member from each ARC node. The purpose of the meeting is to discuss high-level operational requirements, issues that touch upon the ARC network organisation and communication with the ALMA project, and the short- and medium-term evolution of the network and its functions. The venue of this meeting also rotates among the various nodes and ESO. The ARC network management team also visits the nodes at a frequency set by the individual needs of each node. This gives all the involved parties the opportunity to concentrate on the services provided by each of them, to discuss whether they are satisfied with the current arrangements and to establish whether any improvements could be made. Finally, European ARC staff regularly meet during ALMA training and scientific events as well as on a number of other formal or informal occasions.

Information related to the use of the ALMA facility has to be shared with the scientific community. The European ARC webpages⁴ contain high-level information regarding the activities and services of the network as well as links to the local web pages of the nodes, and is a good starting point for users seeking specific information regarding the network. The central point of contact for all ALMA users is the ALMA Helpdesk⁵, which is available to all registered users from the ALMA Science Portal⁶ in one uniform users’ view. There is one Helpdesk for all global ALMA users, but queries from European users are automatically directed to and addressed by

the European ARC. As part of the common user experience, the ALMA Science Portal also shares one unified view for all users across the globe, but has three mirror sites, and users are automatically redirected according to the location from which they are connecting. The only difference between the three ARC mirror sites is the column hosting the Local News, specific to each ARC. Important ALMA information also reaches the European ALMA users via their regional node newsletters, as well as via the newly established European ARC newsletter, which will be issued every three months.

The experience after seven years of ARC network collaboration, backed up by research into the performance of geographically dispersed teams (Huang, 2012), shows that communication is often the Achilles heel of the collaboration: team members simply cannot interact as easily as in a centralised team. Good communication is therefore essential in keeping a distributed network functional. It should have low thresholds, should use all media and formats that people find convenient (telephone, video connections, face-to-face meetings), and must be regular.

The European ARC user support model

The staff at ESO and the ARC nodes work together to provide optimal support to users during the complete lifetime of a project, from proposal preparation, through the creation of the scheduling blocks (SBs), to delivery of the calibrated



science products to the users, and, if required, to additional data reduction support. Personalised face-to-face support is the biggest success of the European ARC network and the *raison d'être* of the ARC nodes. In what follows we describe this model in more detail.

Users with newly approved observing projects are notified by email and assigned to an ARC Contact Scientist (CS), usually from the local ARC node. The ARC CS works with the PI and the Phase II team at ESO to create the SBs. The PI is notified when the SBs are ready for approval and the CS draws their attention to (and, if necessary, explains) any significant issues so that the PI can check and finally approve the SBs. Once all Phase II material is approved by the PI and technically validated, it is submitted to the ALMA Archive ready for scheduling and eventual execution. PIs can then monitor the progress of their projects in terms of observations and data reduction via dedicated tools.

After the successful execution of the project and subsequent data delivery, the PI can ask for face-to-face support for regular or advanced data reduction. Face-to-face support can also be requested for the purposes of proposal preparation or archival research. A complete, synchronised mirror of the ALMA Archive is kept at ESO⁷, and is a valuable resource for data mining. ALMA datacubes are particularly complex and the scientific information which they carry can be used for scientific goals other than the ones in the original proposal. In

order to ensure that the archive as well as ALMA itself are exploited to their full potential, the nodes also provide support for users wishing to carry out archival research.

Requests for face-to-face support are usually received via the ALMA Helpdesk. Requests made directly to the nodes are likewise transmitted to the Helpdesk. Once a node is made aware of a visit request, support staff at this node are responsible for arranging the details of the visit. Visits are usually made to a user's regional node as national funding bodies expect this. However, if a certain area of expertise is required, a visit to a node other than the local node can be arranged, if this will provide the user with the best possible support. Each visitor is assigned a single member of staff at that ARC node for all aspects of support.

After a visit, the user is encouraged to submit (anonymously, if so desired) feedback via a web form. Feedback is also required from the node support staff in order to discuss any technical aspects of the support or successful data reduction of technically challenging projects that other nodes might encounter in the future. At the time of writing, 89 formal face-to-face requests have been recorded in the Helpdesk from Cycle 0 to Cycle 2, with the majority asking for support with data reduction. This number does not include less formal visits involving users at close proximity to a node, who meet with ARC node staff in order to get extra help with their data interpretation, future proposals, etc.

Diversity: A strength within a weakness

To all intents and purposes, the network for the European ARC nodes already operates as a virtual organisation (Travica, 1997) obeying two structural conditions: geographical dispersion of the organisational units (nodes) and the use of information technology to support work and communications. A virtual organisation resembles a traditional organisation in its inputs and outputs. It differs in the way in which it adds value during the journey between these inputs and outputs (Economist, 2009). The coordination of such a structure implies an understanding of the cultural and interpersonal differences, and its successful operation relies on smooth communications, a common aim and a shared sense of responsibility, all the while respecting the distinctiveness of each individual organisational unit. Subsequently, the challenges such a structure faces are many, starting from establishing a seamless information flow, to ensuring that all decisions are understood and executed in exactly the same manner by all parties involved, as well as building a common sense of purpose, sharing risks and responsibilities and finally jointly enjoying and benefitting from a successful outcome.

The weakness as well as the strength of the ARC network lies in its heterogeneous structure: nodes have different organisations, funding schemes, community size and expertise, and — perhaps

Figure 3. A panoramic view of ALMA antennas on the Chajnantor Plateau.



more importantly — mandates from their funding agencies. This means that they constantly have to keep a balance among, sometimes conflicting, requirements coming from their users, funding bodies, the ARC network and the ALMA project itself. At the same time, such differences foster the development of new ideas and new concepts of user support, impose flexibility, and broaden the scope of the network.

In order to keep the ARC network a lively entity, with the flexibility to respond to external factors, such as varying funding situations, changing user needs, and unplanned tasks, it is necessary to identify a number of items that are crucial for the ARC network to maintain:

Face-to-face user support. In this area, the European ARC is unique in that many more users in Europe make use of this service compared to the other executives, and the service is valued extremely highly, as shown by feedback⁸. A distributed support network that is geographically close to the users and makes optimal use of the large body of millimetre/submillimetre interferometric expertise in Europe implies a clear competitive advantage for European astronomers.

Unique scientific or technical expertise. Within the European ARC network there are several expertise areas that are unique within the ALMA project, including Solar observation, polarimetry, high frequency and long-baseline phase correction and array combination. European ARC nodes have contributed particularly extensively to ALMA commissioning in these areas, and are in an ideal position to provide optimal specialised user support.

Enhanced services. The European ARC network has a long tradition of providing software packages to ALMA and to the user community. These range from packages that assist the Observatory (e.g., the data packager or the water vapour radiometer correction software), to user support and science analysis software, such as radiative transfer codes.

General ALMA development. To maintain its role as a premier observational facility



in the coming decades, ALMA maintains a healthy long-term development programme. Advanced observing modes and capabilities are rolled into the array operational environment to respond to the evolving challenges of astrophysical research. Some examples from the early years of ALMA development are the new Band 5 receivers and millimetre-wave very long baseline interferometry (VLBI) capabilities. Many of the ARC nodes are involved in the development of new ALMA capabilities, their implementation at the observatory and the future user support needs.

The network for the ARC nodes closely coordinates the development of these areas of expertise to ensure global coverage, avoid overlap and stimulate inter-node collaborations.

The evolution of the ARC network

The ARC nodes have been a great asset in attracting young people who aspire to get close to the operational side of the ALMA project and pursue a career in science. Staff at ARC nodes are scientists who are trained in operating the facility, understand its technical aspects, gain valuable technical skills and provide user support to facilitate the best science return from the facility. However, one of the most challenging issues that the network continually faces is to retain the expertise acquired over the years, as about half of the people in the network are on fixed-term contracts. Having to import expertise is a healthy way of renewing the “population” of the network. It does however require a robust training scheme that ensures skill transfer among both staff and nodes, on timescales that

Figure 4. The view out of the ALMA Array Operations Site (AOS) Technical Building, that houses the ALMA correlator.

do not interfere with the smooth functioning of the network and the services provided. To this aim, training workshops are regularly organised inside the network, covering both procedural (e.g., Contact Scientist training) and operational (e.g., data reduction, use of calibration pipeline, etc.) skills.

As ALMA observations become more standardised, and experience in the community with ALMA data grows, user support at the nodes will shift from direct assistance with technical and/or practical aspects, to pushing the ALMA capabilities to the limit, by supporting large, data-intensive projects and enabling advanced scientific analysis. User support provided by the ARC nodes may, therefore, progressively acquire a more science-oriented character, while maintaining the basic support necessary to new users or use of new ALMA capabilities. To accommodate the needs of an increasingly demanding ALMA user community, the ARC nodes work towards strengthening their areas of expertise, such as polarimetry, (millimetre-wave) VLBI, Solar observations, or the enhancements of synergies between ALMA and the other facilities that each of the ARC nodes is actively supporting.

Furthermore, driven by the needs of their communities, already established mandates or the requests from their funding agencies, some ARC nodes already act as, or are developing towards, general support centres. Such centres provide support for a multitude of instruments and facilities operating in the (sub)millimetre and radio regimes, maximising the

synergies between ALMA and various other (European and non-European) facilities.

The European ARC network is an ever-evolving structure, due to both its organisation and the nature of the support it is providing. It is therefore not only the expertise and type of support that may change, but the number of nodes may evolve with time, as well. New nodes (or CoEs) may join the network just as old nodes might leave as a result of the changing needs of the user base or decisions by the funding agencies.

Concluding remarks

In January 2015, the ARC network was reviewed by an external committee. Receiving an independent assessment of the key aspects of the network turned out to be an extremely useful exercise. It clearly brought up the strengths of the network and the reasons behind the network's success. At the same time, it motivated an honest discussion on its vulnerabilities that has helped to establish a course of action that takes into account the evolving needs of both the network and the European ALMA user community.

Undoubtedly, the reasons behind the continuing success of the network are the mutual benefits: the nodes have become an integral part of the ALMA project, they enhance their expertise and provide a service greatly appreciated by their communities and their funding agencies. While ALMA has been extensively advertised through well-organised community events, users appreciate direct help from well-known experts close to their home institutes. At the same time, the European ARC gains from the large pool of expert staff working at the nodes, securing user support at a level that would have been impossible without them. ARC node staff are also actively using the facility in order to pursue their own scientific and technical interests. In addition to enhancing their expertise, this connection increases their motivation and involvement and makes them effective ambassadors of the ALMA project.

In order to ensure the continuation of the seamless functioning of the network,



ALMA (ESO/NAO/JRAO), C. Padilla

efforts have to be made towards maintaining the goodwill that has developed, primarily as a result of the good communications, and also in securing the recognition of the skills and the professionalism of the ARC node staff, and their subsequent level of engagement. A good way to maintain the latter is by establishing their high level of involvement in the commissioning efforts of new capabilities, thus bringing visibility as well as added knowledge.

Flexibility is an essential quality of the network. The quick reaction of the ARC network to the huge workload brought about by the, originally unaccounted, demand for quality assurance is an example demonstrating that the network is flexible enough to deal with complications when they arise. However, nothing should be taken for granted, given the differences in the organisational and funding schemes behind each individual node. The balance that the network has achieved to date needs to be maintained. The ARC at ESO has neither the duty nor the wish to control the detailed management of the nodes. The nodes will continue to contribute the amount of effort that is beneficial to them, taking into account their own needs and those of the community that they support. Ultimately, the capacity of the network to develop and deliver in the long term will critically depend on its ability to function as a single distributed team.

Figure 5. A view across the Chajnantor Plateau.

Acknowledgements

This project requires a huge amount of work and dedication. Its implementation and continuous success would not have been possible without the hard work of all former and present members of the European ARC network. We also thank the different funding agencies that support the individual ARC nodes, and together make the existence of this network possible.

References

- Andreani, P. & Zwaan, M. 2006, *The Messenger*, 126, 43
- 2009, *The virtual organisation*, *Economist*, online edition, 23 November
- Huang, L. 2012, *Mitigating the negative effects of geographically dispersed teams*, (Irvine: University of California)
- Shaver, P. & van Dishoeck, E. 2002, *The Messenger*, 110, 44
- Travica, B. 1997, in Gupta, J. N. D., *Association for Information Systems, Proc. American Conference on Information Systems*, Indianapolis, 417

Links

- ¹ Joint ALMA Observatory: <http://www.almaobservatory.org>
- ² National Astronomical Observatory Japan: <http://www.nao.ac.jp/en/>
- ³ US National Radio Astronomy Observatory: <http://nrao.edu/>
- ⁴ European ARC web pages: <http://www.eso.org/sci/facilities/alma/arc.html>
- ⁵ ALMA helpdesk: <http://help.almascience.org>
- ⁶ ALMA Science Portal: <http://www.almascience.org>
- ⁷ ALMA archive at ESO: <https://almascience.eso.org/alma-data/archive>
- ⁸ ALMA Cycle 3 User Survey: <https://almascience.eso.org/news/alma-cycle-3-user-survey-3>

ALMA Cycle 0 Publication Statistics

Felix Stoehr¹
 Uta Grothkopf¹
 Silvia Meakins¹
 Marsha Bishop²
 Ayako Uchida³
 Leonardo Testi¹
 Daisuke Iono³
 Kenichi Tatematsu³
 Al Wootten²

¹ ESO

² National Radio Astronomy Observatory,
 Charlottesville, USA

³ National Astronomical Observatory of
 Japan, Mitaka, Tokyo, Japan

The scientific impact of a facility is the most important measure of its success. Monitoring and analysing the scientific return can help to modify and optimise operations and adapt to the changing needs of scientific research. The methodology that we have developed to monitor the scientific productivity of the ALMA Observatory, as well as the first results, are described. We focus on the outcome of the first cycle (Cycle 0) of ALMA Early Science operations. Despite the fact that only two years have passed since the completion of Cycle 0 and operations have already changed substantially, this analysis confirms the effectiveness of the underlying concepts. We find that ALMA is fulfilling its promise as a transformational facility for the observation of the Universe in the submillimetre.

Introduction

The Atacama Large Millimeter/submillimeter Array (ALMA) was designed and built as a world-leading submillimetre observatory that would produce transformational science on a broad range of astrophysical topics. Early Science observations began in 2011 in response to increasing pressure from the astronomical community to use the facility, even though only a small fraction of the final capabilities were available. Eventually, ALMA was offered in Cycle 0 for observations with sixteen 12-metre antennas, four frequency bands covering 84–116 GHz (Band 3), 211–275 GHz (Band 6), 275–373 GHz (Band 7), and

602–720 GHz (Band 9), baseline lengths of up to 400 metres and limited observing modes and correlator capabilities. The capabilities that were offered correspond to about 25 % of the final collecting area, 40 % of the frequency bands, only 2 % of the achievable angular resolution and a small fraction of the observing and correlator modes of the completed observatory.

Science observations for ALMA Cycle 0 were carried out from 1 October 2011 through 31 January 2013. The vast majority of the calibrated datasets were delivered to the users by the first quarter of 2013; the last dataset was delivered in mid-August 2013.

Methodology

In this section, we summarise the methodology applied in order to compile the ALMA bibliography. A more detailed version, along with lessons learned from the first two years of maintaining this important resource, can be found in Meakins et al. (2014).

The ALMA bibliographic database is jointly maintained by the librarians at ESO and the National Radio Astronomy Observatory of the USA (NRAO), together with administrative support from the National Astronomical Observatory of Japan (NAOJ). The bibliographic database has been built using the extensive experience accumulated by the librarians in the context of similar telescope bibliographies at their institutes (NRAOpapers¹ and ESO telbib²).

For the purposes of this study, only refereed publications that appeared in print at the time of writing and that make direct use of ALMA data are considered. Papers that only cite values or results derived from ALMA data from the literature are excluded. Also excluded are publications that describe instrumentation or software, merely mention ongoing projects, suggest future observations, or develop models or run simulations without actual use of data. This definition corresponds to the *Best Practices for Creating a Telescope Bibliography*, the IAU/Commission 5 endorsed guidelines for the construction and maintenance of

bibliographies related to observatory or telescope bibliographies³.

Compilation of the ALMA bibliography consists of a multi-step workflow that starts with the screening of core journals in astronomy as well as of various other journals and arXiv/astro-ph eprints (journals routinely screened are A&A, A&Arv, AJ, AN, ApJ, ApJS, ARA&A, EM&P, Icarus, MNRAS, Nature, NewA, NewAR, PASJ, PASP, P&SS, and Science). However, in this article only papers that have been fully published and have received their final bibcode are considered. All papers that contain at least one ALMA-related keyword are visually inspected by the librarians to decide whether or not they qualify for inclusion in the database. Bibliographic details (authors, titles, publication details, etc.) along with other metadata are imported from the Smithsonian Astrophysical Observatory (SAO)/National Aeronautics and Space Administration (NASA) Astronomical Data System (ADS).

For each record in the bibliography, a variety of parameters are identified and added by the librarians. Most importantly, this includes the ALMA project code(s) of the observations that were used, the ALMA partner to whose share the observing time was attributed and the observing type (Standard, Large, Target of Opportunity, Science Verification, etc.). At this point, archive flags are assigned to project codes without overlap between authors of the paper and Principal Investigators/Co-Investigators (PIs/Cols) of the Observing Programme (see section on archival research below).

ALMA's User Policies require authors not only to include the official ALMA acknowledgement text in their publications, but also the ID number of the ALMA Programme of the data used, formatted according to the ADS data-tag⁴ specification. This allows the creation of links between publications and data, which forms not only the basis of most of the results presented here, but also allows readers of the articles to immediately access the data in the ALMA Science Archive⁵. Additionally, in the near future, archival researchers can find publications related to the data records in the ALMA Science Archive.

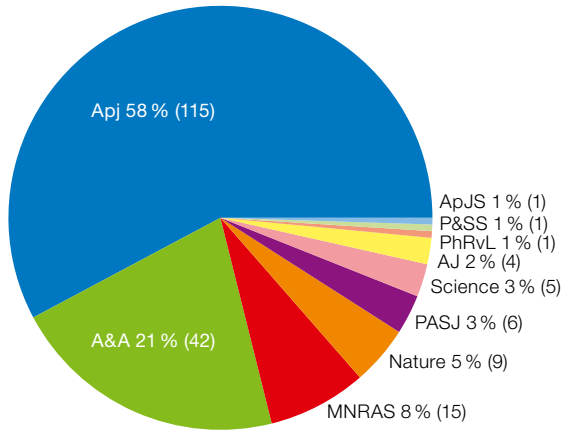


Figure 1. Distribution of ALMA Cycle 0 publications by refereed journal.

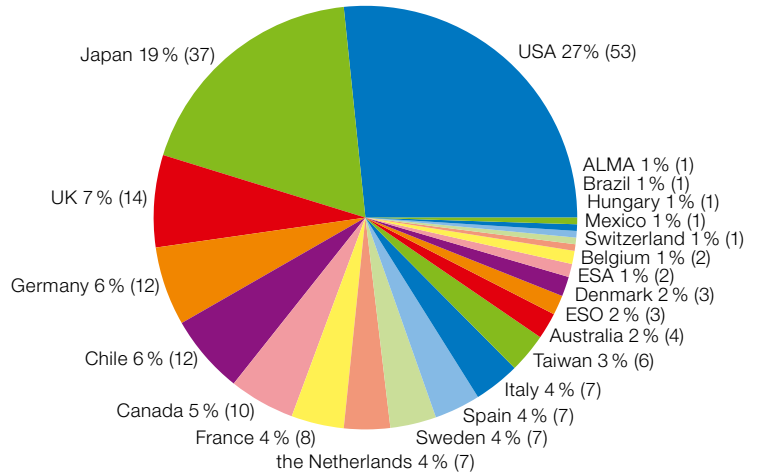


Figure 2. Geographical distribution of the first authors of ALMA Cycle 0 publications.

A large and increasing fraction of authors (about 85 %) know these policies well and place the statement and the data tag in their publications. Furthermore, we regularly check the arXiv.org preprint server and contact the authors by email if the acknowledgement or data tag are missing from a paper or are incorrect. Feedback from contacted authors is extremely positive with the result that 98 % of the ALMA publications that go to press carry the acknowledgement statement and data tag. The remaining publications without data tags are those that were put on the preprint server only when the publication was already in press. In those cases a member of the library staff identifies the related ALMA Programmes manually and adds the information to the publication database.

Experience from two years of maintenance of the ALMA bibliography has shown clearly that this personal communication is essential to: (a) raise the awareness of authors regarding the ALMA policy concerning the use of ALMA data in the acknowledgements; and (b) to establish a bibliography that is as complete and correct as possible.

General overview of the publications

At the time of writing the number of refereed publications using ALMA data has reached a total of 308 papers, mostly using Cycle 0 data (199, or 65 %) and Science Verification (SV) observations

(76, or 25 %). There are 47 (15 %) papers based on Cycle 1 and 2 data including 3, or 1 %, based on Cycle 1 and 2 Director's Discretionary Time (DDT). In Cycle 0 DDT was not offered. As a single paper can make use of several ALMA Programmes, the sum over the values of the different cycles is larger than 100 %.

In the following we concentrate on publications from Cycle 0 data. All Cycle 0 data were delivered more than two years ago, which allows us to carry out a global and unbiased first analysis.

Journals

A significant fraction of the Cycle 0 ALMA publications (7 %) appeared in non-sector specific, high-impact journals (*Nature* and *Science*), demonstrating the transformational nature of the ALMA Observatory, even in the limited configuration available for Cycle 0 observations. Such a high fraction is uncommon for ground-based observatories in the first years of operations and more in line with that of space missions. The premier journals for ALMA publications are *The Astrophysical Journal* (ApJ) and *Astronomy & Astrophysics*, which together account for 79 % of the refereed publications (see Figure 1). It is noteworthy that nearly a quarter of all papers are published as Letters — in addition to the publications in *Nature* and *Science*. For all regions, ApJ publishes most of the Letters. This, together with the fact that most North American (NA)

authors and many East Asia (EA) authors publish in ApJ, explains the large fraction of ApJ publications.

Countries

The overall publication numbers (Figure 2) are well balanced among the three ALMA partners (NA, EA and ESO [EU]) and are in line, within the uncertainties, with their shares in the Observatory (37.5 % each for ESO (EU) and NA, 25 % for EA). There is a marginally larger fraction of first authors from the ESO members (EU 37 %, NA 33 %, EA 20 %, Chile 4 %, other 6 %), but this is not statistically significant. The fraction of first authors who use data obtained through observing time attributed to a different partner from that of their home institute hovers around 15 %, indicating a healthy mix of the partners in the research groups and mobility of the researchers across the regions.

Distribution by science area

The right-hand side of Figure 3 shows the distribution of Cycle 0 publications according to their scientific categories. This distribution is relatively well balanced. Notable differences in the distribution of scientific categories of accepted proposals that received data (Figure 3, left) are only observed in the galaxy evolution and Solar System categories. A single project is responsible for the over-proportionally large number of publications in the galaxy

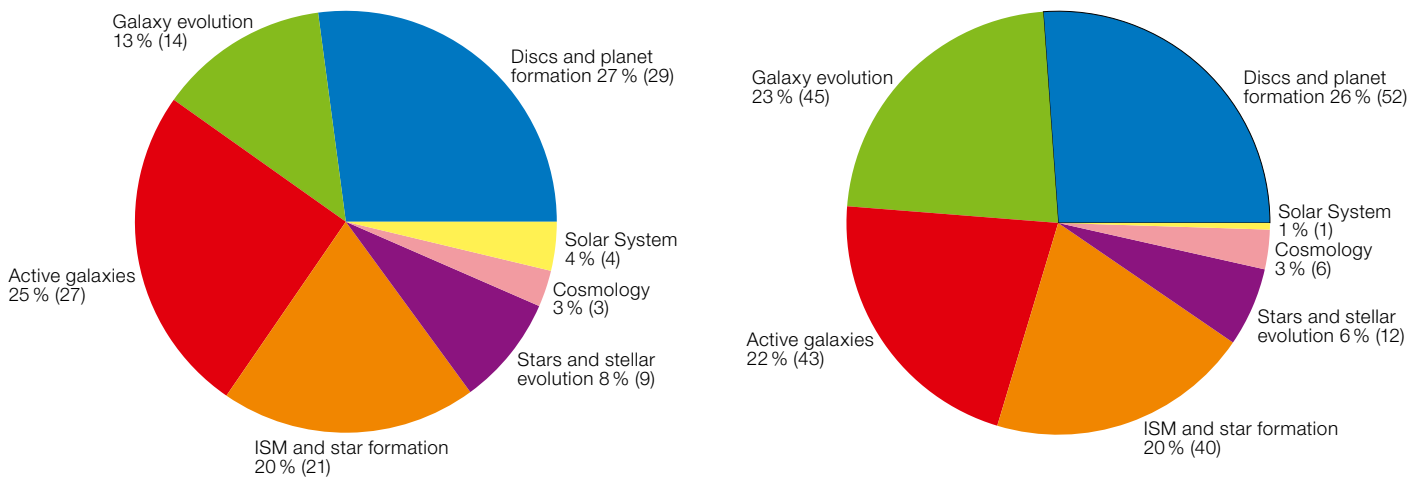


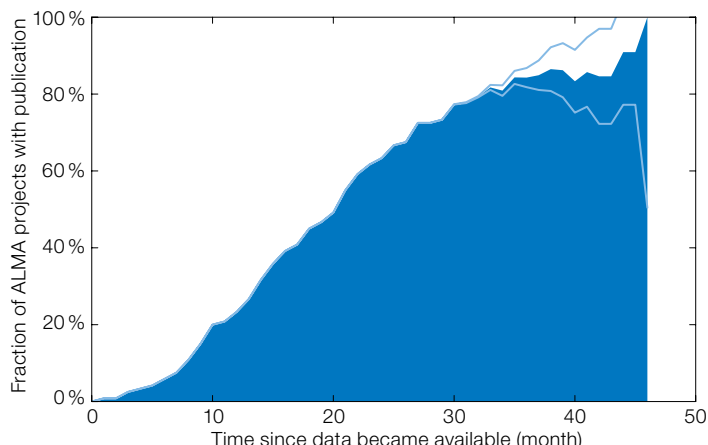
Figure 3. Distribution of the scientific categories of allocated Cycle 0 high priority Programmes (left) and the resulting publications (right).

evolution category. Solar System data in Cycle 0 turned out to be very difficult to obtain, calibrate and analyse and this is considered as the reason for the lower number of publications so far.

Publication fraction

An important measure for a facility is the fraction of Programmes that did receive data and that result in a publication (PI or archival). In other words: how effectively

Figure 4. The fraction of programmes that have had at least one related publication as a function of the time since the data was made available to the PI. The light blue lines show 1σ standard deviations assuming 50% publication probability and weighted by the number of projects that have not yet reached the age to contribute to a bin.

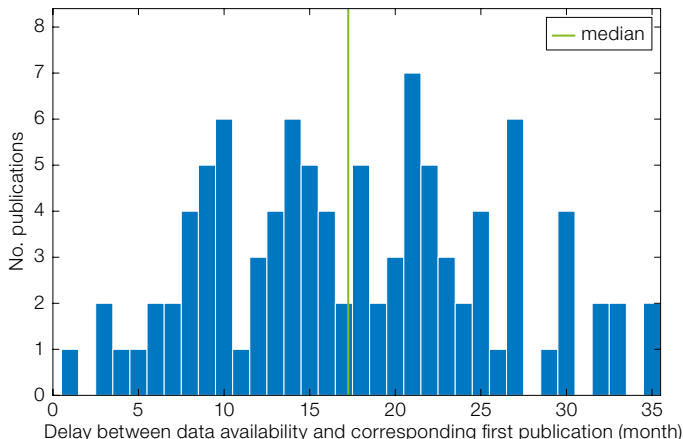


can the data be converted into published science? Figure 4 shows this fraction as a function of time since the data became available to the PI. For each bin only the Programmes that are available for that timespan are taken into account, hence the plot is not strictly cumulative for the left-most bins, which suffer from low number statistics. However we can conclude that the ALMA publication fraction for Cycle 0 is roughly 85%, an extremely high value even when compared to space programmes. Although fully comparable numbers are not available, facilities like the Very Large Telescope (VLT), Hubble Space Telescope (HST) or the X-ray Multi-Mirror Mission (XMM-Newton) have publication fractions in the range of 50–75% (Sterzik et al., p. 2, private communication and Ness et al. [2013] respectively).

The high publication fraction not only indicates that ALMA is a transformational facility, but also suggests that the quality of the ALMA data is extremely high and that the effort of providing science-grade data to users allowed nearly all Cycle 0 PIs, including those with limited previous interferometric or millimetre-wave background, to make effective scientific use of the data. This conclusion is also supported by the results of the ALMA User Surveys.

We speculate that the exceptionally high publication fraction suggests that the Cycle 0 ALMA Proposal Review Committee (APRC) awarded time preferably to high science profile Programmes with a high probability of success (low-risk approach in the selection of the science

Figure 5. The distribution of the time spans from the availability of the data for a Programme until the first resulting publication.



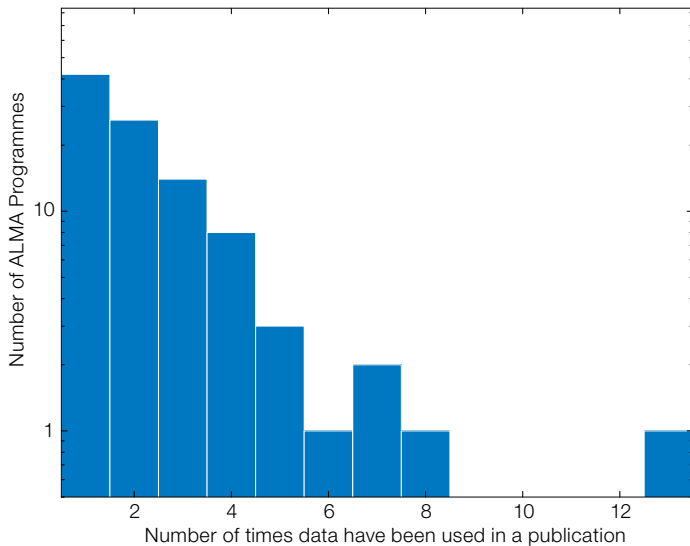


Figure 6. Distribution of the number of times data from a given Programme has been used in a refereed publication.

programme); possibly as a consequence also of the extremely high oversubscription rate of nine for Cycle 0.

Publication delay

Figure 5 shows the time that it takes from the delivery of the data to the PI to the first publication using the data, either by the original proposers or by an archival research team. Up to 32 months the statistics are complete and include 80% of all Programmes. We can therefore safely conclude that the large majority of the ALMA Cycle 0 data were published extremely rapidly. The median value is 1.4 years, which is considerably faster than standard programmes of space missions like XMM or Chandra (both about 2.3 years: Rots et al., 2012; Ness et al., 2013). The ALMA Cycle 0 publication delay is even comparable to the delay for XMM Target of Opportunity Programmes, which have a six-month proprietary period. We believe that the high pressure to obtain time, the transformational nature of ALMA and the fact that ALMA is the first submillimetre observatory in the southern hemisphere, have all contributed to the fast publication rate of Cycle 0 Programmes.

In addition to the novelty of ALMA, we also attribute this effect to the fact that users did not need to spend much time

on data reduction, as they received fully calibrated data and reference images directly from ALMA. In addition, the fact that ALMA provides a comprehensive user-support model, which offers Help-desk support on three continents as well as face-to-face support from proposal preparation to data reduction and analysis (see Hatziminaoglou et al., p. 24), has a very positive impact on the usability of ALMA data by the community. Both claims are again well supported by the results of the ALMA User Surveys.

Multiple use of the data

ALMA Cycle 0 Programmes, which have resulted in at least one publication, produced on average about two publications per Programme. Experience from other observatories shows that the ALMA value is expected to rise with time. After four years, this value for ALMA is already identical to a similar quantity for the VLT averaged over nine years (Sterzik et al., p. 2). More than half of all published ALMA Programmes were used in at least two publications (Figure 6), with Programme 2011.0.00294.S *More than LESS: The first fully-identified submillimetre survey* (PI: Ian Smail) being by far the most published Cycle 0 Programme, with 13 publications to date.

These numbers confirm the richness and quality of ALMA data and indicate that the ALMA archive is a very valuable asset to maximise the scientific return of the facility.

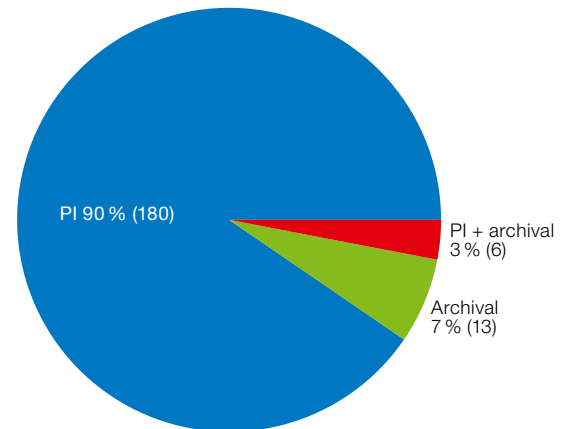


Figure 7. Distribution of publications that use only PI data, only archival data, or a combination of both.

Archival research

A paper is considered as using archival data in the case where there is no overlap between the authors and PI & CoIs of the original Programme from which data were used. Where a publication makes use of archival as well as proprietary data, the paper is tagged “PI + archival”.

The fraction of publications that made use of ALMA archival data has been steadily increasing and has now reached 7% for purely archival publications and an additional 3% for publications making use of Cycle 0 archival data together with ALMA PI data (Figure 7). We expect this fraction to continue to grow with time; even more so for future cycles once full-cube science-grade pipeline products are available. Note that although SV data are also tagged “archival”, in the statistics presented above, only publications making use of data taken as part of Cycle 0 Programmes have been taken into account.

Publications from SV data

In order to test new capabilities, ALMA has been regularly executing SV projects⁶. The resulting data were reduced and made publicly available without a proprietary period. These data have, so far, led to a very large number of refereed publications. The 17 SV projects have been used in 76 publications (4.5 publications per project). Due to the highly

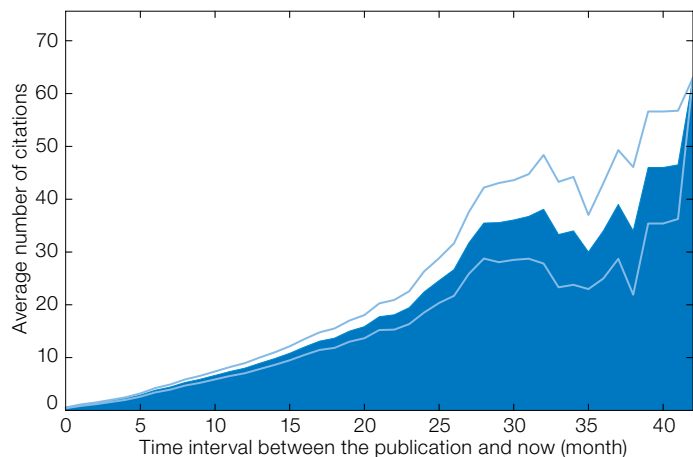


Figure 8. Average number of citations of ALMA publications as a function of time from publication. The light blue lines show the Poisson uncertainty for the counts in each time bin.

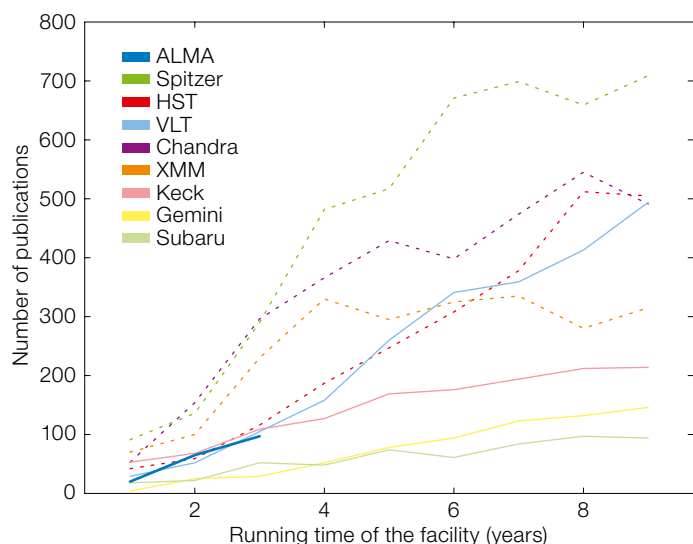


Figure 9. Comparison of the evolution of the number of publications since the first publication for some of the large space-based (dotted) and ground-based (solid, including ALMA as a thick blue line) astronomical facilities.

competitive setting, without a proprietary period, the median timespan between the release of the data and the first corresponding publication is only four months. Multi-use of the data has also been very high, with one SV dataset (2011.0.00009. SV, Orion KL Band 6) having been used in 18 publications.

Scientific impact

One proxy measurement for scientific impact is the frequency at which publications are cited in the scientific literature. We track citations to ALMA papers using the SAO/NASA ADS services. It is obviously too early to draw final conclusions at this stage; the numbers reported should

be considered only as trends. Figure 8 shows the evolution of the average number of citations to Cycle 0 ALMA papers.

We find that, on average, each Cycle 0 publication receives about ten citations per year, which is higher than the 6.5 citations per year measured for ALMA SV publications. Comparing the average number of citations per paper per year to other facilities has to be done with great care because: (a) the value changes with time; and (b) the methodologies and policies for inclusion and exclusion may vary among observatories. The average number of citations per paper per year for VLT publications is four (measured over the last 15 years and computed from telbib² using citation numbers from SAO/NASA

ADS), which is identical to the value for XMM (measured over 13 years, Ness et al., 2013). When taking only the last three years of VLT publications into account to match the period with the ALMA data, then the average number of citations per paper per year is about five.

When comparing ALMA data papers to those published in 2012–2014, we find that there are one, six and three ALMA papers, respectively, in the most cited 1% of all refereed astronomy articles in 2012, 2013 and 2014. Thus about 4% of all ALMA publications make it into the top 1% most-cited papers per year (computed from SAO/NASA ADS).

Comparison with other facilities

In Figure 9 we compare the number of publications making use of data from major astronomical facilities as a function of the time that they have been operational. In order to be comparable, publications from all ALMA cycles as well as publications using SV data have been included.

Space observatories (dotted lines in Figure 9) have traditionally had much steeper rises in publication numbers than ground-based facilities. This effect may be due to the fact that space probes need to be fully prepared at launch and can ramp up very quickly to full operation, whereas ground-based facilities are usually commissioned gradually while some operations have already begun. In the early years, ALMA's scientific output — measured here by the number of scientific papers — is in line with that of HST, VLT or Keck.

Outlook

In order to close the loop with the PIs and to learn the reasons that prevented PIs from publishing their data, ALMA has initiated a survey, which is sent to PIs of Programmes without a publication two years after the end of the proprietary period. The results of this survey will become part of the monitored elements to constantly improve the operational model and thus optimise the scientific return of ALMA.

Conclusions

We have analysed the publications of the first Early Science proposal cycle (Cycle 0) of ALMA. Although only two years have passed since the end of this cycle, and more publications making use of Cycle 0 data can be expected, a number of conclusions can already be reached.

ALMA is indeed the transformational facility it was designed to be and has effectively opened the submillimetre wavelength regime to general user observations, with Bands 7 and 9 (275–950 GHz) the basis of 64 % of all Cycle 0 publications. All originally foreseen scientific categories — with the exception of observations of the Sun which are not yet fully commissioned — are represented. We find that a very high fraction of Programmes (roughly 85 %) resulted in one or more publications, and on aver-

age, each Cycle 0 publication receives ten citations per year. Publications appear very fast once the data becomes available to the PIs (1.4 years) and the fraction of publications making use of archival data is rising (currently at ~ 10 %). The evolution of the total number of publications is similar to the early evolution of HST, VLT and Keck.

Science Verification data has led to a very large number of publications (76 publications from 17 SV datasets) with very short publication delays (four months), large multiple use (maximum 18) and 6.5 citations per publication per year.

We attribute the success of Cycle 0 in terms of scientific impact to the novelty of the instrument, the high quality of the data, the fact that ALMA delivers fully calibrated and quality-controlled data as well as to the extensive user support in three continents.

Acknowledgements

The ALMA bibliography makes use of the SAO/NASA ADS⁷.

References

- Meakins, S. et al. 2014, Proc. SPIE, 9149, 914926
Ness, J. U. et al. 2014, AN, 335, 210
Rots, A. H., Winkelman, S. L. & Becker, G. E. 2012, PASP, 124, 391

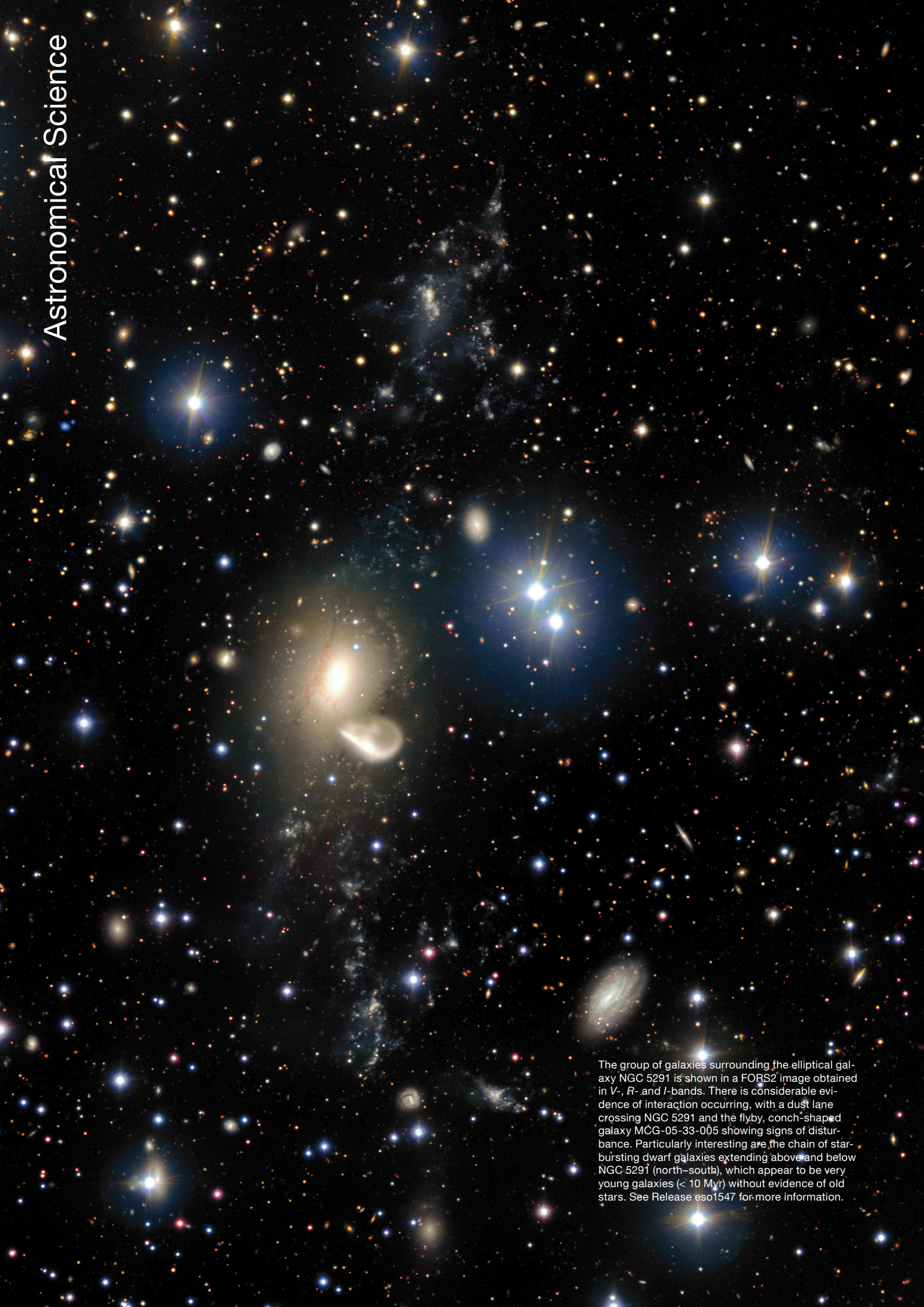
Links

- ¹ NRAOpapers bibliography: <http://library.nrao.edu/papersmethod.shtml>
- ² ESO telbib: http://www.eso.org/sci/libraries/telbib_info.html
- ³ IAU Commission 5 best bibliographic practices: <https://iau-commission5.wikispaces.com/WG+Libraries+-+Best+Practices+for+Creating+a+Telescope+Bibliography>
- ⁴ ADS data tag: <http://vo.ads.harvard.edu/dv/index.html>
- ⁵ ALMA Science Archive: almascience.org/aq
- ⁶ ALMA Science Verification: <http://almascience.org/alma-data/science-verification>
- ⁷ ADS, <http://adswww.harvard.edu/>

J. C. Rogge/ESO



Part of the Atacama Large Millimeter/submillimeter Array (ALMA) during day time. The rare optical phenomenon known as a circumhorizontal arc is formed by the refraction of sunlight in plate-shaped ice crystals suspended in the atmosphere.



The group of galaxies surrounding the elliptical galaxy NGC 5291 is shown in a FORS2 image obtained in V-, R- and I-bands. There is considerable evidence of interaction occurring, with a dust lane crossing NGC 5291 and the flyby, conch-shaped galaxy MCG-05-33-005 showing signs of disturbance. Particularly interesting are the chain of starbursting dwarf galaxies extending above and below NGC 5291 (north-south), which appear to be very young galaxies (< 10 Myr) without evidence of old stars. See Release eso1547 for more information.

The Central Orion Nebula (M42) as seen by MUSE

Peter M. Weilbacher¹
 Ana Monreal-Ibero²
 Anna F. McLeod³
 Adam Ginsburg³
 Wolfram Kollatschny⁴
 Christer Sandin¹
 Martin Wendt^{1,5}
 Lutz Wisotzki¹
 Roland Bacon⁶

¹ Leibniz-Institut für Astrophysik (AIP),
 Potsdam, Germany

² GEPI, Observatoire de Paris, PSL
 Research University, CNRS, Université
 Paris Diderot, Sorbonne Paris Cité,
 Meudon, France

³ ESO

⁴ Institut für Astrophysik, Universität
 Göttingen, Germany

⁵ Institut für Physik und Astronomie,
 Universität Potsdam, Germany

⁶ CRAL, Observatoire de Lyon, Saint-
 Genis Laval, France

The MUSE (Multi Unit Spectroscopic Explorer) instrument, an optical wide-field integral field spectrograph at the Very Large Telescope, has been operating successfully for about a year. Among the impressive sets of data collected during commissioning was a mosaic of the central Orion Nebula (M42), known as the Huygens region. During the past year, we have made the data ready for scientific use, and they are now publicly available to the community. An overview of the observations and their reduction, as well as two possible scientific applications, are presented.

The MUSE integral field spectrograph (Bacon et al., 2012) was commissioned at the Paranal Observatory in the first half of 2014. It covers a field of view of about 1 by 1 arcminute on the sky at a sampling of 0.2 arcseconds per spatial element and has a nominal wavelength range of 480 to 930 nm. An extended mode without an order-separating filter is available, which allows a contiguous data coverage down to about 460 nm. In the future, the instrument will be enhanced with an adaptive optics module and a narrow-field mode, with an eightfold increase in spatial sampling. A summary of the com-

missioning and Science Verification activities was presented in Bacon et al. (2014) and these activities have already amply demonstrated the instrument's capabilities for a variety of astronomical topics. In this article we highlight the Orion Nebula dataset taken during commissioning, which we have reduced and now make available as science-ready cubes¹.

The Orion Nebula

H II regions are stellar nurseries where we can study the interplay between the recently born (massive) stars and the surrounding interstellar medium. One of the best-known and closest examples, at a distance of about 440 pc, is the Orion Nebula (M42; a review is given in O'Dell [2001]). As such, it is one of the favourite targets when a new instrument needs to be validated, on account of its high surface brightness, richness in terms of structures and wealth of previous observations. The nebula was observed during the commissioning of MUSE with the main technical goals of testing offsets larger than the field of view and as a stress test for the data reduction system. The collected data: i) mapped the complete bright core (called the Huygens region) over a field of 6 by 5 arcminutes; ii) achieved a depth similar to previous studies with only 5 seconds exposure time; iii) offered a large spectral coverage ranging from approximately 460 nm to 935 nm; and iv) had reasonably good spa-

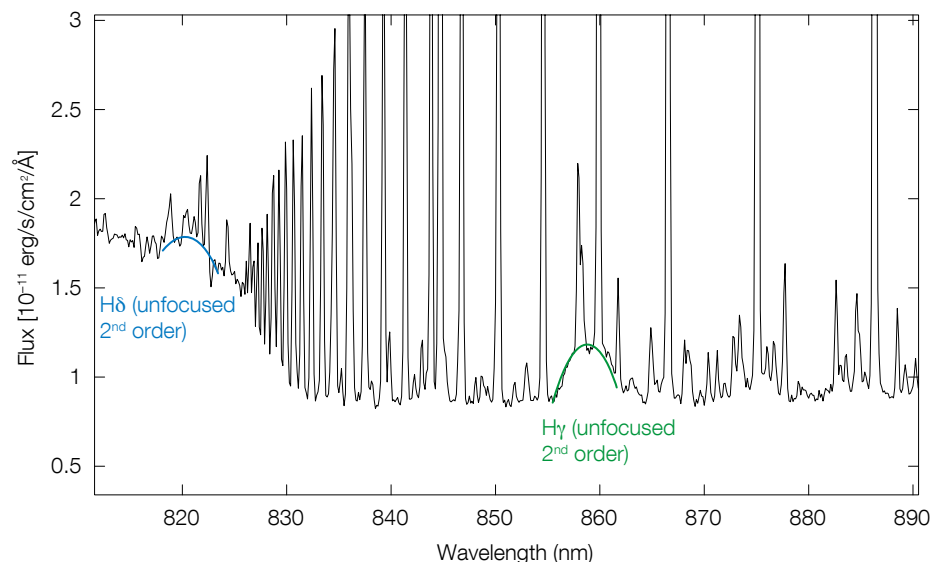
tial and spectral resolution. Since none of the previous datasets obtained using long-slit or integral field spectrographs possessed all these properties simultaneously, it was decided to release the MUSE Orion Nebula data to the community, as a fully reduced and science-ready cube.

Data processing

Basic data processing of each individual pointing was done using the dedicated MUSE pipeline (Weilbacher et al. [2012], and publicly available for download²) and included bias subtraction, flat-fielding and throughput correction, wavelength calibration, geometric characterisation, application of an astrometric solution, correction for atmospheric refraction, application of the barycentric velocity offset and flux calibration. We did not attempt to remove the sky background or the telluric absorption. The 2-Micron All Sky Survey (2MASS) positions of the stars present in each pointing were used to establish the relative positioning between the individual pointings, and all the cubes were merged into a common final cube.

The dataset constitutes one of the first observations with the MUSE extended mode and thus, also one of the first

Figure 1. The red end of one Orion spectrum illustrating the contamination of the data by the broad second order. Broad bumps caused by second order contamination of H δ and H γ are indicated.



opportunities to evaluate the effects of second-order overlap. The central Orion Nebula shows very strong emission lines that are easy to identify, while the second order is unfocused and offset from the expected wavelength calibration. Figure 1 illustrates its appearance in the spectral direction: strong emission lines in the blue create broad bumps in the red region of the spectrum. On top of the first order spectrum, two bumps caused by the second order spectrum of $H\delta$ and $H\gamma$ are clearly identified. These bumps can be modelled and subtracted as background, thereby minimising their effect in the estimation of the line fluxes in the reddest part of the spectra.

Data release

The released data products have a spatial size of 5.9 by 4.9 arcminutes (0.76 by 0.63 pc) at a 0.2 by 0.2 arcsecond sampling and a contiguous spectral coverage of 459.5 to 936.6 nm. They are delivered as FITS files with several extensions, including cubes for the data and the statistical variance, and reconstructed 2D images of the field of view. We provide two versions of the cube, with spectral samplings of 0.125 nm and 0.085 nm, and file sizes of 75 and 110 GB respectively. We also provide an online facility that offers the possibility of extracting only a subsection of the cubes, since by current standards these are rather large files¹.

The combined scope of the spatial and spectral directions is illustrated by the cover page and in Figure 2, which show several of the many possible three-colour composite images that can be extracted from these data. The cover page shows an image constructed from three emission lines of hydrogen: $H\beta$, $H\alpha$ and Paschen 9 (923 nm) and another image from all three ionisation stages of oxygen that have been detected: $[O\ I]6300\ \text{\AA}$, $[O\ II]7320\ \text{\AA}$ and $[O\ III]5007\ \text{\AA}$. As such, the change in colour in the oxygen image nicely traces the ionisation structure of the nebula. This is particularly visible in the Bright Bar, which gradually changes from red ($[O\ III]$), through green ($[O\ II]$) to blue ($[O\ I]$). Figure 2 combines maps of $H\beta$, $[N\ II]6584\ \text{\AA}$ and $[S\ II]6731\ \text{\AA}$; the most striking features in M42 are labelled.

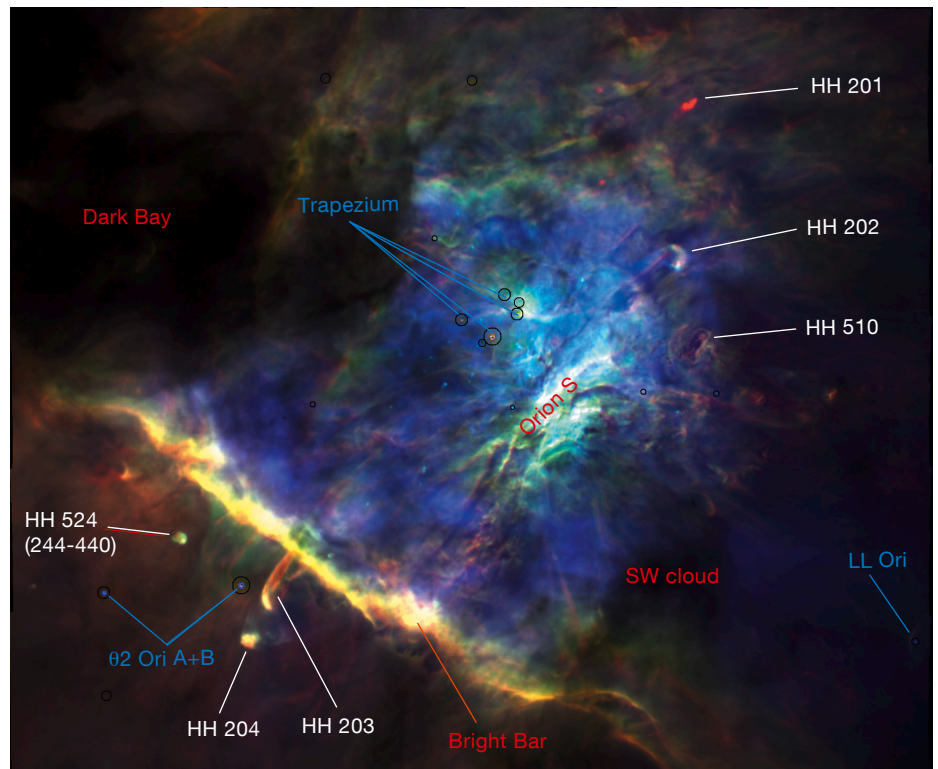


Figure 2. Colour-composite image illustrating the richness of the MUSE datacube in the spatial direction (see also the two images on the cover). $[S\ II]6730\ \text{\AA}/[N\ II]6584\ \text{\AA}/H\beta$ (with annotated features within the image) for blue/green/red channels respectively.

These are: the Bright Bar, the Dark Bay, the Orion-S region and several shock-excited Herbig–Harro (HH) objects. The positions of the brightest stars in the field are marked as well, but the stars are not seen, as the maps are continuum subtracted.

The amount of spectral information conveyed in the cube is illustrated in Figure 3. A nebular spectrum of a bright part of M42 over the full wavelength range extracted from the MUSE data is shown. The bright H I ($H\alpha$, $H\beta$, Paschen series) and He I recombination lines are detected, as well as many collisionally excited lines of several metals, which can be used as diagnostics for the physical and chemical conditions of the warm ionised gas. More interestingly, we also detect many of the much fainter metal recombination lines. The faintest identified lines have fluxes on the order of $4 \times 10^{-15}\ \text{erg cm}^{-2}\ \text{s}^{-1}$.

Extinction structure

An example of the scientific possibilities offered by this set of data is presented in Figure 4, which shows the extinction map derived from the observed $H\alpha/H\beta$ emission line ratio and standard assumptions for the assumed intrinsic $H\alpha/H\beta$ ratio. The Dark Bay and the southwest cloud show the strongest extinction, while regions like the Bright Bar exhibit moderate reddening. This map is qualitatively similar to the reddening map derived by O’Dell & Yusef-Zadeh (2000), who use a different technique (i.e., radio-to-optical surface brightness comparison) and find an extinction peak that is higher by a factor of 1.5 in extinction $c(H\beta)$ with respect to the one found with the MUSE data. This difference can be understood in terms of the differing capacity of both tracers to penetrate the dust, which is higher for the one involving radio emission.

Digging up proplyds by means of line ratio mapping

Although lacking the high angular resolution of Hubble Space Telescope (HST)

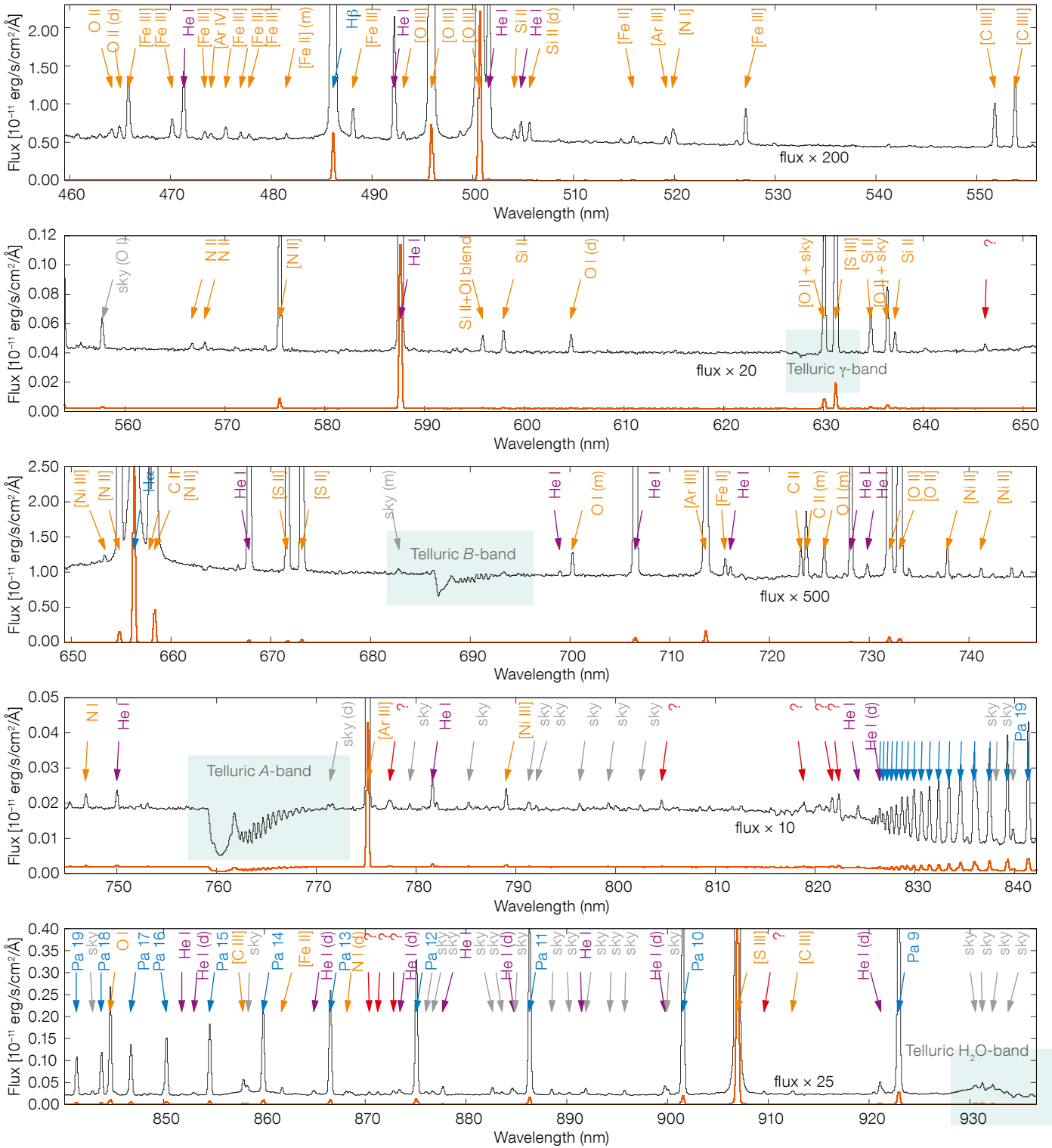


Figure 3. Spectral plots illustrating the richness of the data in the spectral direction: known hydrogen, helium, metal, and sky emission lines are marked with blue, violet, orange, and grey arrows, respectively. A few faint, unknown emission lines are marked in red. The spectrum was extracted from the location of Slit1 of Baldwin et al. (1991).

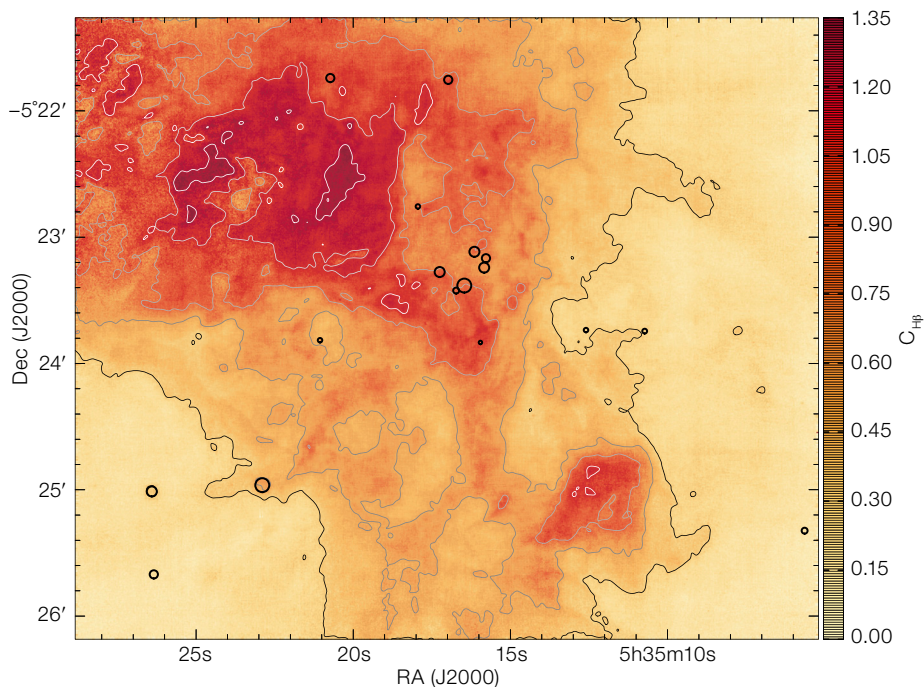


Figure 4. The extinction structure $c(\text{H}\beta)$ over the Huygens region of M42, as traced from the $\text{H}\alpha/\text{H}\beta$ emission line ratio, is shown.



Figure 5. Two Orion proplyds (protoplanetary discs) imaged with HST (left) and MUSE (right). The top row displays object 141-301, the bottom row is 177-341 (nomenclature of O'Dell & Wen [1994]).

imaging, the MUSE Orion dataset can also be used to analyse various small-scale structures of the Orion Nebula, specifically HH objects and proplyds (protoplanetary discs, O'Dell & Wen [1994]). As an example of the drastic

difference in spatial resolution, two Orion proplyds are shown as seen by HST (left) and by MUSE (right) in Figure 5. This analysis is based on two emission line ratios: the parameter usually called $S_{23} = ([\text{S II}] + [\text{S III}])/\text{H}\beta$ (Vilchez & Esteban,

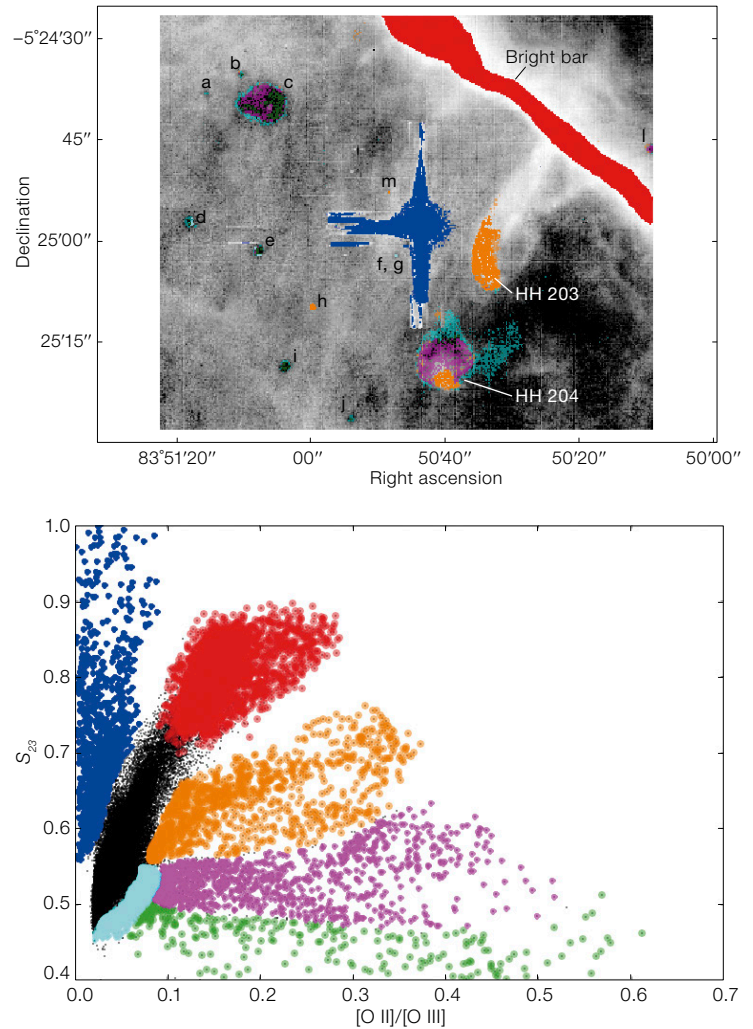
1996), and the indicator $[\text{O II}]/[\text{O III}]$ representing the degree of ionisation. The parameter space for these two line ratios is shown in the lower panel of Figure 6 (of the immense full region observed with MUSE, only a small sub-region south of the Bright Bar is shown here, as this very interesting region hosts two of the major HH objects as well as several proplyds). In this figure, the data points were traced back to their spatial origin in the S_{23} map (upper panel): it is clear that the different structures and objects occupy different regions in this parameter space. This line-ratio diagram can therefore be used as an initial tool to detect these kinds of objects (propyds and HH objects) in other star-forming regions as well.

The Bright Bar (red data points in Figure 6) shows higher S_{23} values than the proplyds (their positions are drawn from Ricci et al. [2008] and marked with characters from a to m) and HH objects, while these show a wider range of degrees of ionisation. Furthermore, the HH outflows and proplyds can be separated into four classes (marked by the orange, magenta, green and cyan data points in Figure 6), depending on their S_{23} and $[\text{O II}]/[\text{O III}]$ values. An initial, tentative, physical interpretation of this empirical finding is that the S_{23} parameter traces the relative contribution of shocks and photo-ionisation to the sulphur excitation, as the presence of shocks locally lowers the ionisation parameter, enhancing the emission of low ionisation (e.g., $[\text{S II}]$) over the high ionisation species (e.g., $[\text{S III}]$). A full discussion of this investigation will be presented in McLeod et al. (2015).

Future perspectives

We have released MUSE datacubes for M42¹. This constitutes the largest integral field mosaic to date in terms of information content. We validated the data in terms of quality as apt for scientific use, and as such potentially useful to address a wide range of scientific questions. Some examples have been presented in this article as well as in Weillbacher et al. (2015) and McLeod et al. (2015). We hope that the astronomical community envisions many more.

Figure 6. The S_{23} parameter map of a sub-region south of the Orion Bright Bar (upper panel); the proplyds from Ricci et al. (2008) are marked with characters from a to m. The S_{23} vs. $[O II]/[O III]$ parameter space of the same region is shown in the lower panel, with the structures colour-coded as in the upper panel.



Acknowledgements

The authors thank the (rest of) the MUSE consortium and the teams that conducted first light and commissioning observations. We are grateful for support from ESO during these activities.

References

- Bacon, R. et al. 2012, *The Messenger*, 147, 4
 Bacon, R. et al. 2014, *The Messenger*, 157, 13
 Baldwin, J. A. et al. 1991, *ApJ*, 374, 580
 McLeod, A. F. et al. 2015, *MNRAS*, submitted
 O'Dell, C. R. & Wen, Z. 1994, *ApJ*, 436, 194
 O'Dell, C. R. 2001, *ARA&A*, 39, 99
 O'Dell, C. R. & Yusef-Zadeh, F. 2000, *AJ*, 136, 382
 Ricci, L. et al. 2008, *AJ*, 136, 2136
 Shields, G. A. 1990, *ARA&A*, 28, 525
 Weilbacher, P. M. et al. 2012, *Proc. SPIE*, 8451, 84510B
 Weilbacher, P. M. et al. 2015, *A&A*, 582, A114
 Vilchez, J. M. & Esteban, C. 1996, *MNRAS*, 280, 720

Links

- ¹ Access to MUSE datacubes and sub-cube extraction tool: <http://muse-vlt.eu/science/m42/>
² MUSE pipeline: <http://www.eso.org/sci/software/pipelines/muse/muse-pipe-recipes.html>

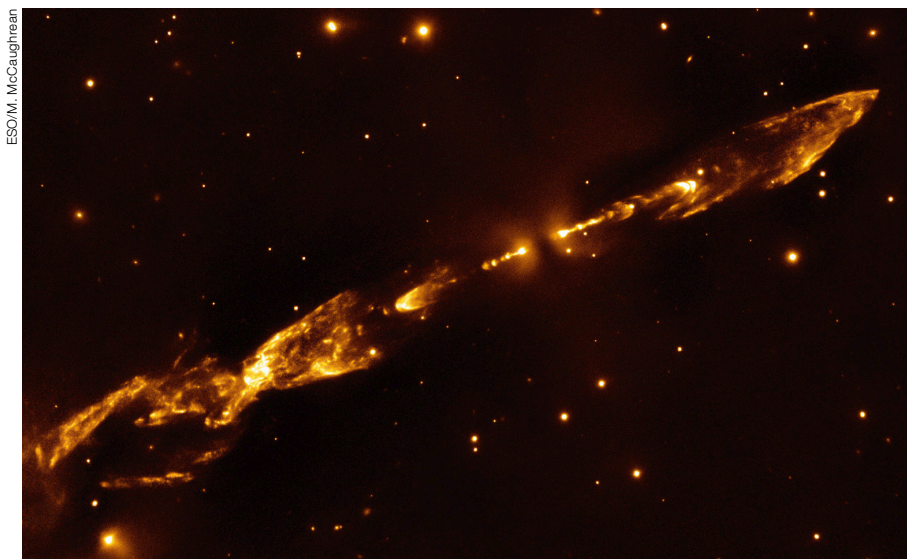


Image in the molecular hydrogen 2.12 μ m line of the Herbig-Haro object HH 212 in the Orion B region obtained with the Infrared Spectrometer And Array Camera (ISAAC). The spectacular collimated bipolar outflow from the central young star shocks against the local cloud material, producing a typical emission spectrum strong in molecular hydrogen, other more complex molecules and ionised gas.

Young Stellar Objects in the Orion B Cloud

Monika G. Petr-Gotzens¹
 Juan M. Alcalá²
 Loredana Spezzi^{1,3}
 Jes K. Jørgensen⁴
 Thomas Stanke¹
 Marco Lombardi^{5,6}
 João F. Alves⁷

¹ ESO

² INAF Osservatorio Astronomico di Capodimonte, Napoli, Italy

³ European Organization for the Exploitation of Meteorological Satellites (EUMETSAT), Darmstadt, Germany

⁴ Niels Bohr Institute, University of Copenhagen, Denmark

⁵ Department of Physics, University of Milan, Italy

⁶ Harvard-Smithsonian Center for Astrophysics, Cambridge, USA

⁷ Department of Astrophysics, University of Vienna, Austria

Wide-field near-infrared imaging surveys offer an excellent opportunity to obtain spatially complete samples of young stars in nearby star-forming regions. By studying their spatial distribution and individual properties, the global star formation characteristics of a region can be established. Near-infrared wide-field imaging observations of a significantly large area in the Orion Molecular Cloud B, obtained with the VISTA telescope on Cerro Paranal are presented. On the basis of photometric selection criteria, we have identified 186 candidate young stellar objects that are associated with the stellar clusters NGC 2068 and NGC 2071, and with the stellar group around HH24-26. Overall, Orion B shows a lot of similarities in its star formation characteristics with other Galactic star-forming regions: a star formation efficiency of a few percent, a stellar mass distribution very similar to that of the Orion Trapezium cluster, and a high observed fraction of circumstellar discs.

VISTA wide-field observations of Orion B

The constellation of Orion is a beautiful night-sky object visible to both southern and northern hemisphere skywatchers, due to its location close to the celestial



equator. Orion is also the nearest region of active high- and low-mass star formation allowing us to study many aspects of the star formation process in great detail.

For the study presented here, we analysed the multi-band photometry of a ~ 1.6 square degree field in the northern part of the Orion Molecular Cloud B, which was observed as part of the Visible and Infrared Survey Telescope for Astronomy (VISTA) Science Verification (SV)

Figure 1. VISTA three-colour (ZJKs) mosaic image of the northern part of Orion B on a logarithmic display. The image covers ~ 1.6 square degree and contains more than 100 000 objects. Clearly visible in the north is the embedded stellar cluster NGC 2071, while the cluster in the centre is NGC 2068.

Orion mini-survey (Petr-Gotzens et al., 2011). The analysed field contains the prominent bright optical reflection nebulosities NGC 2068 and NGC 2071 which, observed at near-infrared wavelengths, beautifully reveal their full nature as young stellar clusters (Figure 1). The ages

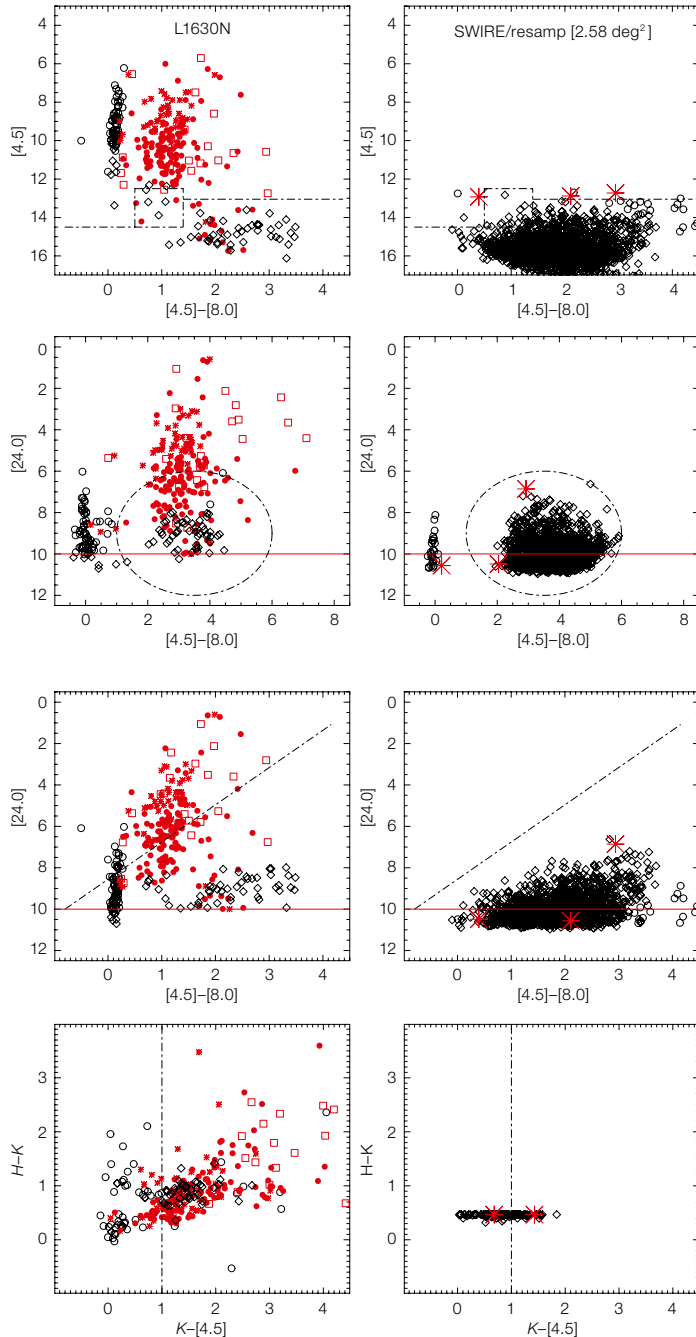


Figure 2. Upper four panels: VISTA/Spitzer colour–magnitude diagrams for objects in Orion B. The dot-dashed lines show fuzzy limits with exponential cutoffs that define the YSO candidate selection criterion in each diagram, excluding contamination from galaxies (diamonds) and field stars presenting normal photospheric colours (black circles). The continuous red lines show hard limits; fainter objects are excluded from the YSO category. Point-like and extended YSO candidates are indicated by red dots and open squares, respectively; YSO candidates with no VISTA morphological classification are indicated by asterisks.

Lower four panels: 2MASS/Spitzer colour–magnitude and colour–colour diagrams for the SWIRE galaxy catalogue. Three objects from the SWIRE catalogue (marked as asterisks) are classified as YSO candidates, according to our selection criteria.

of the clusters have been determined by Flaherty & Muzerolle (2008) to be 1–2 Myr, although star formation appears to be still ongoing, as suggested by the outflow sources that are clearly seen in the north of NGC 2071 and in a chain of young stellar objects to the southwest of NGC 2068. Our VISTA images were obtained through the ZYJHKs filters (0.9–2.2 μm) and achieved excellent sensitivity, e.g., a 5σ detection limit of Ks \sim 18.5 mag,

$J \sim 20.3$ mag and $Z \sim 22.5$ mag. All data reduction was performed by the Cambridge Astronomy Survey Unit (CASU) pipeline¹. We estimate that our survey should have detected, for a population as young as ~ 2 Myr at a distance of about 400 pc (i.e., the case of Orion B), essentially all objects from $\sim 1 M_{\odot}$ down to ~ 5 Jupiter masses (M_{Jup}) in a region showing less than 1 mag of visual interstellar extinction.

Selection of young stellar objects

The region of Orion B that we studied contains roughly 160 000 VISTA sources, among which less than 1% (!) are actually young objects belonging to Orion; the large majority of the sources are foreground and background stars. Efficient and reliable young stellar object (YSO) source selection is therefore a critical task. We employ a multicolour selection method that is based on the combination of *JHKs* near-infrared photometry with that in the mid-infrared, and has been proven to provide an optimal distinction between disc-bearing young stellar objects, reddened field stars and galaxies (Harvey et al., 2007). In detail, the location of an object in each of the colour–colour and colour–magnitude diagrams is compared with well-defined boundaries in these diagrams for the expected locations of young stellar objects (Figure 2). The selection is then decided on a combined probability for a source being a young stellar object, based on its location in colour–colour and colour–magnitude space.

This selection method has been applied very successfully to select YSO candidates in star-forming regions observed within the Spitzer c2d and Spitzer Gould Belt legacy surveys (e.g., Evans et al., 2009; Hatchell et al., 2012). In order to apply the same method, we matched our VISTA catalogue with the Spitzer combined Infrared Array Camera (IRAC) and Multi-Band Imaging Photometer (MIPS) catalogue by Megeath et al. (2012), resulting in ~ 58 500 sources with complete ZYJHKs, IRAC 3.6, 4.5, 5.8 and 8 μm and MIPS-24 μm photometry. Figure 2 shows the VISTA/Spitzer colour–colour and colour–magnitude diagrams used to select the YSO candidates in Orion B, which led to a total number of 188 such candidates that are indicated in Figure 2 with red symbols.

Even though we have used a well-tested, robust YSO selection method, remaining contamination from extragalactic sources, foreground main-sequence cool dwarfs, and background red giants is possible. Using the Galactic stellar population model by Robin et al. (2003), we find that the expected number of background giants in the direction of our observed

area, and within the magnitude limits of our survey, is very low (~ 3 stars). Red background giants generally appear much brighter than young Orion members in the same effective temperature range and are therefore easily distinguishable. Similarly, we find from the following experiment that the number of possible galaxy contaminants is very low: we take the SWIRE (Spitzer Wide-area Infrared Extragalactic) catalogue and select an area the same in size as our target area and then place this sample of extragalactic objects behind the Orion B Molecular Cloud. In practice this means applying extinction to the extragalactic objects according to our extinction map of Orion B. Then, we apply our YSO multicolour selection criteria to the reddened SWIRE catalogue objects and check how many targets would be classified as YSOs. Only three objects from the SWIRE catalogue were classified as YSOs (see also lower right panels of Figure 2). In fact, visual inspection of all 188 YSO candidates revealed two objects which appear extended in the VISTA images and could be clearly identified as galaxies. These were rejected from our sample of YSO candidates, i.e., it now numbers 186 objects. The full YSO candidate source list, including their photometry and further information, is described in Spezzi et al. (2015) and is available in electronic data format at the Centre de Données Stellaires (CDS²).

Almost all of the 186 YSO candidates are consistent with an infrared excess typical for young stars with a disc and/or protostellar envelope, i.e., these are sources of class II or earlier in the Lada classification scheme (see below). Moreover, their spatial distribution clearly follows the cloud extinction, i.e. there is a larger clustering of YSO sources at or close to the highest extinction regions of Orion B. Therefore, we conclude that any remaining contamination by foreground cool main-sequence stars (which we believe are the only remaining considerable “polluters” to our YSO sample) is most likely very low.

Properties of the YSOs: luminosity, mass and discs

Now that we have identified the candidate YSOs, we proceed to explore their detailed properties, such as their lumi-

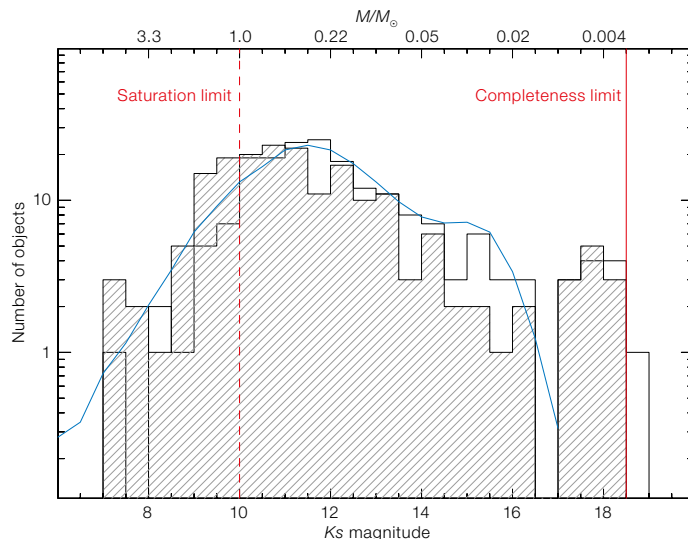


Figure 3. The K_s -band luminosity function (KLF) of the region targeted in Orion B before (empty histogram) and after (line-filled histogram) correction for interstellar extinction. The labels on the upper x -axis indicate the corresponding stellar mass according to the VISTA 2-Myr isochrone. The continuous and dashed vertical lines indicate the completeness and the saturation limit of the VISTA K_s -band photometry, respectively. The continuous curve is the KLF of the Trapezium Cluster, scaled to the peak of the Orion B KLF.

nosities, masses and presence of circumstellar discs. The estimate of the YSO masses is probably the most difficult and we derive it indirectly from the YSOs’ luminosity at K_s -band. Particularly interesting is the frequency mass distribution of the YSOs, i.e., the shape of the mass function, and, related to this, the number of substellar sources. Even though a number of surveys of different star formation regions have been carried out over the last decade, there is still an ongoing debate on the universality or non-universality of the substellar initial mass functions. It appears that, in the environment of a massive stellar cluster, more substellar objects are produced than in low stellar density star-forming environments, such as T-associations.

What is the situation for our studied region in Orion B, which includes the star clusters NGC 2068 and NGC 2071? We constructed the K_s -band luminosity function (KLF) as a proxy for the stellar/substellar mass function. We choose the KLF, rather than the J - or H -band luminosity functions, to minimise the effects of extinction, to maximise our sensitivity to intrinsically red, low luminosity members of this cluster and to make a comparison to the KLF of the nearby Orion Trapezium Cluster presented by Muench et al. (2002).

In Figure 3 we present the observed and de-reddened KLF of our target region in Orion B and overplot, for comparison purposes, the Orion Trapezium KLF. The

KLF of Orion B shows a broad peak at approximately $0.3\text{--}0.7 M_{\odot}$ before it steadily declines into the substellar mass regime. The fraction of substellar objects compared to the total number of YSOs is 28 %, which, after a correction for contamination with field stars, is more like $\sim 20\%$. This, as well as the overall shape of the mass function, is remarkably similar to the Orion Trapezium KLF, which has been reported to have a fraction of substellar objects of $\sim 22\%$ (Muench et al. 2002). We conclude that the star formation environment in Orion B is similarly productive in forming substellar objects as are more massive clusters.

Next, we investigated the circumstellar disc properties of the YSOs. Since YSOs are pre-main sequence objects by definition, the circumstellar discs are protoplanetary discs, i.e., the material surrounding the YSOs are the building blocks for planets. As a matter of fact, our selection criteria has been specifically sensitive to disc-bearing sources and biased against disc-less objects. Hence, it is no surprise that our observations indicate that 97 % of our YSO candidates possess a thick disc and/or a circumstellar envelope. This fraction, however, translates to at most $\sim 85\%$ disc fraction for the complete young stellar sample after accounting for a missed population of disc-less sources.

We further determine the specific nature of the discs from the slope of their spectral energy distributions measured

Region	No. of YSOs	Star formation efficiency (SFE) %	Area (pc ²)	Gas surface density Σ_{gas} ($M_{\odot} \text{pc}^{-2}$)	SFR/Area Σ_{SFR} ($M_{\odot} \text{Myr}^{-1} \text{pc}^{-2}$)
NGC 2071	52	3.8	2.17	180	6.0
NGC 2068	45	5.3	2.12	115	5.4
HH 24-26	14	3.3	0.77	161	4.6

Table 1. Properties of star formation in the substructures in Orion B. The star formation rate (SFR) is derived from the ratio of the YSO mass belonging to a substructure and its age.

over the 2.2 to 24 μm flux points. This so-called Lada classification scheme resulted in 13 % class I sources (envelope plus thick disc dominated YSO), 16 % flat-spectrum sources and 68 % class II sources (thick disc dominated sources). If star formation has been continuous over a period longer than the age of class II sources, the lifetime for each phase can be estimated by taking the ratio of number counts in each class with respect to class II counts and multiplying by the lifetime for class II. According to the statistics of the derived Lada classes in Orion B, we estimate a lifetime of 0.4 and 0.48 Myr for the class I and flat-spectrum phases, respectively. These values agree well with the average lifetimes derived for several star-forming regions observed in the Spitzer c2d legacy survey (Evans et al., 2009).

Spatial clustering and global star formation properties

Looking at the molecular cloud as a whole, the total number of YSOs and their spatial distribution allow us to characterise the efficiency of star formation of a cloud, as well as to establish any preferred star formation mode. The YSO candidates identified in Orion B are located close to the sites of highest extinction, which in turn are associated with the approximate centres of the young stellar clusters NGC 2068 and NGC 2071. We also find a clear concentration of class I and flat spectrum sources at the extinction peak associated with the HH 24-26 group of Herbig–Haro objects, confirming that this region is a place of currently very active star formation. A more detailed analysis of the clustering structures is based on the volume density of YSOs. We calculate that for all the sites of star formation (NGC 2068, NGC 2071, HH 24-26) the volume density

is $\sim 10 M_{\odot} \text{pc}^{-3}$. Following the criteria adopted in the Spitzer c2d legacy survey (Evans et al., 2009), this classifies NGC 2068 and NGC 2071, which each contain more than 35 YSOs, as clusters and HH 24-26 as a stellar group. More than half of all YSO candidates identified in our study belong to NGC 2068 or NGC 2071, hence the majority of star formation in this part of Orion B appears to occur in a clustered mode, which confirms the conclusions of the early study by Lada et al. (1991).

Another interesting aspect is to investigate the efficiency with which Orion B turns molecular gas into stars. Intuitively one might think that more massive molecular clouds are more active in forming stars, but some studies have shown that it is rather a question of how much of a cloud's mass lies above a gas surface density threshold of $\Sigma_{\text{gas}} \sim 129 M_{\odot} \text{pc}^{-2}$ (Lada et al., 2010; Heiderman et al., 2010).

We determined the overall molecular cloud mass and the gas surface density in our studied region of Orion B and in the respective substructures, i.e., in the clusters and group, using our extinction map and assuming a distance to Orion B of 400 pc. The extinction map was constructed from our multi-band near-infrared photometry utilising the near-infrared colour excess method (see details in Spezzi et al., 2015). The measured extinction is converted to a gas column density and gas mass surface density via the well-known relationship $N_{\text{H}}/A_{\text{V}} = 1.87 \times 10^{21} \text{ atoms cm}^{-2} \text{ mag}^{-1}$.

Furthermore, the star formation efficiency (SFE) for each of the clusters is derived from the gas mass associated with each and their mass in stars, i.e. $\text{SFE} = M_{\text{stars}} / (M_{\text{stars}} + M_{\text{cloud}})$. The results are presented in Table 1. These clearly suggest that NGC 2071 and HH 24-26 are active sites of star formation, while NGC 2068 appears to be in a more evolved state. The overall SFE is $\sim 4\%$ on average, which is generally consistent with the values measured for Orion A and B, and for

the majority of star-forming regions in the Galaxy (e.g., Federrath & Klessen, 2013).

Pre-main sequence isochrones in the VISTA photometric system

The CASU data reduction pipeline provides photometrically calibrated images and source catalogues in the VISTA filter system. However, the commonly used theoretical isochrones for low-mass stars and brown dwarfs by Baraffe et al. (1998) and Chabrier et al. (2000) are in the Cousins photometric system. Therefore, we transformed these isochrones into the specific VISTA photometric system and made them available to the community at the CDS website². Please refer to Spezzi et al. (2015) for details of the procedure adopted to perform the conversion of the evolutionary model isochrones. These VISTA isochrones should be a valuable tool for use in wide-field VISTA-based searches for very low-mass stars and brown dwarfs in other star-forming regions.

Acknowledgements

We would like to thank the CASU astronomical data centre for their support and for providing the reduced catalogues and images. Also, the commissioning work of the VISTA telescope and camera carried out by the UK-based VISTA consortium has been greatly appreciated. JMA acknowledge financial support from INAF, under the PRIN2013 programme Disks, Jets and the Dawn of Planets.

References

- Baraffe, I. et al. 1998, A&A, 337, 403
- Chabrier, G. et al. 2000, ApJ, 542, 464
- Evans, N. J. et al. 2009, ApJS, 181, 321
- Federrath, C. & Klessen, R. S. 2013, ApJ, 763, 51
- Flaherty, K. M. & Muzerolle, J. 2008, AJ, 135, 966
- Harvey, P. et al. 2007, ApJ, 663, 1149
- Hatchell, J. et al. 2012, ApJ, 754, 104
- Heiderman, A. et al. 2010, ApJ, 723, 1019
- Lada, C. J. et al. 1991, ApJ, 371, 171
- Lada, C. J. et al. 2010, ApJ, 724, 687
- Megeath, S. T. et al. 2012, AJ, 144, 192
- Muench, A. A. et al. 2002, ApJ, 573, 366
- Petr-Gotzens, M. et al. 2011, The Messenger, 145, 29
- Robin, A. C. et al. 2003, A&A, 409, 523
- Spezzi, L. et al. 2015, A&A, 581, 140

Links

- ¹ CASU VISTA pipeline: <http://apm49.ast.cam.ac.uk/surveys-projects/vista/vdfs>
- ² Vizier at CDS: <http://vizier.cfa.harvard.edu/viz-bin/VizieR?-source=J/A+A/581/A140>

Revealing the Complex Dynamics of the Atmospheres of Red Supergiants with the Very Large Telescope Interferometer

Keiichi Ohnaka¹
 Gerd Weigelt²
 Karl-Heinz Hofmann²
 Dieter Schertl²

¹ Instituto de Astronomía, Universidad Católica del Norte, Antofagasta, Chile

² Max-Planck-Institut für Radioastronomie, Bonn, Germany

Massive stars lose a significant fraction of their initial mass when they evolve to red supergiants before they end their life in supernova explosions. The mass loss greatly affects their final fate. However, the mass loss from these dying supergiants is not yet understood well. Here we present our efforts to spatially resolve the dynamics of the atmospheres of red supergiants with the Very Large Telescope Interferometer (VLTI) and the AMBER instrument to clarify the physical mechanism behind the mass loss. The VLTI/AMBER's combination of milliarcsecond spatial resolution and high spectral resolution allows us to spatially resolve stellar atmospheres and extract the dynamical information at each position over the star and the atmosphere — just like observations of the Sun.

Mass loss from red supergiants

Although massive stars are short-lived and rare in number, they have a great influence on their surrounding environment. For example, powerful stellar winds and supernova (SN) explosions can trigger or quench star formation activities. They also play an important role in the enrichment of carbon, nitrogen and oxygen in the interstellar medium. Hot massive stars are also the primary source of ionising radiation in galaxies. Nevertheless, the evolution of massive stars is not yet well understood. One of the major reasons is our poor understanding of the mass loss. Particularly at the ends of their lives, massive stars experience intense mass loss. In the red supergiant (RSG) phase, the mass-loss rate dramatically increases up to $\sim 10^{-4} M_{\odot} \text{ yr}^{-1}$. Some extreme RSGs appear to have shed as much as a few solar masses.

Obviously, such drastic mass loss affects the final fate of massive stars. For example, the mass loss in the RSG phase is a key to understanding the progenitor mass of SNe Type IIp, which are the most common core-collapse SNe.

Despite its importance, the mass-loss mechanism in RSGs is one of the long-standing problems in stellar astrophysics. It is often argued that dust forms in the cool atmosphere of RSGs, and that radiation pressure on dust grains initiates a mass outflow, dragging the gas along. However, it is still controversial how and where dust forms in RSGs and there is currently no viable theory for the mass loss from RSGs. How can observations help to improve our understanding of the mass loss?

Need for high spatial and high spectral resolution

The stellar winds of RSGs are considered to be accelerated within ten stellar radii from the star, and therefore, a better understanding of the dynamics of this region — the outer atmosphere — is of paramount importance for solving the mass-loss problem. However, the outer atmosphere is very complex, as the best-studied RSG Betelgeuse (α Ori) illustrates. On the one hand, its ultraviolet image taken with the Hubble Space Telescope shows a chromosphere extending up to two to three stellar radii (Gilliland & Dupree, 1996). On the other hand, the radio map taken at 7 mm with the Very Large Array reveals cooler gas at 1000–3500 K, which also extends to about two stellar radii (Lim et al., 1998). Infrared spectroscopic and interferometric observations also suggest the presence of a molecular outer atmosphere, known as the MOLsphere, at 1000–2000 K extending to about 1.3 stellar radii (Ohnaka et al. [2011] and references therein). This means that the hot chromospheric gas (6000–8000 K) and cooler neutral and molecular gas (1000–3500 K) coexist within a few stellar radii. Perhaps the hot chromospheric gas is confined in magnetically active regions with a small filling factor and embedded in more massive cool material (Harper & Brown, 2006).

Given the complex, multicomponent nature of the outer atmosphere, it is necessary to spatially resolve this key region, in order to clarify how the RSG winds are accelerated and understand the physics behind the mass loss. However, this is easy to say but hard to do because of the angular scale of the outer atmosphere. Even the angular diameter of the closest RSG, Betelgeuse, is a mere 42.5 milliarcseconds (mas). We need milliarcsecond spatial resolution and high spectral resolution to spatially resolve the detailed structures of the outer atmosphere and extract information about its dynamics.

Velocity-resolved aperture-synthesis imaging of stellar atmospheres with VLTI/AMBER

The near-infrared VLTI instrument AMBER (Petrov et al., 2007), which combines milliarcsecond spatial resolution achieved by infrared long-baseline interferometry and high spectral resolution of up to 12 000, provides us with a unique opportunity to spatially resolve the dynamics of the outer atmosphere. We have been working on spatially resolving the velocity field in the outer atmosphere of the best-studied RSGs, Betelgeuse and Antares (α Sco), with AMBER. We focus on the CO first overtone lines near 2.3 μm . These lines are ideal for probing the properties of the upper photosphere and the outer atmosphere.

Taking advantage of AMBER's high spatial and high spectral resolution, we have carried out 1D aperture-synthesis imaging of Betelgeuse in the individual CO lines with a spatial resolution of 9.8 mas, which is more than four times smaller than the star's angular diameter (Ohnaka et al., 2011). To be precise, the reconstructed 1D images represent the 1D projection of the actual 2D images of the star obtained by squashing them onto the direction in the sky defined by the linear uv Fourier plane coverage of our observations. Figure 1 presents the 1D projection images reconstructed in the blue wing, line centre and red wing within one of the observed CO lines as well as in the continuum. As seen in the figure (top left insets), AMBER's spectral resolution allows us to not only resolve the individ-

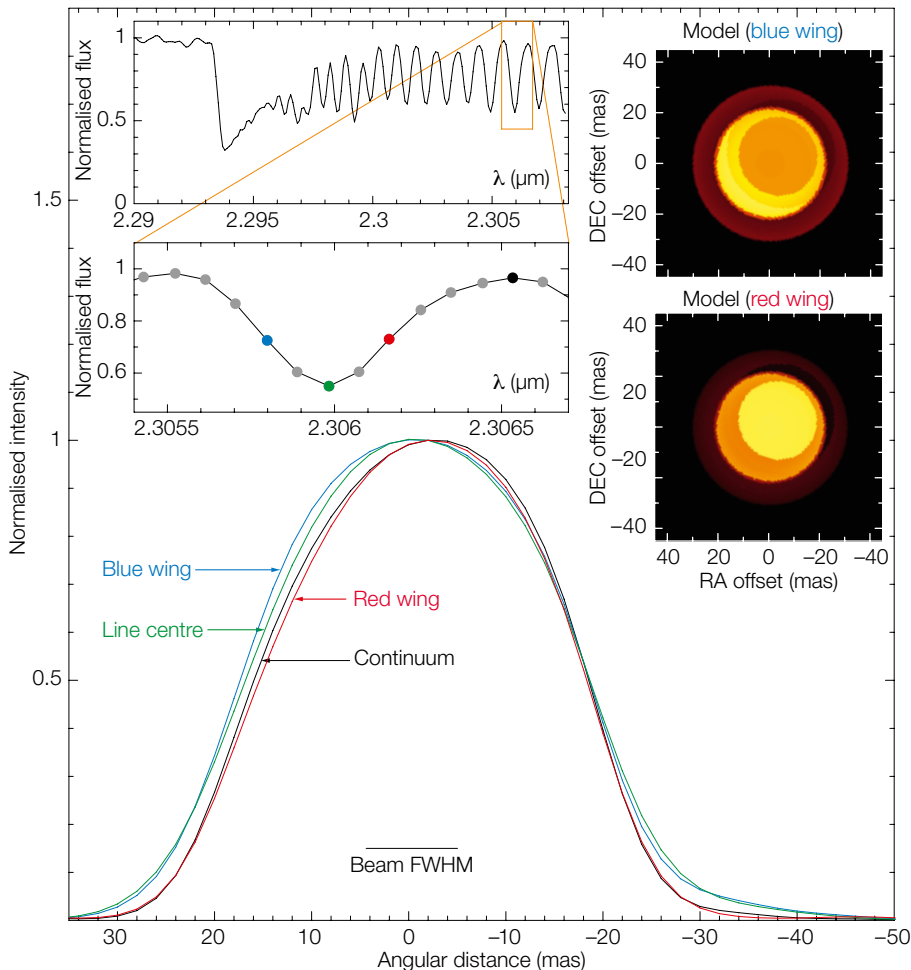


Figure 1. Velocity-resolved aperture-synthesis imaging of Betelgeuse with VLTI and AMBER. The upper left insets show the observed CO line spectrum of Betelgeuse with an expanded view of the 2.306 μm line. The 1D projection images reconstructed in the blue wing, line centre, and red wing within one of the observed CO lines as well as in the continuum are plotted at the bottom. The wavelengths of these 1D images are marked with the blue, green, red and black dots in the lower of the left insets. The 1D images are convolved with a beam of full width at half maximum (FWHM) 9.8 mas. The upper right insets present 2D images of our model in the blue and red wings of the line.

ual CO lines, but also to have approximately ten wavelength points across each CO line profile. The reconstructed 1D images in the line centre and the blue wing clearly reveal an extended atmosphere up to 1.3 stellar radii compared to the continuum image (see the profiles in Figure 1). This is the first study to image the extended, molecular outer atmosphere (MOLsphere) of an RSG in individual CO first overtone lines.

More interestingly, the star appears differently in the blue wing and red wing of the line profile. While the 1D image in the blue wing (blue line) shows the asymmetrically extended atmosphere as in the line centre, the 1D image in the red wing (red line) shows no signature of the extended atmosphere. Rather, it closely follows the continuum image (black line). This is unexpected. If the line depth is the same in the blue wing and red wing of a line, the star should appear extended by the same amount compared to the continuum. However, if the atmosphere is inhomogeneous (for example, the gas in some regions in the atmosphere is moving outward, while it is moving inward in other regions), the star can appear differently in the blue and red wings of the line.

We examined this idea with a simple model. The upper right insets in Figure 1 show 2D images of our model in the blue

wing and red wing. We assumed a large gas clump, which is upwelling slowly at 0–5 km s^{-1} . This produces blueshifted absorption, leading to a lower intensity in the blue wing image (seen as the orange circular region in the upper right inset). On the other hand, the gas outside this clump is downfalling much faster at 20–30 km s^{-1} , which produces redshifted absorption. Therefore, as the lower right inset shows, the intensity outside the clump is lower in the red wing image (seen as the orange crescent-like shape). Obviously, the model images in the blue wing and red wing appear differently. The 1D projection images computed from these 2D model images can explain the observed change in the 1D images within the CO line profiles reasonably well. Therefore, we have spatially resolved the inhomogeneous velocity field of the outer atmosphere of Betelgeuse, which is characterised by vigorous upwelling and downdrafting motions of a gas clump as large as the radius of the star. Our velocity-resolved aperture-synthesis imaging, which is possible only with AMBER’s high spectral resolution, opens an entirely new window to probe the dynamics of stellar atmospheres and winds.

Spatially resolved spectra of stellar atmospheres—observing stars as in Solar observations

The high spatial and high spectral resolution images reconstructed from the AMBER data also allow us to extract the spatially resolved spectrum at each position of the stellar disc and the atmosphere. Instead of plotting the 1D images as in Figure 1, we can make a strip of the colour-coded intensity at each wavelength. By putting these strips side by side, we obtain a 2D spectrum (Figure 2), in which the intensity is represented in colours as a function of the wavelength (horizontal axis) and the angular distance from the star (vertical axis). This is equivalent to high-resolution long-slit spectroscopy data with an angular resolution of 9.8 mas.

The 2D spectrum shows a number of spikes sticking out upward and downward at the wavelengths of the CO lines. They correspond to the extended atmosphere detected in the 1D images shown

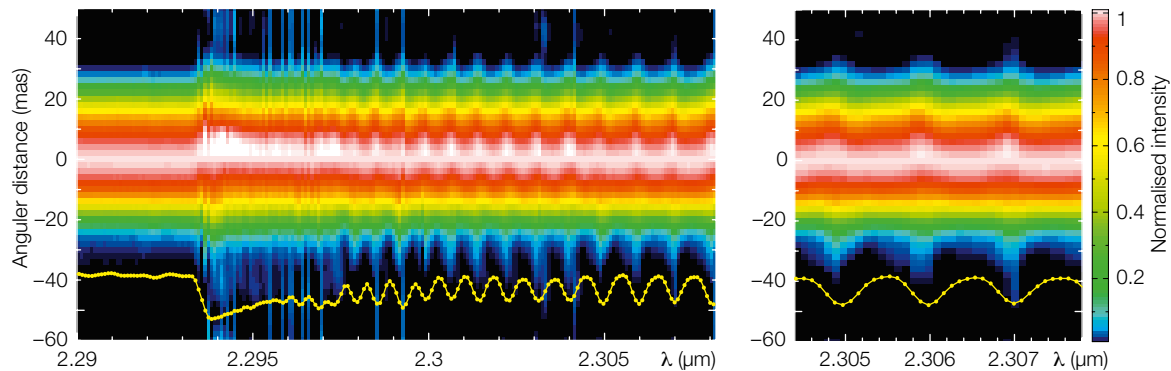


Figure 2. Spatially resolved 2D spectra of Betelgeuse reconstructed from the 1D aperture-synthesis images obtained with AMBER (left: from 2.29 to 2.308 μm ; right: an enlargement for three CO lines). The spatially unresolved spectrum is shown in yellow at the bottom of both plots.

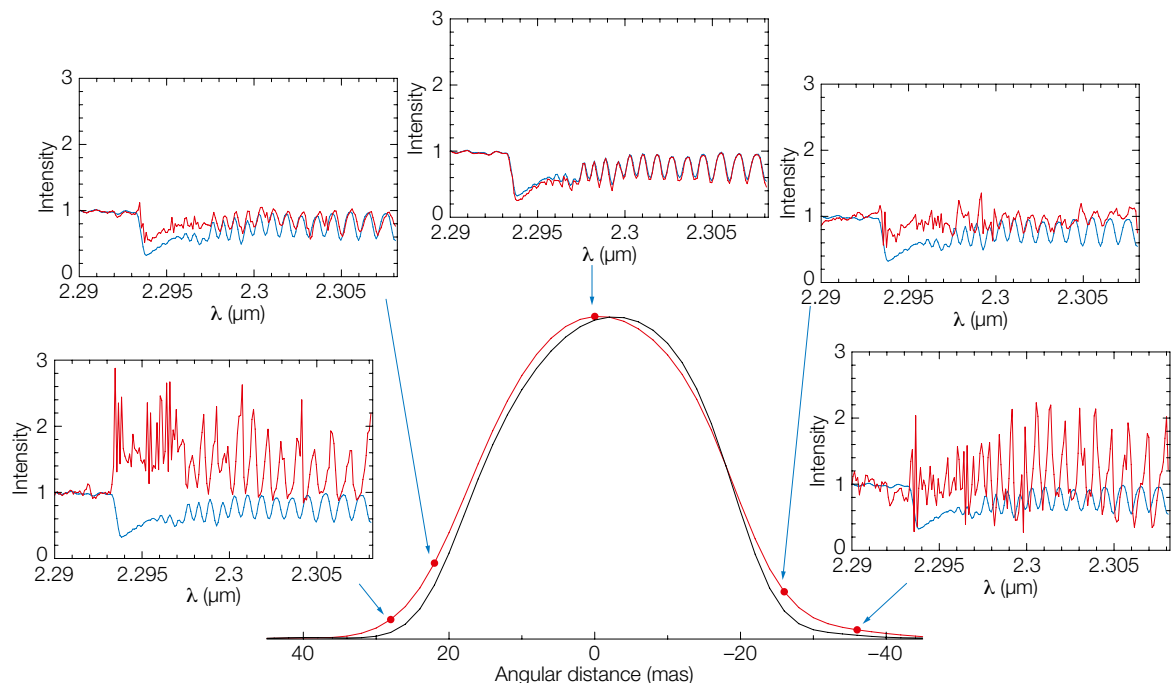


Figure 3. Spatially resolved CO line spectra of Betelgeuse extracted at five representative positions in the 1D image (red: CO line centre image, black: continuum image). In each panel, the spatially resolved spectrum is plotted in red, while the spatially unresolved spectrum is plotted in blue. All spectra are normalised to 1 in the continuum.

in Figure 1. We clearly see that the extended atmosphere is asymmetric with respect to the centre of the star: it is more extended in one direction (downward in the figure) than in the other direction (upward in the figure). The asymmetry of the extended atmosphere in the CO lines also gives rise to the wiggle running along the middle of the 2D spectrum horizontally. A closer look at the 2D spectrum, shown in Figure 2 (right), reveals that the spikes appear only in the blue half within the CO line profiles, reflecting the fact that the extended atmosphere is seen only in the blue wing and the line centre, as plotted in Figure 1.

We can extract the spatially resolved spectrum at each position by taking a horizontal cut of the 2D spectrum. Fig-

ure 3 shows the spatially resolved spectra at five representative positions derived in this manner. While the spectrum at the centre of the stellar disc (angular distance 0 mas) follows closely the spatially unresolved spectrum (that is, obtained by conventional spectroscopy), the spatially resolved spectra from the extended atmosphere (angular distances +28 and -36 mas) show prominent emission. The spectral line features become weak near the limb of the star (angular distances +22 and -26 mas), because the emission from the extended atmosphere and the absorption from the stellar disc cancel out due to the finite beam size. This result — the spectral lines turn from absorption to emission in the spatially resolved spectra of the atmosphere — is exactly what is expected from Kirchhoff's laws.

Our result demonstrates the feasibility of obtaining spatially resolved spectra over the stellar disc and atmosphere of stars other than the Sun. Moreover, it is straightforward to derive the (line-of-sight) velocity of the gas at each position and obtain a 2D map of the velocity field. We are currently working on such programmes for the RSG Antares and the red giant R Dor.

Velocity-resolved imaging of the temporally variable atmosphere of Antares

We also carried out velocity-resolved aperture-synthesis imaging of another well-studied RSG, Antares, with AMBER (Ohnaka et al., 2013). We observed in the same wavelength region with the CO

first overtone lines as in the above observations of Betelgeuse, at two epochs, one year apart. Figure 4 shows the reconstructed images across one of the observed CO lines, in which the continuum image is subtracted to enhance the extended component. As in the case of Betelgeuse, the extended atmosphere of Antares appears differently across the line profile, which means that we have spatially resolved a similar inhomogeneous velocity field in Antares as well. Moreover, while the line profiles observed at two epochs exhibit very little change (the black and red lines in the top row of the figure), the aperture-synthesis images reveal noticeable time variations. The extended atmosphere is seen in the red wing and line centre in 2009, while it is seen in the blue wing and line centre in 2010. This implies a significant change in the velocity field within one year.

What causes the vigorous, turbulent motions in the outer atmosphere?

Our velocity-resolved aperture-synthesis imaging of Betelgeuse and Antares has revealed vigorous, inhomogeneous upwelling and downdrafting motions of large gas clumps in the molecular outer atmosphere extending to at least 1.3 stellar radii. These gas motions are qualitatively similar to the motions of the much hotter chromospheric gas extending to two to three stellar radii (Lobel & Dupree, 2001). The complex gas dynamics are very different from the stationary, monotonic acceleration of the stellar winds, which is often adopted in the modelling of the circumstellar envelope.

What can be responsible for the inhomogeneous velocity field in the outer atmospheres of Betelgeuse and Antares (and perhaps RSGs in general)? The turbulent motions of large gas clumps may be reminiscent of large convective cells. However, the density of the outer atmosphere at 1.2 stellar radii derived from the observed images is $\sim 10^{-14} \text{ g cm}^{-3}$, which is more than six orders of magnitude higher than predicted by the current 3D convection simulations for RSGs (e.g., Chiavassa et al., 2011). This suggests that while convection can induce inhomogeneities in the deep photospheric layers as observed (e.g., Montargès et al., 2014), it

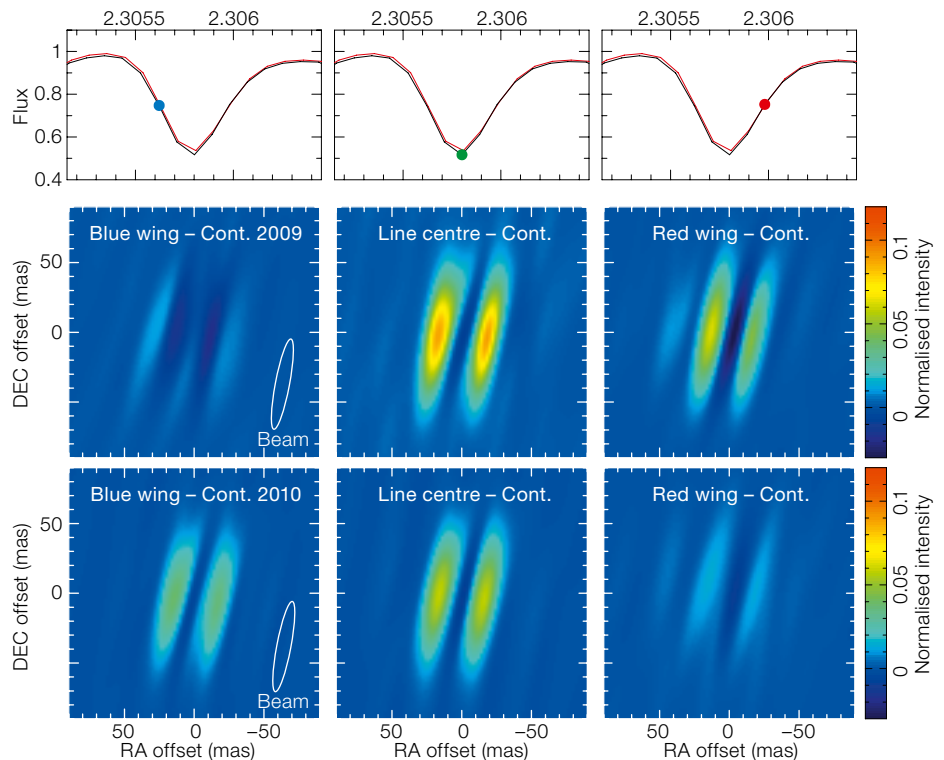


Figure 4. Continuum-subtracted aperture-synthesis images of Antares in the blue wing, line centre, and red wing (left to right) within one of the observed CO lines. The top row shows the line profiles observed in 2009 (black) and 2010 (red), with the

wavelengths of the reconstructed images marked with the dots. The middle and bottom rows show the images obtained in 2009 and 2010, respectively. The beam is quite elongated because of the elongated uv plane coverage.

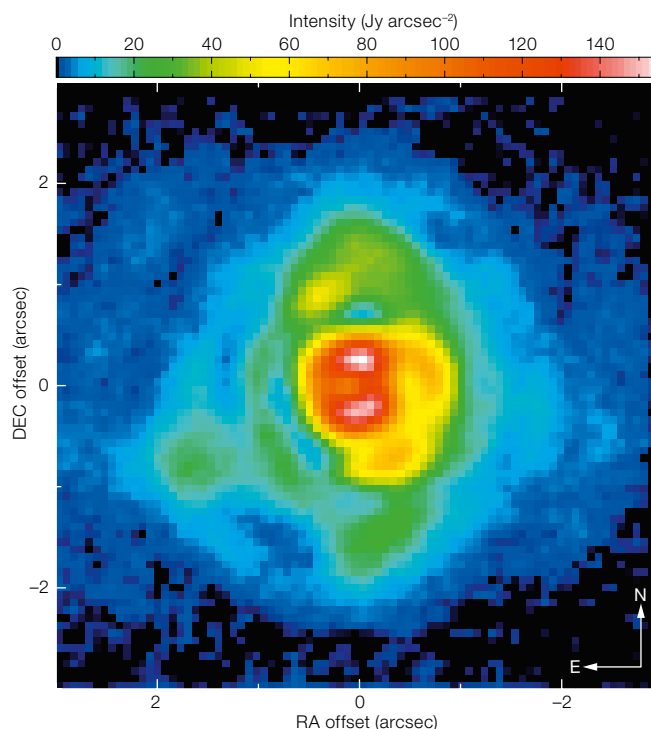


Figure 5. VISIR image of Antares obtained at $17.7 \mu\text{m}$ (Ohnaka, 2014). The central star is subtracted to clearly show the clumpy circumstellar envelope.

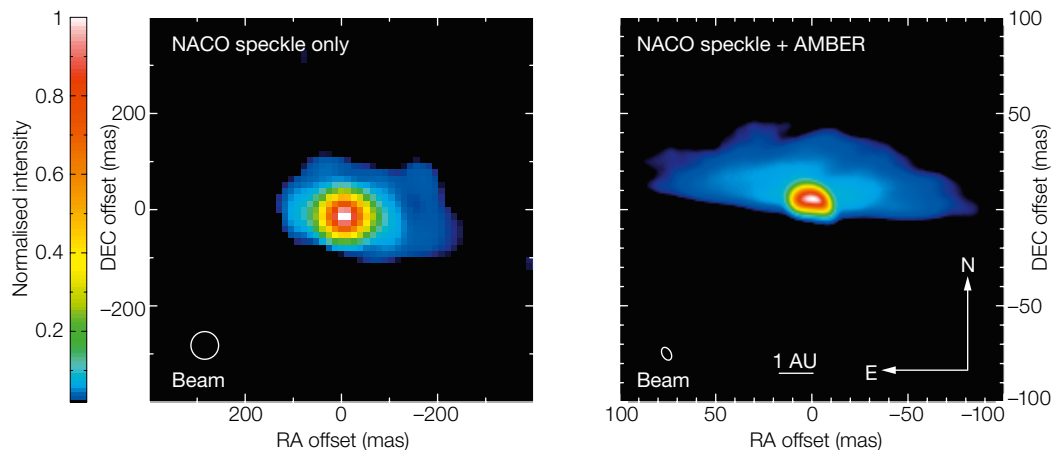


Figure 6. Aperture-synthesis imaging of the dust disc and the half-obscured central star of the red giant L_2 Pup (Ohnaka et al., 2015). Left: Image reconstructed from the speckle interferometric data obtained with NACO. Right: Image reconstructed by combining the NACO speckle data and the AMBER data.

is not sufficient to lift up the atmosphere to the observed 1.3 stellar radii.

What else can be causing the detected, inhomogeneous, vigorous gas motions? Given the detection of magnetic fields on Betelgeuse (Aurière et al., 2010), the magnetohydrodynamical (MHD) process might be responsible. However, at the moment, there is neither an observational smoking gun nor a self-consistent theoretical model to explain it. An alternative scenario is radiation pressure on molecular lines (Arroyo-Torres et al., 2015). The physical mechanism behind the vigorous turbulent motions in the outer atmosphere of RSGs remains to be unveiled.

The inhomogeneous velocity field in the outer atmosphere is likely the seed of the clumpy structures seen in the circumstellar envelope of Betelgeuse and Antares on larger spatial scales. The VLT spectrometer and imager for the mid-infrared (VISIR) imaging of Betelgeuse in the mid-infrared show an asymmetric, clumpy circumstellar envelope extending up to 2 arcseconds (or 94 stellar radii, Kervella et al., 2011). Our $17.7 \mu\text{m}$ image of Antares taken with VISIR, shown in Figure 5, also reveals clumpy dust clouds at 0.8–1.8 arcseconds, which correspond to 43–96 stellar radii. These dust clouds may have formed from large, upwelling gas clumps that were further accelerated and have managed to escape the star’s gravitational potential.

Next steps

We can push velocity-resolved aperture-synthesis imaging one step further to probe the gas dynamics throughout the atmosphere. The velocity-resolved imaging in different molecular or atomic lines forming in different atmospheric layers allows us to obtain a 3D picture of the dynamics, from the deep photospheric layers to the outer atmosphere. Furthermore, the combination of this tomographic velocity-resolved aperture-synthesis imaging with the VLTI and the Atacama Large Millimeter/submillimeter Array (ALMA) observations of molecular lines will help us understand how energy and momentum propagate throughout the atmosphere to the innermost circumstellar envelope and pin down the driving force of the RSG mass loss. At the same time, we will be able to carry out imaging of the surface and atmosphere of RSGs more efficiently and for more stars with the second generation VLTI instruments GRAVITY and the Multi AperTure mid-Infrared Spectro-Scopic Experiment (MATISSE). Their accuracy and sensitivity, combined with spectral resolution of 4000–5000, will enable us to obtain detailed images of RSGs in many more spectral lines than have been explored up to now.

While the VISIR image of Antares (Figure 5) implies a link between the formation of dust clouds and the turbulent motions of large gas clumps in the outer atmosphere, we have yet to clarify where and how dust forms in RSGs. To illustrate that the imaging with VLTI is also promis-

ing for this goal, we show our recent results for the red giant L_2 Pup in Figure 6 (Ohnaka et al., 2015). We succeeded in aperture-synthesis imaging at $2.2 \mu\text{m}$ by combining speckle interferometric observations with the Nasmyth Adaptive Optics System and the high resolution near-infrared camera (NACO) on the VLT and long-baseline interferometric observations with AMBER and VLTI. The reconstructed image with a beam size of $5.6 \times 7.3 \text{ mas}$ has revealed not only the nearly edge-on dust disc, but also the half-obscured central star within the equatorial dust lane. The second generation VLTI instrument MATISSE, which will enable us to carry out aperture-synthesis imaging in the thermal infrared from 3 to $13 \mu\text{m}$, will provide an excellent opportunity to probe the dust formation in RSGs extensively. Therefore, in the coming years, we can expect to obtain a comprehensive picture from the photosphere to the outer atmosphere to the inner circumstellar envelope, which is indispensable to finally solving the mass-loss problem.

References

- Arroyo-Torres, B. et al. 2015, *A&A*, 575, A50
- Aurière, M. et al. 2010, *A&A*, 516, L2
- Chiavassa, A. et al. 2011, *A&A*, 535, A22
- Gilliland, R. L. & Dupree, A. K. 1996, *ApJ*, 463, L29
- Harper, G. M. & Brown, A. 2006, *ApJ*, 646, 1179
- Kervella, P. et al. 2011, *A&A*, 531, A117
- Lim, J. et al. 1998, *Nature*, 392, 575
- Lobel, A. & Dupree, A. K. 2001, *ApJ*, 558, 815
- Montargès, M. et al. 2014, *A&A*, 572, A17
- Ohnaka, K. et al. 2011, *A&A*, 529, A163
- Ohnaka, K. et al. 2013, *A&A*, 555, A24
- Ohnaka, K. 2014, *A&A*, 568, A17
- Ohnaka, K. et al. 2015, *A&A*, 581, A127
- Petrov, R. G. et al. 2007, *A&A*, 464, 1

Beyond Phase 3: The FORS1 Catalogue of Stellar Magnetic Fields

Stefano Bagnulo¹
John D. Landstreet^{1,2}
Luca Fossati³

¹ Armagh Observatory, College Hill,
Armagh, United Kingdom

² University of Western Ontario, London,
Canada

³ Space Research Institute, Austrian
Academy of Sciences, Graz, Austria

Over the course of a decade of operations, more than 200 nights of telescope time have been granted for magnetic field measurements with the FORS1 instrument on the VLT. Motivated by some conflicting results published in the literature, we have studied the instrument characteristics and critically revised previous magnetic field detections obtained with FORS1. Our study has led to the publication of a catalogue of 1400 magnetic field measurements of a sample of 850 different stars, together with their intensity spectra. This catalogue includes nearly all the circular spectropolarimetric measurements taken during ten years of operation. Here we summarise some of the lessons learned from the analysis of the FORS1 stellar spectropolarimetric archive.

The twin Focal Reducer and low dispersion Spectrograph FORS1/2 instruments (Appenzeller et al., 1998), operated at the Paranal Observatory, have been one of the great success stories of the Very Large Telescope (VLT) instrumentation. These two instruments are versatile tools for observing faint objects, primarily with direct imaging and low-resolution multi-object spectroscopy over the full optical band. FORS1 was in use from 1999 until 2009; FORS2 is still in regular use. In addition to its imaging and spectroscopic capabilities, FORS1 was equipped with polarimetric optics, and when FORS1 was retired, its polarisation optics system was moved to FORS2 and is still available.

The FORS polarimeters were originally intended for observations of rather faint objects. Examples are: broadband and emission-line linear polarisation spectra of pre-main sequence Herbig Ae and Be stars and faint classical Be stars; meas-

urement of the interstellar polarisation of extragalactic stars; intrinsic polarisation of the nuclei of Seyfert galaxies and AM Herculis white dwarfs; and circular spectropolarimetry of line and continuum radiation of magnetic white dwarfs with fields of hundreds of Tesla (100 Tesla = 1 megaGauss, MG) or more. However, it turned out that a non-negligible fraction of FORS1 time was used instead to measure relatively weak fields of bright stars.

Measuring magnetic fields with FORS

Magnetic field measurements with FORS are possible mainly as a consequence of the physics of the Zeeman effect. A spectral line formed in a stellar atmosphere permeated with a strong magnetic field splits into numerous components, one group (π components) centred on the wavelength of the unsplit line, and two other line groups (σ components) shifted to shorter and longer wavelengths around the π components. In a white dwarf with a field of some MG, this splitting is clearly visible in the normal intensity profiles of the common H Balmer lines, and provides a measure of the mean magnetic field strength $\langle |B| \rangle$ averaged over the visible stellar hemisphere. In addition, if the field has a large line-of-sight component, the groups of σ components are circularly polarised in opposite senses.

On account of this combination of line splitting and polarisation, the mean wavelength of the spectral line of a magnetic star, as seen in right circularly polarised light, will be at a slightly different wavelength from that of the same line seen in left circularly polarised light. This wavelength difference is proportional to the mean line-of-sight component of the field $\langle B_z \rangle$, averaged over the visible stellar hemisphere. If the difference between the two line profiles is measured, there will be net circular polarisation of one sign in one wing of the average line, and of the other sign in the other wing. Thus an observational signature of a magnetic field is net circular polarisation in the wings of a spectral line, correlated with the sign of the slope of the line.

With FORS, measurements of this kind were expected to detect even rather weak fields of a few kG using the very broad

Balmer lines of white dwarfs, and in fact such weak fields have been detected (e.g., Aznar Cuadrado et al., 2004). It was not obvious that FORS1 could be used to measure the weaker (hundreds of G) magnetic fields of upper main sequence stars, as such measurements are mainly carried out using sharp metal lines with spectropolarimeters of much higher resolving power than that of FORS. However, an experiment carried out in 2001 to try to measure the kG magnetic field of the known magnetic “peculiar A” (Ap star) HD 94660 revealed that not only is the field of this star readily detectable using the star’s Balmer lines, but that it is also easily measured using the metal line spectrum (Bagnulo et al., 2002). This was a very surprising result. Since almost all the spectral lines are blended, it was expected that the polarisation signature in metal lines would largely cancel out, but in fact the circular polarisation remains closely connected with the local line slope, and magnetic fields are easily detectable.

The principle of magnetic field measurements is summarised in Figure 1. In the upper panel, the black solid line shows the uncorrected detected intensity profile. The red solid line is the reduced Stokes V profile ($P_V = V/I$) in % units. Photon noise error bars are centred on -0.5% and appear as a light blue background, on which the null profile (also offset by -0.5% for display purposes) is superposed (blue solid line). The null profile is an experimental estimate of the error, and should be scattered around zero with the same full width at half maximum (FWHM) as the light blue error bars. Spectral regions, highlighted by green bars above and below the spectra, have been used to determine the $\langle B_z \rangle$ value from H Balmer lines, and the magenta bars highlight the spectral regions used to estimate the magnetic field from metal lines.

The four bottom panels of Figure 1 show the best-fit, obtained by fitting with a straight line, P_V as a function of the quantity $\propto \lambda^2(1/l) (dl/d\lambda)$; where $l(\lambda)$ is the intensity spectrum. The slope of the fitting line is proportional to the mean longitudinal magnetic field. For quality check purposes, the magnetic field $\langle N_z \rangle$ is also measured from the null profile, and is expected to be zero within the error bars.

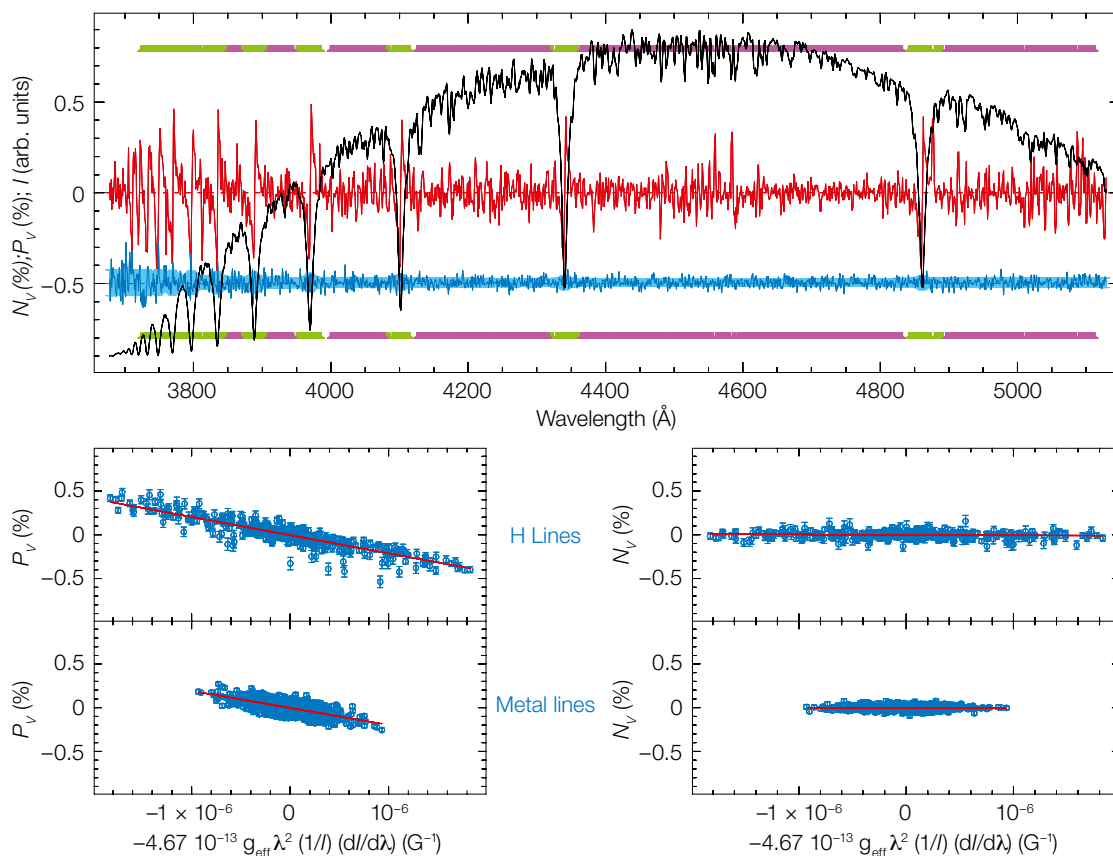


Figure 1. An example of FORS magnetic field measurements: the case of the Ap star HD 94660. The upper plot shows the intensity and Stokes V profiles and the four lower panels show the straight line best fits for P_V . See text for more details.

In this example the field values ($\langle B_z \rangle \sim -2000$ G and $\langle N_z \rangle \sim 0$ G) are determined with a formal precision of ~ 40 G for Balmer lines and ~ 25 G for metal lines, i.e., with an error bar even smaller than from H Balmer lines! With this result, it became clear that FORS1 could be used for measuring magnetic fields in main sequence stars and a large new parameter space for the study of stellar magnetic fields was opened up to investigation with this instrument.

Searching for magnetic fields with FORS

The possibility of using a spectropolarimeter on an 8-metre telescope to observe magnetic fields in stars other than white dwarfs very quickly led to surveys of various kinds of stars little studied before. Wade et al. (2005; 2007) carried out an extensive search for magnetism in pre-main sequence Herbig Ae stars, and discovered a field in the southern star HD 101412, although only at about the 5σ significance level in a single observation. Bagnulo et al. (2006) used

FORS in multi-object mode to search for magnetic fields among magnetic Ap stars (already known to have fairly strong fields) in open clusters. Since stellar ages can be precisely determined from cluster ages, it was possible to use these data to demonstrate that Ap magnetic fields decline strongly with time on the main sequence (Landstreet et al., 2008). A similar investigation, but on field stars, was started by Hubrig et al. (2006).

Hubrig, Schoeller and their collaborators started a number of surveys of Herbig stars, HgMn and PGa stars (the hotter extension of the HgMn stars, with rich P II, Mn II, Ga II and Hg II spectra), pulsating B stars, normal B stars, classical Be stars, and O-type stars (see Hubrig et al. [2009] and references therein). They reported the discovery that magnetic fields are often present in all these kinds of stars. Other programmes focused on compact stars, such as hot subdwarfs (O'Toole et al., 2005) and central stars of planetary nebulae (Jordan et al., 2005), with reports that both these categories of stars are often magnetic.

Not long after a number of magnetic field measurement programmes were started and carried out on FORS1, the Echelle Spectropolarimetric Device for the Observations of Stars (ESPaDONs) high-resolution spectropolarimeter was commissioned on the Canada–France–Hawaii Telescope. When results from the two polarimeters were compared, it became clear that a number of field discoveries reported for a wide variety of stellar types, often on the basis of one or two FORS detections at the 3σ to 5σ level, were not consistent with the non-detections, sometimes with substantially smaller uncertainties, obtained with ESPaDONs (Silvester et al., 2009; Aurière et al., 2010; Shultz et al., 2012). This led us to become concerned by the possibility that FORS data were not being correctly interpreted, and/or that there were subtle problems with FORS in spectropolarimetric mode that had not been identified by observers.

As a result, we started a large project aimed at fully understanding the situation. This began with a basic paper describing

in detail the theory of data reduction in two-beam spectropolarimeters with beam-swapping (Bagnulo et al., 2009). Then we created routines for automatic frame classification and data reduction (particularly with the help of the late ESO software developer, Carlo Izzo). The new suite of programmes (partially based on the ESO FORS pipeline, see Izzo et al. [2010]) was then used to completely re-analyse almost all the magnetic field measurements made with FORS1, in a homogeneous way.

During data reduction, a number of choices have to be made (for example, about how to best deal with spectrum extraction, with cosmic rays, etc.). Use of different reduction algorithms may have small but non-negligible effects on the final measurements, but it is not always obvious how to distinguish a better from a worse choice. Our software tool allowed us to study the effects of various algorithms on a large data sample, sometimes only to conclude that it is not possible to identify the optimal reduction choices, and that the small ambiguities introduced by the data reduction should be considered as additional noise to the final measurement. Most importantly, our analysis of the full dataset allowed us to firmly conclude that the accuracy, claimed for certain measurements, placed demands on FORS1 stability that were probably not realistic, and may well be very difficult for any Cassegrain instrument to meet.

Non-photon noise

While it is very natural to predict that instrument flexure can have a negative impact on the accuracy of a measurement, perhaps it is not so obvious to understand exactly how and why instrument flexure may be responsible for a spurious polarisation signal in a spectral line. In order to understand this, it is necessary to remember that polarimetry is a differential technique, i.e., by definition, both linear and circular polarisations are measured through the difference of two signals. In particular, Stokes V is given by the difference between right- and left-hand circular polarisation (RHP and LHP, respectively). In the case of FORS, the RHP and LHP signals are

obtained by introducing a $\lambda/4$ retarder waveplate and a Wollaston prism into the optical path. A grism (and perhaps an order separator filter) are then introduced in the optical train to perform spectral analysis, and finally a CCD records the intensity of two spectra originally circularly polarised in opposite directions. If the original signal is non-polarised, then after perfectly accurate flatfielding and wavelength calibration, the two spectra are identical, and their difference is only due to noise. If the spectral line is polarised (for instance due to the Zeeman effect), then its LHP and RHP spectra appear slightly offset, and their difference is a non-zero Stokes V spectrum.

The LHP and RHP spectra could be offset as a result of any tiny imperfection in the wavelength calibration. By applying the beam-swapping technique, the LHP and RHP spectra exchange their position in the optical path (this is possible with a simple 90° rotation of the $\lambda/4$ waveplate between subsequent measurements). In this way, most instrumental features cancel out even without the use of calibrations. Beam-swapping can cure some systematic offsets between the beams, e.g., when both RHP and LHP are offset by the same amount after the retarder waveplate rotates, or when there is a systematic offset between RHP and LHP that remains constant as the retarder waveplate rotates. However, it cannot compensate for a differential offset between the RHP and LHP spectra as the retarder waveplate rotates. Some simple numerical simulations (see Bagnulo et al., 2009 and 2013) show that an offset of this kind as small as 1/100 of the FWHM of a spectral line may create a detectable spurious polarisation signal.

In many cases, with FORS, spectral lines are sampled with a few pixels at most, hence a differential flexure of the order of a small fraction of a pixel may produce a spurious signal. It is not always possible to avoid such small amounts of flexure in a Cassegrain mounted instrument, and the occurrence of spurious spikes in the Stokes V spectra is more likely in narrower than in broader lines. Spurious signals due to flexure may sometimes be distinguished from Zeeman signatures by taking into account that the wavelength-integrated Stokes V profile due to Zeeman

effect is zero: therefore a spike in Stokes V that does not obey this rule is likely to be ascribed to flexure.

Instrument flexure is not the only possible source of spurious signals: variations in guiding or even seeing effects may cause the same effect if combined with a less-than-perfect relative wavelength calibration of the RHP and LHP (for details see Bagnulo et al., 2013).

The revised incidence of magnetic fields in various classes of stars

Full data reduction carried out with our suite of programs allowed us to test whether the numerous but controversial detections of apparently significant magnetic fields in a wide variety of stars were robustly reproduced using the best reduction choices identified by our experiments. One of our findings was that uncertainties may be of the order of 30% larger than that expected from photon-counting statistics alone. Our work showed that most of the detections reported on the basis of single $3-5\sigma$ field measurements were spurious (Bagnulo et al., 2012). Some FORS1 field discoveries, usually those at a higher significance level, were confirmed, for example those in the white dwarfs WD0446-789 and WD2359-434 and in the β Cep star ξ^1 CMa. However, the reports that large fractions of pulsating B stars, classical Be stars, normal B stars, O stars, and HgMn peculiar B stars possess weak magnetic fields, as claimed in the articles cited by Hubrig et al. (2009), were generally not confirmed. The discovery that about half of the Herbig Ae/Be stars possess a magnetic field was also not confirmed (Wade et al. [2007] had suggested an occurrence of $\sim 10\%$, consistent with that for main sequence A and B stars). Similarly, we could not confirm any of the field detections in hot subdwarfs and central stars of planetary nebulae — null results were then reported in detail by Leone et al. (2011), Jordan et al. (2012) and Landstreet et al. (2012).

Study of these spurious results, and also the systematic examination of the fairly large body of magnetic field measurements carried out on magnetic Ap stars, allowed us to obtain a clearer

understanding of the strengths and limitations of FORS for measuring weak magnetic fields. In general we found that FORS measurements of a single star are internally consistent at approximately the level expected from the uncertainties derived with our reduction programmes (Landstreet et al., 2014). However, there are occasional measurements that deviate from the expected behaviour by a few σ . We call these inconsistent measures occasional outliers, and find that they seem to occur in a few percent of measurements. Thus field discoveries based on single measurements significant at the 4–5 σ level cannot be considered as definite detections.

A public catalogue of FORS1 magnetic field measurements

As a final outcome of our study of the FORS1 archive, we have published a nearly complete catalogue of re-reduced FORS1 magnetic field measurements (Bagnulo et al., 2015). The FORS1 archive includes about 1400 observing series, for a total of more than about 12 000 scientific frames, obtained within the context of almost 60 observing programmes, using more than 2000 hours of telescope time and about 340 hours of shutter open time. The content of our catalogue is available at Catalogue de Données Stellaires (CDS¹) and Bagnulo et al. (2015) includes an abridged version in the form of a printable table.

This catalogue is not the definitive, ultimate reduction of the FORS1 magnetic dataset however. As discussed in all our earlier papers, several different choices made during data reduction are equally reasonable, but lead to somewhat different results. However, the reductions leading to our catalogue are based on reasonable choices applied in a consistent way to all the FORS1 field measurements. In this respect our catalogue offers a more homogeneous overview than a simple collection of the same measurements in the literature. Our catalogue may be used also for a number of statistical studies, many of them presented in detail by Bagnulo et al. (2012; 2015) and Landstreet et al. (2014).

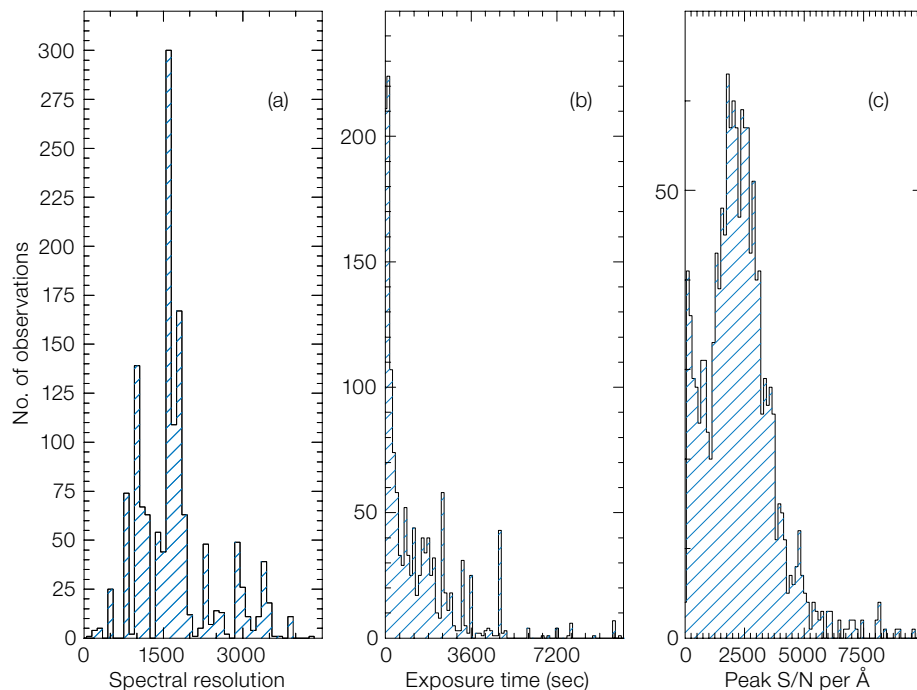


Figure 2 shows three histograms that we have built using data extracted from the FORS1 archive: the distribution of the adopted spectral resolution, the distribution of the exposure time, and the distribution of the peak signal-to-noise reached after an observing series. Looking at this figure, a number of very interesting features are apparent. Panel (a) shows that users wanted to have the highest possible resolution (in fact, magnetic fields are probably best measured at a higher resolution than offered by the FORS grisms), even at the expense of dramatic light losses, as spectral resolution > 1000–1500 could be obtained only by setting the slit width to sub-arcsecond values. On the other hand, panel (b) tells us that light losses were probably not so much of an issue: many observations were carried out with just a few seconds of shutter time, clearly on very bright targets. The high overhead of such short exposures is the main reason for the large discrepancy between assigned telescope time and shutter time. In effect, many programmes were carried out on FORS1 not because it was on an 8-metre telescope, but because it was the only spectropolarimeter available at ESO at the time (see Bagnulo et al., 2012).

Panel (c) shows the distribution of the peak signal-to-noise ratio (S/N) of the

Figure 2. Some statistical data from the analysis of the FORS1 archive of circular spectropolarimetric data. Figure 2a shows the spectral resolution deduced from the analysis of arc lines. The histograms in Figures 2b (shutter time) and 2c (S/N) refer to an observing series (typically composed of eight individual exposures).

observing series used for field measurements. It is interesting to note that even with an 8-metre telescope and with very bright stars, photon noise cannot be pushed down arbitrarily far, due to the CCD saturation limit and the non-negligible amount of CCD readout overheads. The typical maximum electron counts that one can reach in a FORS frame in a 1 Å spectral bin without saturation is generally < 10⁶ (the exact figure depends on the grism dispersion and on seeing), and the typical maximum S/N that can be achieved with a series of eight exposures is 2000–3000. Depending on the spectral type of the star, this corresponds to an error bar of a few tens of Gauss.

The relationship between peak S/N and error bar is shown in Figure 3, which shows that the highest precision that can be achieved, without ridiculously long overheads for CCD readout, is of the order of tens of Gauss (remember that to improve the detection threshold by a factor of two one would need four times the number of exposures). In conclusion,

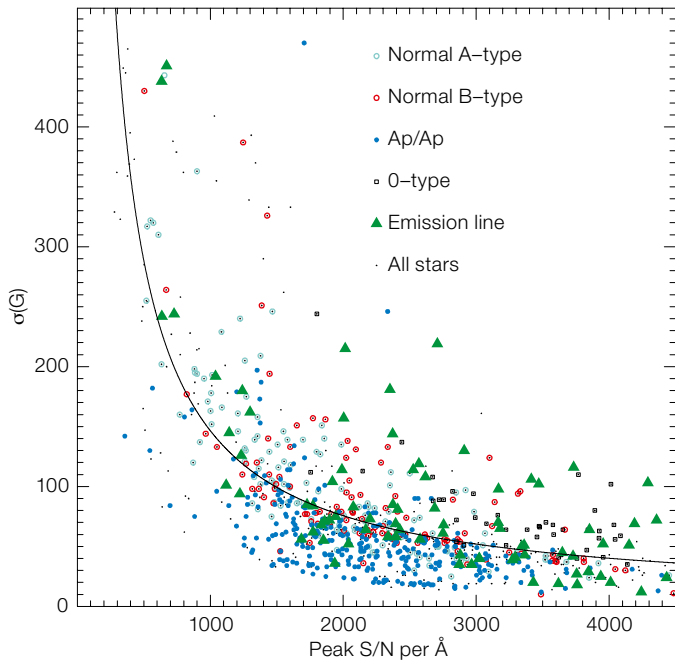


Figure 3. The error bar $\sigma(G)$ from the analysis of all spectral lines as a function of the peak S/N per \AA for various kinds of stars.

satellite and powerful instrument for magnetic field measurements. It is also suitable for projects where enough time is allocated so that initial field discoveries at the few σ level can be confirmed by repeated measurements.

References

- Appenzeller, I. et al. 1998, *The Messenger*, 94, 1
 Aurière, M. et al. 2010, *A&A*, 523, 40
 Aznar Cuadrado, R. et al. 2004, *A&A*, 423, 1081
 Bagnulo, S. et al. 2002, *A&A*, 389, 191
 Bagnulo, S. et al. 2006, *A&A*, 450, 777
 Bagnulo, S. et al. 2009, *PASP*, 121, 993
 Bagnulo, S. et al. 2012, *A&A*, 538, 129
 Bagnulo, S. et al. 2013, *A&A*, 559, 103
 Bagnulo, S. et al. 2015, *A&A*, 583, A115
 Hubrig, S. et al. 2006, *AN*, 327, 289
 Hubrig, S. et al. 2009, *The Messenger*, 135, 21
 Izzo, C. et al. 2010, *SPIE*, 7737, 7737-29
 Jordan, S. et al. 2005, *A&A*, 432, 273
 Jordan, S. et al. 2012, *A&A*, 542, 64
 Landstreet, J. D. et al. 2009, *A&A*, 481, 465
 Landstreet, J. D. et al. 2012, *A&A*, 541, A100
 Landstreet, J. D. et al. 2014, *A&A*, 572, A113
 Leone, F. et al. 2011, *ApJ*, 731, 33
 Manso Sainz, R. 2011, *ApJ*, 731, L33
 O'Toole, S. J. et al. 2005, *A&A*, 437, 227
 Silvester, J. et al. 2009, *MNRAS*, 398, 1505
 Shultz, M. et al. 2012, *ApJ*, 750, 2
 Wade, G. A. et al. 2005, *A&A*, 442L, 31
 Wade, G. A. et al. 2007, *MNRAS*, 376, 1145

Links

- ¹ FORS1 polarimetric star catalogue: <http://cdsarc.u-strasbg.fr/viz-bin/qcat?J/A+A/583/A115>
² FORS2 Exposure Time Calculator: <http://www.eso.org/observing/etc/bin/gen/form?INS.NAME=FORS+INS.MODE=spectro>

even if the error bars were determined only by photon noise, FORS could not achieve the same precision reached with high resolution spectropolarimeters such as ESPaDOnS and HARPSpol.

Complemented by the FORS Exposure Time Calculator², Figure 3 may be used as a tool for planning measurements of magnetic fields with FORS2. More details are given in Bagnulo et al. (2015).

In terms of field measurement accuracy, FORS cannot compete with a high resolution spectropolarimeter sitting on a thermally and mechanically isolated bench (like ESPaDOnS and HARPSpol) and is not the optimal instrument to search for very weak fields ($\leq 100\text{--}200$ G) in bright stars. However, when used with faint objects known or expected to have fields detectable at the several σ level (in particular in objects with broad spectral lines), FORS is an extremely ver-

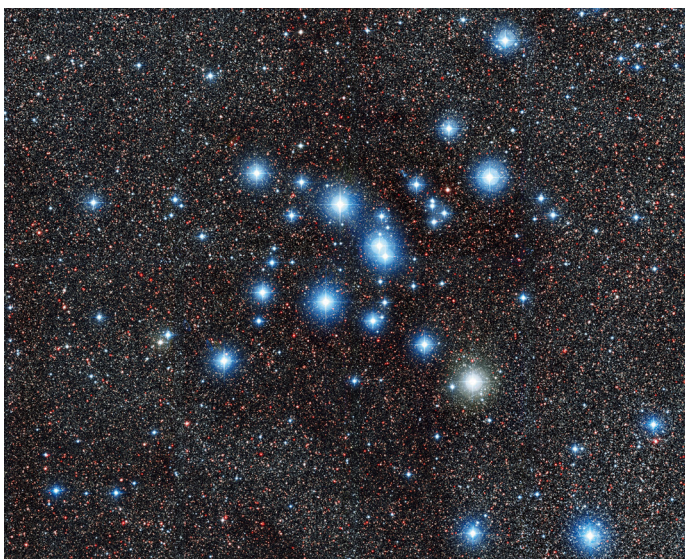


Image of the open cluster NGC 6745 (M7) obtained with the Wide Field Imager (WFI) on the MPG/ESO 2.2-metre telescope. *B*, *V* and *I* filters were combined. NGC 6745 is a young (~ 200 Myr old) open cluster of about 100 stars situated at about 340 pc in the Galactic Plane. See Photo Release eso1406 for further details.



The Prime Minister of Italy, His Excellency Matteo Renzi (centre), visited Paranal on 24 October 2015 and is shown watching the sunset with the ESO Director General Tim de Zeeuw (left).

The signing of an agreement between members of an international consortium of institutes and ESO to build the HARMONI E-ELT instrument took place at Oxford University on 22 September 2015. See [ann15070](#) for details.



Rainbows on the Southern Sky: Science and Legacy Value of the ESO Public Surveys and Large Programmes

held at ESO Headquarters, Garching, Germany, 5–9 October 2015

Magda Arnaboldi¹
Marina Rejkuba¹
Bruno Leibundgut¹
Giacomo Beccari¹

¹ ESO

This was the third ESO workshop on the science from Large Programmes and the second on Public Surveys. By design, this workshop covered all areas of research in observational astronomy, providing a forum for the presentation of the most recent scientific results from these programmes and fostering discussions on the planned developments enabled by large and coherent time allocations on ESO telescopes. Several aspects of the legacy value of such programmes – technological, archival content, access to data, time domain and sociological – were evaluated and set a reference for future developments of ESO services to the community.

Introduction: Large Programmes and Public Surveys at ESO

The ESO Large Programmes were introduced in 1996, following the recommendation of a working group nominated by the Observing Programmes Committee (OPC), with the aim of focusing on specific science goals that require large time allocations, typically more than ten nights (100 hours) and/or observations that span up to four observing periods. Since then, about 13 % of the total available science time on ESO telescopes has been allocated to Large Programmes and more than 150 such programmes have been scheduled at the La Silla Paranal Observatory. A Large Programme is selected after a dedicated discussion that involves the whole OPC (in addition to the panels), and these programmes are expected to target scientific projects that are not possible within the regular time allocation and are relevant for a large fraction of the astronomical community.

Since 2010, ESO Public Surveys, on the Visible and Infrared Survey Telescope for Astronomy (VISTA), the VLT Survey Telescope (VST), the Very Large Telescope

(VLT) and the New Technology Telescope (NTT), were added to the portfolio of programmes enlarging the observational perspectives available to the community. The Public Surveys lead to an increase in the legacy value of data from ESO telescopes on account of their homogeneity and uniformity for the sky area covered and often include a time-domain component. In 2010 and 2011, the nine imaging Public Surveys started on VISTA and the VST, and were soon followed by the spectroscopic Public Surveys: PESSTO (Public ESO Spectroscopic Survey of Transient Objects) on the NTT; and Gaia-ESO, LEGA-C (Large Early Galaxy Astrophysics Census) and VANDELS (A deep VIMOS survey of the CANDELS Fields), all on the VLT. The raw data from all Public Surveys are immediately public. In addition, these programmes produce science data products, reduced images and spectra, as well as catalogues of astrophysical measurements extracted from the science data. The science data products delivered by the Public Surveys, and published via the ESO Science Archive Facility (SAF), support new ways of conducting research and effectively enlarge the scientific community using ESO services.

ESO regularly organises workshops that present an overview of the scientific advances enabled by the use of its facilities and provide a forum for input by the community on promising new projects and programmes. The assessment of the scientific return from the Large Programmes was the goal of two workshops in 2003 (Wagner & Leibundgut, 2004) and in 2008 (Mathys & Leibundgut, 2009); the presentation of, and the first results from, the imaging Public Surveys were discussed in 2012 (Arnaboldi & Rejkuba, 2012). The first Large Programmes workshop in 2004 included a discussion with the community on surveys, which ultimately led to the establishment of ESO Public Surveys. The 13 ongoing ESO Public Surveys and a representative set of recently completed Large Programmes were now the focus of the workshop referred to as the Rainbows2015 workshop¹ and reported here.

The workshop covered all areas of observational astronomy and the presentations were organised in seven sessions: planets; stars; the Milky Way and Local Group;

extragalactic astronomy; galaxy evolution; the high-redshift Universe and cosmology; and the legacy value of Public Surveys and Large Programmes. Keynote speakers provided an overview of the recent advances and open questions when introducing their topic; the overviews were followed by invited talks from the Large Programme and Public Survey principal investigators (PIs) and by additional oral contributions. A concise summary of the content of the workshop is presented.

Legacy of Large Programmes and Public Surveys

The workshop was opened by Bruno Leibundgut, starting with a session on the legacy value of Large Programmes and Public Surveys. The session focused on the interplay between the research topics in observational astronomy and the feedback from the concept of the legacy value of Large Programmes/Surveys. The legacy of an observing programme starts with the curation and archiving of its data and Alex Szalay covered these aspects in his keynote talk on the Sloan Digital Sky Survey (SDSS) projects. As the workshop progressed, it became clear that the legacy can provide a variety of different metrics for the assessment of the success of these projects. Building on well-known parameters, like the number of publications and citations, other measures are the number of public releases, training of young researchers, engagement of the wider population, as, for example, via the citizen science projects such as the Galaxy Zoo, enlarging the network of scientific collaborations, as well as independent archive science and serendipitous discoveries that open new fields. Alex Szalay made the point that the way the science is done in astronomy research is changing. Fast progress is now coming from multiwavelength and time-domain analysis of data, thereby shifting the focus from smaller programmes driven by hypothesis to projects managing terabytes of data. Szalay argued that the equivalent of “microscopes” and “telescopes” for managing large volumes of data are the new instruments that are needed.

Guinevere Kauffmann elucidated very interesting points about some further

changes in how research is being done and emphasised the need to coordinate efforts, transparency and the sharing of data and tools. The contributed talk by Sara Ellison further explored the use of neural networks for data mining of the SDSS archive, while Marc Moniez emphasised the impact of the upcoming Large Synoptic Survey telescope.

Cosmology, galaxy evolution and extragalactic astronomy

The first half of the workshop focused on cosmology, galaxy evolution and extragalactic astronomy. Three keynote speakers introduced the main areas: Richard Ellis (cosmology and the high-redshift Universe), Natascha Foerster-Schreiber (galaxy evolution) and Guinevere Kauffmann (extragalactic astronomy and the local Universe). These fields are rapidly developing thanks to the modern facilities, and even more progress is anticipated from ongoing and future surveys. Many recent advances were enabled by ESO telescopes and featured in the invited talks that covered, among other topics: the search for high-redshift quasars (talk by Bram Venemans); the first objects that reionised the Universe (Laura Pentericci, Bo Milvang-Jensen); surveys of samples of quasars which allow the intergalactic and circumgalactic medium to be probed (talks by Trystyn Berg, Sebastian Lopez, Valentina D’Odorico and Tom Shanks); surveys of galaxies establishing galaxy growth, luminosity function evolution and star formation history across a range of redshifts (Storm Dunlop, Adriano Fontana, Rebecca Bowler and Lidia Tasca); and cosmology constraints from the mapping of the large-scale structure at $z \sim 1$ (Luigi Guzzo). Synergies with upcoming surveys, such as Euclid, were also mentioned.

At lower redshift and in the local Universe, results were presented on dark matter–baryon connections via gravitational lensing (Alastair Edge, Hendrik Hildebrandt and Piero Rosati), on the kinematics of the outer halos of early-type galaxies (Claudia Pulsoni), and the diversity of dusty molecular tori in active galactic nuclei (Klaus Meisenheimer). In general, the focus appears to be shifting from large-area redshift surveys towards the need for high quality, deeper obser-



Figure 1. Participants of the Rainbows2015 workshop in the entrance hall of ESO Headquarters.

vations targeting the physics of galaxies (Ross McLure and Arjen van der Wel) and cosmology.

Dissecting galaxies into stars, planets and ... black holes

The Milky Way, the Local Group and the physics of stars and planets were covered during the central part of the workshop. Hans-Walter Rix reviewed the composition and dynamics of the Milky Way disc around the Solar Neighbourhood and to large radii. Maurizio Salaris described the recent advances and challenges in stellar astrophysics: he pointed out that specific details of the models have large uncertainties and their predictions can only be constrained by observations. The surveys of the Milky Way (Vista Variables in the *Via Láctea* [VVV], the VST Photometric $H\alpha$ Survey [VPHAS+] and Gaia-ESO) are providing large samples that enable star formation (Philipp Lucas), stellar evolution and Galactic chemical evolution (Rodolfo Smiljanic) to be addressed, in addition to providing a first complete view of the Milky Way Bulge (Dante Minniti, Manuela Zoccali, Chris Wegg and Matthieu Portail), and Disc (Sofia Randich, Boris Gaensicke). Variable stars were investigated as distance indicators (Wolfgang Gieren), as well as pop-

ulation tracers in the Milky Way (Dante Minniti) and its satellites — the Magellanic Clouds (Vincenzo Ripepi). The search for the most metal-poor stars in the halo (Piercarlo Bonifacio), the chemical enrichment of ultra-faint dwarf spheroidal galaxies (Georges Kordopatis), and the census of circumstellar discs in nearby star-forming regions (Giacomo Beccari) were also covered. Mariya Lyubenova presented a new stellar spectral library, based on X-shooter observations.

Reinhard Genzel presented the results from the Galactic Centre Legacy Programme. This is actually a series of many programmes that together comprise a long-term coherent monitoring experiment, which has unambiguously established that there is a Schwarzschild–Kerr black hole at the centre of the Milky Way, if general relativity is applicable. This programme continues to test the physical processes in the vicinity of the Milky Way black hole and will enter a new phase in the coming years when the star S2 will again pass very close to the black hole, in 2018. Several instruments will measure this event, including the newest addition to the Paranal suite, aptly called GRAVITY.

The last session of the workshop covered time domain astrophysics, such as supernovae (Stephen Smartt, Stefano

Benetti and Cosimo Inserra) as well as proper motion and parallaxes (Radostin Kurtev), and ending with a review of results on the characterisation and formation of planets. Didier Queloz gave an exciting overview of the field, highlighting how far we have come from the first discoveries of planets around other stars, to the physical characterisation of the most extreme planetary systems. The High Accuracy Radial velocity Planet Searcher (HARPS) on the ESO 3.6-metre is leading this field and has provided a census of the super-Earth and Neptune-mass planet population around Solar-type stars (Francisco Pepe), while the VLT Interferometer provides exquisite resolution to zoom into the early stages of planet formation and protoplanetary disc physics (Jean-Philippe Berger).

Closing the loop: Legacy of Large Programmes/Public Surveys and archives

The closing session returned to data archiving and access as one aspect of the contribution to the legacy value of Large Programmes and Public Surveys. The SAF is the collection point for Large Programme and Public Survey products and the primary point of publication/availability of these products to the ESO community as laid down by ESO Council resolution #104 from 17–18 December 2004. Phase 3 — the process of preparation, validation and ingestion of science data products for storage in the SAF, and subsequent data publication to the scientific community (Arnaboldi et al., 2014) — ensures the coherent legacy and data return via the ESO SAF.

Following the publication of the first data release from ESO Public Surveys in December 2011, the survey science data products in the ESO SAF cover more than 11 500 square degrees (Optical/near-infrared: 4336 / 9445 square degrees) with more than 35 TB of data consisting of 2.7×10^5 files, with more than 2.6×10^6 spectra (Jörg Retzlaff). The data releases from ESO Public Surveys include high-level science catalogues. Statistics on the data access and download from the SAF were shown, including the cumulative number of archive users of these products, amounting to twice the number of PIs and Co-Is listed in the

ESO Public Survey teams. Currently archive papers contribute about 25% to the total number of refereed papers from ESO facilities each year.

The support to the community is further enhanced by the availability of science data products from the science archives at the Wide Field Astronomy Unit at the Institute for Astronomy, University of Edinburgh (Nicholas Cross) which provides extensive programmatic access via SQL queries to their data assets. The requirements on survey project design that must include not only new instrumentation, but also dedicated services for data processing, storage, effective publication and retrieval, was highlighted in the case of the next generation spectroscopic surveys planned for the 4-Metre Multi-Object Spectroscopic Telescope (4MOST; talk by Eduardo Gonzalez-Solares).

Clearly the wealth of data available through Public Surveys and Large Programmes transforms our view of the Universe into an N -dimensional space where correlations and information can be mined, and extracted to test and formulate new theories. On account of the web and fast-evolving archive tools, a large pool of users can now share the scientific method and join the astronomical community. Diversity, openness, curiosity and the unexpected are concepts that can change our way of doing astronomical research, and become attributes of what is meant by “legacy value”.

Concluding remarks

Scientific discoveries are driven by strongly motivated, highly interested individuals supported by leading-edge technology developments. The community shares these discoveries and benefits via technology advances in archiving and data transfer. At the workshop we celebrated the achievements of the successful PIs and their teams who pursue important questions in observational astrophysics with ESO facilities.

The large variety of programmes and progress in different science fields

generated a vibrant atmosphere and led to vigorous discussions during lunches and coffee breaks. The programme was dense and diverse, with many excellent presentations. The talks from the Rainbow2015 workshops can be found on the workshop page¹. The photograph of the workshop participants is shown in Figure 1.

Several sociological aspects distinguished this workshop from those in the past:

- A number of Large Programme/Public Survey PIs could not attend the workshop and delegated the invited talks to younger members of their teams. Hence there was a healthy attendance by young astronomers presenting the results from the large team efforts — a new generation of European scientists is clearly taking up a more prominent role.
- The selection of Large Programme presentations invited by the Scientific Organising Committee triggered some healthy responses from the Large Programmes community. In addition to the inevitably limited selection of invited talks, several other Large Programme teams submitted requests for a contributed talk and participated in the scientific discussions.
- There was a strong representation of the Public Survey panels (Joint VISTA/VST and the Spectroscopic panel) and their members took part in the discussions and interacted with the PIs of the Public Surveys.
- Surveys and Large Programmes empower the wider community to discover the Universe. In this sense they are the effective implementation of the IAU statement “The Universe: yours to discover”.

References

- Arnaboldi, M. & Rejkuba, M. 2012, *The Messenger*, 150, 67
Arnaboldi, M. et al. 2014, *The Messenger*, 156, 24
Mathys, G. & Leibundgut, B. 2009, *The Messenger*, 135, 53
Wagner, S. & Leibundgut, B. 2004, *The Messenger*, 115, 41

Links

¹ Workshop programme: <http://www.eso.org/sci/meetings/2015/Rainbows2015/program.html>

Modern Instruments, their Science Case, and Practical Data Reduction

held at Masaryk University, Brno, Czech Republic, 31 August–12 September 2015

Petr Kabath¹
 Michel Dennefeld²
 Michele Gerbaldi²
 Ernst Paunzen³
 Vladimír Karas¹

¹ Astronomical Institute of Czech Academy of Sciences, Ondřejov, Czech Republic

² Institut d'Astrophysique de Paris, France

³ Department of Theoretical Physics and Astrophysics, Masaryk University Brno, Czech Republic

The Astronomical Institute of the Czech Academy of Sciences organised, jointly with its local partners from Masaryk University, and international partners OPTICON, ESO and the IAU, a two-week practical training course in astronomy for young researchers. The summer school is briefly summarised: lectures covered a wide range of theoretical and observational topics and the emphasis of the practical work was on the analysis of archival data.

Introduction

The Czech Republic is an active but relatively young ESO Member State, having joined in 2007. Therefore, it is extremely important to broaden the expertise of young Czech astronomers with regard to the newest available instrumentation and observing facilities. In 2014, the first workshop with this goal, entitled “Seven Years in Chile: The Accomplishments and Goals of Czech Astronomers at ESO”, brought together Czech researchers at Villa Lanna in Prague (see Kabath et al., 2014). It was decided that the next step would be the organisation of a summer school, potentially with international participation.

In early 2015, the Optical Infrared Co-ordination Network (OPTICON¹) agreed to join forces and to co-organise an event within the traditional framework of the Network of European Observatories in the North (NEON) schools, aimed at the education of early-stage researchers in astronomy. Usually, the format of OPTICON schools comprises observing, archival data analysis or awareness-



raising courses. The latter topics were chosen, with a special focus on a hands-on approach to archival data, together with presentations of other European telescopes accessible via the OPTICON Access programme. Finally, to broaden participation even further, the help of International Astronomical Union (IAU) was also obtained, within the International School for Young Astronomers (ISYA) scheme (sponsored by the Norwegian Academy of Sciences and Letters), to sponsor the participation of a few more students from outside the European Union.

The summer school took place in Brno, Czech Republic, on the modern campus of Masaryk University between 31 August and 12 September 2015. Over the course of two weeks, the campus lecture hall witnessed a series of education sessions presenting the modern observatories of Europe, be it ESO, La Palma, Observatoire de Haute Provence (OHP), Calar Alto, Pic du Midi or other facilities, along with their instrumentation and the most recent scientific highlights, ranging from the theoretical background to modelling and astrophysical interpretation. The school was organised under the auspices of the Czech Ministry of Education, Youth, and Sports, and the presence of the Czech Ambassador to Chile enhanced the recognition of the event.

Figure 1. All the participants at the summer school photographed on the steps of the lecture theatre at Masaryk University, Brno.

The school was attended by 39 participants representing astronomy Masters and PhD students, and also several young postdoctoral researchers, mainly from EU Member States, supported by OPTICON. Additionally, nine students received support from the Czech Republic from local funding schemes. Moreover, IAU grants allowed the participation of seven non-EU students, from Armenia, Egypt, Iran and Ukraine. In total, 17 states were represented.

Programme

The school opened on 1 September 2015 with a speech from the Deputy Minister of Education, Youth and Sports of the Czech Republic, Robert Plaga, followed by welcoming speeches from the organising institutions. The Czech vice-president of the ESO Council, Jan Palouš, gave a lecture about the Czech road to becoming an ESO member.

The scientific part of the programme was supported by 15 lecturers from leading European institutions, including ESO, Institut d'Astrophysique de Paris (IAP), Instituto de Astrofísica de Canarias (IAC)

Tenerife, Calar Alto Observatory, Stanford University, Deutsche Luft und Raumfahrt (DLR) Berlin, the Czech Academy of Sciences and Masaryk University. The lecturers came from various fields in astronomy and astrophysics and covered topics of galaxies, black holes, stellar physics and exoplanets. Some lectures described technical aspects of the observatories, their operation and instrumentation, as well as future prospects and planned projects, whilst others presented modern observing methods and the most recent scientific discoveries. An overview of the current observing possibilities in Russia was also given by a Russian colleague.

The lectures were accompanied by projects under the supervision of experienced tutors, whose hard work, enthusiasm, professional experience and careful preparation were especially appreciated. The tutors were: Giacomo Beccari (ESO Garching), Remi Cabanac (Université Toulouse), Anthony Herve (Czech Academy of Sciences), David Jones (IAC, Tenerife), Juan Carlos Munoz (ESO Chile), Korajka Muzic (ESO Chile), Martin Netopil (Masaryk University [MU], Brno), Ernst Paunzen (MU, Brno), Hadi Rahmani (Laboratoire d'Astrophysique de Marseille, LAM) and Marek Skarka (MU, Brno). Each project group included four students and the topics were mainly aimed at teaching data reduction techniques and work with archival data, that is to say a hands-on approach to data. The instrumentation covered imagers in the optical and near-infrared as well as multi-object and long-slit spectroscopy. A specific spectropolarimetry project was also offered, with real (remote) observations from the Pic du Midi 2-metre telescope, under the leadership of its director, Remi Cabanac.

In addition, during a career session, the experience of established astronomers was shared with students and the career prospects for young researchers were presented, giving rise to a very lively and constructive discussion.

Finally, a proposal-writing session and an Observing Programmes Committee simulation exercise were organised by Czech colleagues with experience in ESO's operational procedures, Adela Kawka and Ernst Paunzen. Students had



Figure 2. Some of the students engaged in project work.

to discuss in panels, with real (old) proposals provided, as if they were a real Observing Programmes Committee (OPC). At the end, students handed over their feedback and in the last part of the exercise, in an open discussion, the whole proposal process was discussed with senior astronomers. This was a unique opportunity to acquire insight into the OPC procedures and gain some hints on how to write high-quality proposals and thus increase one's chances of getting telescope time.

Social events played an integral role in the school as well, including an opening reception in the campus hotel Campea, a guided tour through the historical city of Brno, and an afternoon organised by the Center of Technology Transfer of Masaryk University with cooperation of high-tech companies (Moravian Instruments). Students had a chance to foster new friendships and collaborations and interacted informally with experienced researchers. Furthermore, the picturesque region of Moravia was also presented.

On 11 September, the school ended with conference-style presentations of the student projects. The presentations of the results were of excellent quality, given the fact that the students had had a relatively short time for project work. In the evening a farewell dinner took place, again at Hotel Campea. The formal and informal feedback obtained from the participants was clearly positive, with new ideas generated for improvement of future events.

We believe that this kind of summer school is of enormous importance and impact for early-stage researchers, especially because it is not always easy to acquire hands-on experience with the most modern telescopes and instruments. We are happy to acknowledge the contributions of the lecturers and tutors, as well as significant financial support from ESO, OPTICON, the IAU, the Academy of Sciences of the Czech Republic and, last but not least, our local host Masaryk University. Hopefully, this summer school marks an important milestone for modern Czech astronomy and will also contribute to the competitiveness of European students in astronomy, for whom it was a unique astronomy education event of its kind.

All presentations, as well as the student project contributions from the last day of the school, can be found on the school website² and on the OPTICON website¹.

Acknowledgements

Petr Kabath would like to acknowledge funding from MSMT grant LG14013.

References

Kabath, P. et al. 2014, *The Messenger*, 156, 58

Links

¹ OPTICON: <http://www.iap.fr/opticon/>

² Summer School website: <http://awareness2015.physics.muni.cz/>

Science and Technology with the E-ELT

held at the Ettore Majorana Foundation and Centre of Scientific Culture, Erice, Sicily, 8–20 October 2015

Giuseppe Bono¹
Isobel Hook²
Suzanne Ramsay³

¹ Università di Roma Tor Vergata, Italy

² Lancaster University, United Kingdom

³ ESO

This international PhD school in the F. Lucchin cycle was the first to bring together Masters and PhD students with an interest in all aspects of the science and technology of the European Extremely Large Telescope (E-ELT). It was fitting that this school was held within a year of the project formally entering the construction phase. An overview of the topics covered during the school is presented.

In total 51 students from 16 countries attended the school. As may be inferred from the title, the programme for the school was very broad. For example, experts in the adaptive optics (AO) systems with which the E-ELT will be equipped were scheduled alongside astronomers specialising in the theoretical foundations of resolved and unresolved stellar populations or the expansion of the Universe. The lecturers each gave two one-hour lectures on their subjects. They typically reviewed the state of the art in each field in the first hour and, in the second, highlighted the application of that technology to the E-ELT, or the potential of the E-ELT to further develop the field.

E-ELT technology

Lecturers from ESO presented the background and specifics of the European Extremely Large Telescope, including the history and the final telescope design (Roberto Gilmozzi), the current status of the project (Roberto Tamai), the science drivers and the instrumentation programme (Suzanne Ramsay) and the adaptive optics (Enrico Marchetti). Bruno Leibundgut presented the Very Large Telescope (VLT) programme. Talks on specific aspects of instrumentation were also offered: in high spectral resolution spectroscopy (Livia Origlia), polarimetry

(Christoph Keller), high time resolution science and instrumentation (Andrew Shearer) and IFU spectroscopy (Sebastian Kamann). The second lecture given by Sebastian also included homework for the students: identification of individual sources from integral field spectra of the innermost cluster regions of M92.

Fundamental subjects, such as infrared astrophysics and the optimisation of telescopes and instruments for that wavelength regime, were presented by Tom Herbst, while Michel Dennefeld described spectrographs and spectroscopy. The lessons about the infrared atmosphere were further developed by Norbert Przybilla in his lecture on sky modelling.

The technologies and techniques of AO will play a very significant role for astronomers using the E-ELT, so a number of lectures covering the many flavours of AO were presented by Roberto Ragazzoni, Simone Esposito and Enrico Marchetti. Laura Schreiber described how to fit point spread functions (PSFs) to data taken with AO instruments and, along with Giuliana Fiorentino, led the students in a practical exercise of analysing images taken with different AO techniques (multi-conjugate, single conjugate and ground layer adaptive optics [MCAO, SCAO and GLAO]). The aim of the tutorial was to challenge the students to identify the technique used for the observations via the characteristics of the observed PSF across the field of view of the instrument. Giuliana further discussed how to do deep near-infrared photometry with AO instruments.

E-ELT science

The key science cases for the E-ELT were also presented, starting with the basics of the subject and then expanding to describe the way in which the sensitivity and angular resolution of a 40-metre-class telescope would revolutionise each field. The possibilities for increasing our understanding of the Solar System were shown by Benoit Carry, with Markus Kasper detailing current and future work on exoplanets with the Spectro-Polarimetric High-contrast Exoplanet Research instrument (SPHERE) on the VLT and the Planetary Camera and Spectrograph (PCS)

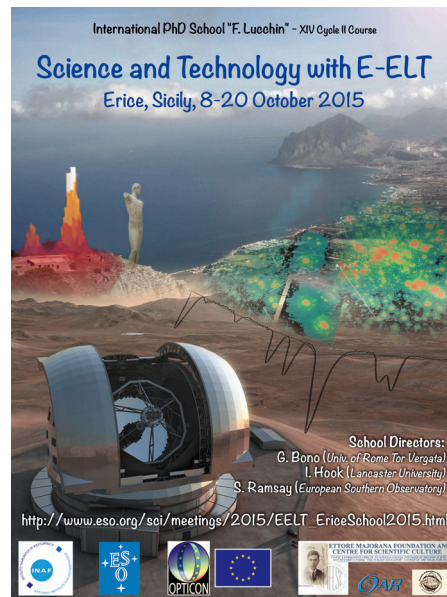


Figure 1. Poster for the International PhD School "F. Lucchin".

on the E-ELT. The role that exoplanets are going to play for the E-ELT was also covered in the lectures by Livia Origlia, together with the pros and cons of high resolution near-infrared spectroscopy. The E-ELT contribution to the understanding of protoplanetary discs was included in the lectures by Miwa Goto.

The processes for understanding the physics of stars themselves were covered in great detail. Suzanne Ramsay discussed their formation and feedback into the interstellar medium. Observations and analysis of single stars — blue supergiants (Norbert Przybilla) and red supergiants (Miguel Urbaneja-Perez), were discussed as well as their use for distance determinations. France Allard introduced the topic of the atmospheric modelling of stars, in particular ultra-cool dwarfs. She also discussed the ongoing effort in improving the input physics of the current atmosphere models of low-mass stars. This topic was then advanced by Maria Bergemann who discussed the use of 3D atmospheric models and the challenges resulting from the new understanding of the abundances of Solar-type stars. Maurizio Salaris presented the latest results and open questions on the advanced evolutionary phases of low- and intermediate-mass stars. Variable stars and their impact on stellar astro-



Figure 2. The School group photograph looking across Bonagia Bay.

physics and cosmology were presented by Marcella Marconi, Laura Inno, Matteo Monelli and Massimo Dall’Ora. A comprehensive review of surveys for transient and variable objects was given by Michel Dennefeld together with current and future strategies for spectroscopic follow-up of transients.

Eline Tolstoy and Patricia Sanchez-Blazquez described the study of resolved and unresolved stellar populations respectively, while the physical and the chemical ingredients to build up synthetic colour–magnitude diagrams were further expanded by Santi Cassisi. The chemical enrichment of the Galactic Disc using classical Cepheids was introduced by Giuseppe Bono, together with the role that optical and near-infrared spectroscopy will play in constraining the metallicity distribution in nearby Local Group stellar systems.

Moving outside the Galaxy, Fabrizio Fiore gave two lectures on active galactic nuclei (AGN) and supernova (SN) feedback. The status of studies of the high-redshift Universe was reviewed by Richard Ellis, together with the spectroscopic and photometric synergies with the James Webb Space Telescope (JWST). Bruno Leibundgut presented the case for the accelerating Universe as revealed by studies of SNe. Joe Liske and Carlos Martins then showed how a direct measurement of this acceleration and of the funda-

mental physical constants could be achieved with great precision using the E-ELT.

All the lectures are available online at the school webpages¹.

Student participation

The students were not simply passive participants in the school. Aside from their questions to, and interactions with, the lecturers, around half of the students took the opportunity to give 10-minute presentations of their own Masters or PhD work. These presentations were of impressively high quality and the breadth of topics matched beautifully that of the school itself — from new detectors to cosmology. A novel innovation was that the final three days of the school were chaired by the students themselves. All the student chairs rose very well to this additional challenge and performed in a most professional manner.

The long duration of the school and the 9:00–19:00-hour schedule of lectures plus tutorial homework and talk preparation led to an intense two weeks for all concerned. Nevertheless it was not all work. A half-day excursion took in the Marsala museum, housing the Nave Punica and the dancing Satyr in the Mazzara museum. This was followed the next day by an expert guided tour of Selinunte and its temples. The school’s location in the small hill town of Erice afforded many opportunities for the informal interactions over lunch and dinner

that are so critical for forming strong working relationships. They were also facilitated by the beautiful terrace overlooking the Bonagia Bay that was the venue for the coffee and tea breaks (see Figure 2).

The co-directors and authors of this short report sincerely hope that this school will have informed and enthused the generation of astronomers who will be the prime users of the new facility. In closing, the students were challenged to ask what they can now do for the E-ELT. We look forward to the results!

Acknowledgements

The school was only possible thanks to the considerable efforts of many people. The authors would like to thank in particular the lecturers for their informative and entertaining lectures. The local organising committee bore the brunt of the day-to-day work on such a school. We gratefully acknowledge all the work done by Vittorio Braga, Michele Fabrizio, Hildegard Haems, Laura Inno, Samantha Milligan and especially Giuliana Giobbi for all their help with the practicalities of the school. It is also a pleasure to thank the Director of the Majorana Centre, Dr Fiorella Ruggiu, with her administrative and technical staff for their steady and warm support in solving the many problems that turn up in the organisation of an International School. The school was supported financially by OPTICON, ESO, the Istituto Nazionale di Astrofisica, the Laboratorio Nazionale di Ottica Adattiva and by the Ettore Majorana Foundation and Centre of Scientific Culture. OPTICON is supported by the European Commission’s FP7 Capacities programme (Grant number 312430).

Links

¹ School webpages: http://www.eso.org/sci/meetings/2015/EELT_EriceSchool2015.html

Staff at ESO

Eleonora Sani

I've always been fascinated by natural behaviour — why things work in one way rather than another. But, sincerely, I hadn't thought to become an astronomer. I started to be interested in astronomy just by chance when I was in my late teens. Walking in the city centre I saw an amateur telescope in a shop and thought, "Well it would be nice to look at stars and galaxies with such a thing!"

I became enthusiastic about going around the countryside camping and looking at the sky with my brand-new telescope, but still astronomy was not my first choice for future studies. I started studying physics at the University of Florence with some vague idea of taking a Masters in quantum physics or something related to the super-small world. But then, when I had to choose my specialisation I realised that astrophysics is the most complete discipline, because it spans the range from atomic physics, Solar studies, radiation processes, plasma physics and complex dynamics to cosmology, and entails the use of many different kinds of technologies, from ground-based facilities to satellites and many more. How can a researcher desire more than having almost all these fields rolled into one?

I had taken the first step, but still had to choose the topic for my degree thesis (and thus, once more, an important challenge for the future). I was interested in observational work on Solar spectroscopy and had already contacted one team, since the Observatory of Arcetri (where I was supposed to finish my Masters) had a great tradition in such studies. But then I had a meeting with the director, Professor Franco Pacini, and he convinced me that working in extragalactic astronomy with a recently formed team of young researchers would be really stimulating. So once more I changed my plans and started a curriculum centred on supermassive black holes and their co-evolution with galaxies. My PhD and my first postdocs were great periods, during which I started my own project based on Very Large Telescope data and had the opportunity to visit the Max Planck Institut für extraterrestrische Physik in Garching to work on both satellite and interferometric data.

My first experience with an 8-metre-class telescope came when I went to Paranal to observe with the Infrared Spectrometer and Array Camera (ISAAC) for my own project. I remember how nervous and excited I was at the same time because of the scientific challenge and I was also a bit fascinated by the skills of the



Eleonora Sani

support astronomers, who appeared to me as super-heroes!

Now I have become part of this team, supporting VLT Unit Telescope 1 and I am in training as the instrument scientist for the K-band Multi-Object Spectrograph (KMOS), a jewel of infrared technology. I am not a super-hero for sure, but will face new challenges and exciting times in the future with the new generation of facilities.

Fellows at ESO

Matthieu Béthermin

I was born in Paris in 1985 and grew up in Suresnes in the western suburbs. From there, the night sky was a sort of bright orange haze caused by all the sodium streetlights. The city of light was certainly not the best place to enjoy the faint and diffuse Milky Way. At a young age, I was already fascinated by the question of our origins. Everything about astronomy, dinosaurs, and prehistoric

men attracted me. But this was nurtured only through reading books and watching TV documentaries.

One of the main events that pushed me towards astronomy, paradoxically, happened on a crowded urban highway in the south of Paris. I was ten years old. After being stuck in a traffic jam for three hours trying to re-enter Paris after a weekend, my parents had decided that Paris was no longer a place to bring

up kids. A few months later, we moved to the south of France. There, I discovered why people say the night sky is black and I saw the Milky Way for the first time. This was beautiful. I started to explore this new world with binoculars and then with a small telescope. After observing the Andromeda Galaxy and reading that the light from there had travelled 2.5 billion years before hitting my retina, I was so fascinated that I decided I wanted to study the cosmos.

I thus started to study physics and maths, since this is the first requirement towards becoming an astrophysicist. I always loved physics and how it connects the world of numbers to reality and paradoxically gives sense to events through abstraction. I first studied at the Lycée du Parc in Lyon and then at the Ecole Normale Supérieure in Cachan, near Paris. During this period I had a six-week internship at the Nançay radio telescope studying pulsars under the supervision of Ismael Cognard. I discovered the large gap between amateur and professional astronomy. There was no long night-sky observing, but high-tech instruments and massive use of computers. Thus it was decided: I definitely wanted to become astrophysicist!

I then studied for my Masters in astrophysics in Paris. I discovered far-infrared surveys during a hands-on session on data analysis. I really liked the challenge of extracting galaxies in data with a very limited resolution. These surveys were also essential to understanding the star formation history of the Universe. The subject was scientifically interesting and challenging and I decided to do my PhD thesis on this topic supervised by Hervé Dole, and in close collaboration with Guilaine Lagache.

The goal of my thesis was to identify the galaxies at the origin of the cosmic infrared background. This background is the relic of all the dust emission across cosmic time and is very important for the understanding of the formation of stars in the Universe. The newborn stellar populations emit a lot of ultraviolet light, which cannot escape the clouds of dust in the vicinity where the stars were born. But the dust re-emits the energy of this light in the far-infrared, allowing us to study this hidden star formation.

Unfortunately, these distant galaxies cannot be detected directly in the data of the Spitzer and Herschel far-infrared space observatories. I thus developed statistical tools to detect the signature of these distant galaxy populations in the faint fluctuations they cause in the cosmic infrared background. After a three-year PhD thesis and a further two-year post-doc at the Commissariat à l'énergie atomique (CEA) Saclay (France) with



Matthieu Béthermin

Emanuele Daddi, my collaborator and I finally managed to identify the galaxies at the origin of the infrared background and the dark-matter halos which host them. We found that in the early Universe, about 10 billion years ago, a large fraction of the stars were formed at a very rapid pace in few very massive galaxies hosted by massive overdensities. The nature of these gigantic star factories, forming 100 times more stars than the Milky Way, was very hard to explain.

After these few years of hard but exciting work, I had the amazing opportunity to come to ESO as a Fellow to pursue my own research programmes, aimed at unveiling the nature of these galaxies. Being independent so early in a research career is extremely stimulating. I continue to use Herschel data and have found gigantic gas reservoirs in these giant galaxies in the young Universe. But, a revolution in my research field is starting with the Atacama Large Millimeter/sub-millimeter Array (ALMA).

ALMA is especially designed to observe the dust in distant galaxies. It is equivalent to a virtual telescope of up to 10 kilo-

metres diameter with a resolution and sensitivity in the submillimetre matching the performance that the Hubble Space Telescope can reach in the visible. For the first time, the dust in distant galaxies is not seen as a faint blob, but we can study the detail and find surprising morphologies.

As an ESO Fellow, I had the honour to go to observe at ALMA as astronomer on duty. The basecamp of ALMA from which the telescope is controlled offers a breathtaking view of the Atacama Desert and the Andean volcanoes. But the high site at 5000 metres above sea level, on a gigantic plateau, where the array is installed, is even more incredible. Operating such ultra-high technology facilities in such a tough environment is challenging. My experience at ALMA was probably one of the highlights of my career as an astronomer, and this was thanks to the ESO Fellowship!

Ke Wang

I grew up in the suburb of Chongqing, in southwest China, a place famous for its delicious Sichuan cuisine. There, in summer, temperatures can reach 40°C, so families would gather in the front yard after supper to enjoy the cool evening breeze. My brother and I would play with our dog and cat before falling asleep in the starry light. It was at that time I became fascinated by the charming beauty of the night skies. Then I started a long journey to find out “what these shining little dots are”. I conducted my first observations using a homemade toy telescope, targeting the Moon and Jupiter, without knowing that Galileo Galilei did the same thing almost 400 years before. “How great it would be, if I could own a real telescope,” I thought. Astronomer soon topped the list of my dream careers. Also included in that list were astronaut, athlete, archaeologist and history teacher. After running several marathons, my injured meniscus warned me that being an athlete was not a good option.

In high school I did well in natural sciences, was interested in many fields, but physics was always my favourite. So I was really excited to find out that there is a field combining the fun parts of both

fields, called astrophysics. I started to read any book about astronomy that I could find, even though some of them turned out to be science fiction (which I actually enjoyed). Book hunting continued throughout my university study at Beijing Institute of Technology (BIT), where I was usually the only visitor to the astronomy section in the library. However BIT did not have an astronomy group. In the final year of my study at BIT, I became a frequent visitor to the neighbouring Peking University (PKU) for seminars in the Department of Astronomy, and naturally conducted my bachelor thesis there, on the habitable zones around Solar-like stars. After a valedictory presentation at BIT I was awarded a place in the PhD programme at PKU, exempt from the entry exam.

Right after my bachelor study I had no idea which topic I would do for a PhD, but I knew I would like to observe using telescopes. Luckily, at PKU we had one year to experience the different subjects being studied at the Department before making the decision. During that year I made my first observing trip to the Purple Mountain Observatory (PMO) 14-metre radio telescope and observed molecular lines in a sample of infrared dark clouds (IRDCs). I was amazed by the (already) gigantic dish and its spherical dome. Although images made by radio telescopes are not (yet) as stunning as optical telescopes, I appreciated the physics one can derive even from a spectrum. Also the fact of “seeing the invisible” (even in the day time!) at radio wavelengths is attractive. So that’s it, radio astronomer!

Soon after I returned from the PMO 14-metre, I was awarded a position in the pre-doctoral programme at the Harvard-Smithsonian Center for Astrophysics (CfA), in the Submillimeter Array (SMA) group. For the first time I flew outside China and moved to Cambridge, Massachusetts, USA. The CfA is one of the hot spots on the world map of astronomy, and the SMA was the first interferometer working at submillimetre wavelengths. With the Atacama Large Millimeter/submillimeter Array (ALMA) coming online in a few years, I knew I was at a good place at a good time. I dived into the sea of knowledge, eagerly learning the fundamentals and the practical aspects of radio interferometry, not only from text-



Ke Wang

books but also from textbook authors and a Nobel Prize Laureate. It was such a privilege to work with people who had actually built and maintained a cutting-edge interferometer: there is no better way to gain a solid understanding of radio interferometry. So I felt that it was like an award to join the SMA remote operations team, controlling the telescope array from a comfortable room at the CfA every week. Early mornings in Boston’s wild winters, clearing the heavy snow in front of the rear door in order to enter the building on time for my SMA observations, is a special memory.

More enjoyable was of course to fly to Hawaii and drive up to the Martian-like landscape of Mauna Kea, home to the SMA and a family of world-class telescopes. Literally above the clouds, watching the array of telescopes moving under my command felt so good! I was also a frequent user of other interferometers and single-dish telescopes including the Jansky Very Large Array (JVLA), the Combined Array for Research in Millimeter-wave Astronomy (CARMA), the Caltech Submillimeter Observatory (CSO) and the Green Bank Telescope (GBT). I used these telescopes to obtain deep, high-resolution images of IRDCs in order to study the initial fragmentation leading to the formation of massive stars and clusters. These observations were later published by Springer as my PhD thesis.

Having spent three years in the USA, I convinced my girlfriend to venture to Europe, a slightly more exotic continent where we did not understand the local

languages. Soon I found myself in the Netherlands, but outside Holland, for a ten-month European Erasmus post-doctoral fellowship at the Kapteyn Astronomical Institute, University of Groningen. That was before my PhD thesis defense. In Groningen, I extended my research horizon to another wavelength range, using data from the Herschel space telescope. In addition to the iconic tulip fields and windmills, I appreciated the Dutch enthusiasm for cycling. I was totally shocked at how efficient the sky is over this land in converting clouds into rain. By the end of my fellowship I could handle sudden rains as elegantly as the locals.

I joined ESO Garching on the occasion of ESO’s 50th anniversary in October 2012. ESO is a unique place in many aspects, from its international, intergovernmental nature to its internal organisation, from the high quality of science it delivers to its frequent exposure in social media. That gives us the opportunities to witness the, usually hidden, political and engineering aspects of a modern observatory, and how decisions are made to shape the next decades of European and world astronomy. Science wise, I was a little surprised to hear “there is no group at ESO”, but few months later I fell in love with the way it is organised: everyone belongs to the ESO family. As an ESO Fellow, I enjoy the freedom of being an independent researcher and at the same time, the rare opportunity to work for the largest ever ground-based astronomy project — ALMA. I have continued to expand my expertise in radio interferometry, gained from the SMA and

the JVLA, to a variety of duties at the European ALMA Regional Centre, such as astronomer on duty (on-site observing), contact scientist, data quality assurance, software testing, tutoring new users, etc. ALMA is revolutionising our understanding of the Universe, and I am proud to be part of the team. Undoubtedly knowing more details of ALMA benefits my own research. On the personal side, although I'm allergic to alcohol and so cannot enjoy the Oktoberfest, we are super happy to find the Alps only one hour away! How can one not fall in love with skiing in the Alps!

My ESO Fellowship has just come to an end, but thanks to the Deutsche Forschungsgemeinschaft (DFG), I can continue my research at ESO as an Associate. It turns out that I am the first to successfully bring a DFG grant to ESO! Currently I am leading an ESO Public Survey towards an all-sky sample of cold molecular clumps discovered by the Planck satellite. After all these rewarding years, the time has come when I can contribute to the community.

Looking up at the crystal-clear sky over Chajnantor on the way to a night shift

at the ALMA Operations Support Facility, my thoughts went back to the yard in my childhood. From my toy telescope to the real telescopes I've operated (or climbed) so far: the PMO 14-metre, SMA, CSO 10-metre, JVLA, GBT 100-metre, CARMA, the Institut de Radioastronomie Millimétrique (IRAM) 30-metre, Effelsberg 100-metre, the Heinrich Hertz Submillimeter Telescope (SMT) 10-metre and ALMA, and I am thankful for the boundless love, help, luck and fortune which, combined, have made my childhood dream come true. I look forward to the even more exciting years to come.

Personnel Movements

Arrivals (1 October–31 December 2015)

Europe

Agnello, Adriano (IT)	Fellow
Arrigoni Battaia, Fabrizio (IT)	Fellow
Bonnefond, Sylvain (FR)	Student
Bordelon, Dominic (US)	Library Technology Specialist
Johnston, Tania (UK)	ESO Supernova Coordinator
Kurowski, Przemyslaw (PL)	Software Engineer
Lu, Hau-Yu (TW)	Fellow
Nilsson, Maria Theresa (SE)	Student
Stroe, Andra (RO)	Fellow

Chile

Bellhouse, Callum (UK)	Student
Diaz, Mariano (CL)	APEX Site Administrator
Dupeyron, Jorge (CL)	Network & Windows Specialist
Gallenne, Alexandre (FR)	Fellow
Haeussler, Boris (DE)	Operations Staff Astronomer
Hibon, Pascale (FR)	Operations Staff Astronomer
Jaffe Ribbi, Yara Lorena (VE)	Fellow
Klement, Robert (CZ)	Student
Lillo Box, Jorge (ES)	Fellow
Muñoz, César (CL)	Student
Muñoz-Mateos, Juan Carlos (ES)	Operations Staff Astronomer
Plunkett, Adele (US)	Fellow
Vogt, Frédéric (CH)	Fellow

Departures (1 October–31 December 2015)

Europe

Balestra, Andrea (IT)	Software Engineer
Cabrera Ziri Castro, Ivan (VE)	Student
Chira, Roxana-Adela (DE)	Student
Erm, Toomas (SE)	Electronics Engineer
Geier, Stephan (DE)	Fellow
Haase, Jonas (DK)	Astronomical Data Archive & Pipeline Software Specialist
Jamialahmadi, Narges (IR)	Student
klein Gebbinck, Maurice (NL)	Software Engineer
Oezener, Betuel (DE)	HR Advisor
Rahoui, Farid (FR)	Fellow
Zafar, Tayyaba (PK)	Fellow
Zahorecz, Sarolta (HU)	Student

Chile

Duran, Carlos (CL)	Electronic Engineer
Parra, Ricardo Nelson (CL)	Electronics Engineer
Smeback, Russell (US)	JAO Head of Administration
Vigan, Arthur (FR)	Operations Astronomer

ESO, the European Southern Observatory, is the foremost intergovernmental astronomy organisation in Europe. It is supported by 16 countries: Austria, Belgium, Brazil, the Czech Republic, Denmark, France, Finland, Germany, Italy, the Netherlands, Poland, Portugal, Spain, Sweden, Switzerland and the United Kingdom. ESO's programme is focused on the design, construction and operation of powerful ground-based observing facilities. ESO operates three observatories in Chile: at La Silla, at Paranal, site of the Very Large Telescope, and at Llano de Chajnantor. ESO is the European partner in the Atacama Large Millimeter/submillimeter Array (ALMA). Currently ESO is engaged in the design of the European Extremely Large Telescope.

The Messenger is published, in hard-copy and electronic form, four times a year: in March, June, September and December. ESO produces and distributes a wide variety of media connected to its activities. For further information, including postal subscription to The Messenger, contact the ESO education and Public Outreach Department at:

ESO Headquarters
Karl-Schwarzschild-Straße 2
85748 Garching bei München, Germany
Phone +49 89 320 06-0
information@eso.org

The Messenger:
Editor: Jeremy R. Walsh;
Design, Production: Jutta Boxheimer;
Layout, Typesetting: Mafalda Martins;
Graphics: Ed Janssen.
www.eso.org/messenger/

Printed by Color Gruppe
Geretsrieder Straße 10
81379 München, Germany

Unless otherwise indicated, all images in The Messenger are courtesy of ESO, except authored contributions which are courtesy of the respective authors.

© ESO 2015
ISSN 0722-6691

Contents

Telescopes and Instrumentation

Sterzik M. et al. – The Scientific Return of VLT Programmes	2
Lo Curto G. et al. – HARPS Gets New Fibres After 12 Years of Operations	9
Willez J. et al. – VLTi: First Light for the Second Generation	16
Amico P. et al. – The First Component of the Adaptive Optics Facility Enters Operations: The Laser Traffic Control System on Paranal	19
Hatziminaoglou E. et al. – The European ALMA Regional Centre Network: A Geographically Distributed User Support Model	24
Stoehr F. et al. – ALMA Cycle 0 Publication Statistics	30

Astronomical Science

Weilbacher P. M. et al. – The Central Orion Nebula (M42) as seen by MUSE	37
Petr-Gotzens M. G. et al. – Young Stellar Objects in the Orion B Cloud	42
Ohnaka K. et al. – Revealing the Complex Dynamics of the Atmospheres of Red Supergiants with the Very Large Telescope Interferometer	46
Bagnulo S. et al. – Beyond Phase 3: The FORS1 Catalogue of Stellar Magnetic Fields	51

Astronomical News

Arnaboldi M. et al. – Report on the ESO Workshop “Rainbows on the Southern Sky: Science and Legacy Value of the ESO Public Surveys and Large Programmes”	57
Kabath P. et al. – Report on the ESO/OPTICON/IAU Summer School “Modern Instruments, their Science Case, and Practical Data Reduction”	60
Bono G. et al. – Report on the International PhD School “Science and Technology with the E-ELT”	62
Staff at ESO – E. Sani	64
Fellows at ESO – M. Béthermin, K. Wang	64
Personnel Movements	67

Front cover: Two emission line composite images from the MUSE study of the bright centre of the Orion Nebula (M42, NGC 1976), featured in the article by Weilbacher et al., p. 37, are shown. The upper image is in ionised hydrogen emission from the lines of H β , H α and Paschen 9 (9229 Å) and coded blue, green, red respectively. The lower image is formed from the three lines of oxygen, neutral – [O I] 6300 Å, singly ionized – [O II] 7320 Å and doubly ionised – [O III] 5007 Å (coded blue, green, red).
Credit: Weilbacher et al.

